THE SYNTHESIS, ELECTROCHEMISTRY AND REACTIVITY OF BINUCLEAR COPPER(I) COMPLEXES AS MIMICS OF PROTEIN ACTIVE SITES

Thesis by

Robert Paul Kreh

In Partial Fulfillment of the Requirements

for the Degree of

Doctor of Philosophy

California Institute of Technology

Pasadena, California

1981

(Submitted September 2, 1980)

ACKNOWLEDGMENTS

Many people made contributions toward the work presented in this thesis. I will no doubt forget to mention a few, but some who come to mind are listed below:

My interest in chemistry was first generated by Lillian Abramson at Montgomery Blair High School (Silver Spring, Maryland). This interest was kindled by Professors Gynith Giffin, Thomas McGrath, Neil Potter and Robert Nylund at Susquehanna University (Selinsgrove, Pennsylvania). At Caltech, I have enjoyed the guidance of my research advisor, Robert Gagné, and I appreciate the freedom he has allowed me in making many decisions on my own. I also thank Dave Evans, Harry Gray and Sunney Chan for many helpful discussions.

The Gagné research group has been great. In the early days, there were Judy Allison with her laugh, Carl Koval with his electrochemistry and Tom Smith with his great knowledge of inorganic chemistry. More recently, trials and tribulations have been shared with Cliff Spiro, George Lisensky, Mike Ingle, Bill Marritt, Dave Marks, Larry Henling, and Rich Durand. John Dodge and Mike McCool deserve a special word of thanks for their work on the crystal structures presented in this thesis. I am especially grateful to Pat Anderson, the group secretary, for her help and cooperation whenever it was needed.

I would also like to thank Henriette Wymar for an excellent job of typing this thesis.

The chemistry staff here at Caltech has been very helpful and understanding, and in particular, special thanks go to Jan Mitchell and Sally Muir of the analytical lab.

I have enjoyed the support and companionship of many friends here at Caltech. Jan and Mark Mitchell have been the best of friends for the past three years. Their support was invaluable. Various members of the Chan research group, including Randy Morse, Tom Stevens and Gary Brudvig, have helped with social diversions (?) along the way. I also have enjoyed the friendships of Jim and Patty Eisenach and Sridhar.

This thesis is dedicated to my parents, Dave and Louise, because they gave me the support and freedom to pursue whatever I chose in life and taught me to do it with the best of my ability.

ABSTRACT

A series of binuclear copper(I) complexes has been synthesized and characterized as potential models for binuclear copper protein sites.

The first group of compounds was prepared by the condensation of 2-hydroxy-5-methylisophthalaldehyde with a variety of primary amines (RNH_2) followed by the addition of $Cu(CH_3CN)_4BF_4$ and pyrazolate (pz), 3,5-dimethyl pyrazolate (Me_2pz) and 7-azaindolate (aza) anions (X) to yield $Cu_2^I ISOIM(R)_2(X)$. A crystal and molecular structural analysis of $Cu_2^I ISOIM(Etpy)_2(pz)$ (R = 2-(2′-pyridyl)ethyl) showed each copper bound to the phenoxide oxygen, as well as to one imine and one pyrazolate nitrogen. The pyridine nitrogens were not coordinated to copper, but an intermolecular Cu-Cu interaction (2.97 Å) was observed. Overall coordination about copper(I) is best described as highly distorted pyramidal, with long axial (Cu-Cu) coordination. The copper-copper interaction appears to be associated with a ca. 600 nm (solid state) absorption which is not present in solution or in the solid state for compounds with bulky "side arms" (R). All compounds are proposed to be three-coordinate in solution, but they have exhibited no tendency to bind additional ligands such as CO or pyridine. Most of the binuclear copper(I) complexes gave quasi-reversible electrochemical behavior, with two distinct one-electron processes. The reduction potentials were varied over a wide range by modifications of the side-arms (R) and the bridge (X), with the most positive potentials observed for R = t-butyl and X = 3,5-dimethylpyrazolate (E_1^f = +0.239,

E_2^f = +0.80 V vs. nhe). Biological implications of the observed reactivities and redox properties of these compounds are discussed.

The reaction of N,N,N′,N′-tetrakis-(2-pyridylmethyl)ethylenediamine (TPEN) with $Cu(CH_3CN)_4BF_4$ yielded $Cu_2^I(TPEN)(BF_4)_2$. A complete crystal and molecular structural analysis showed each copper to be bound to two pyridine nitrogens, and an intramolecular Cu-Cu interaction (2.78 Å) was found. The tertiary nitrogens do not appear to be coordinated to the coppers. $Cu_2^I(TPEN)(BF_4)_2$ reacts with CO to yield $Cu_2^I(TPEN)(CO)_2(BF_4)_2$, and the crystal and molecular structure of this dicarbonyl adduct was also determined. Each copper was found in similar distorted tetrahedral geometries, but the bond lengths and bond angles around each copper are slightly different. This is manifested in two carbonyl stretching frequencies.

Investigation of the dioxygen reactions of Cu_2^IISOIM(R)$_2$(pz), where R = a variety of alkyl, aromatic and heterocyclic groups, indicated ligand oxidation and pyrazolate dissociation upon oxygenation. As a result, the synthesis of new binuclear three-coordinate copper(I) complexes was proposed for investigation of their dioxygen reactivities. The proposed ligands were synthesized by the condensation of 2-hydroxy-5-methylisophthalaldehyde with 2-(2′-aminoethyl)pyridine and 2-(2′-aminoethyl)-1-methylimidazole, but the desired cuprous complexes were not isolated in pure form.

TABLE OF CONTENTS

CHAPTER I

Introduction

Hemocyanin, tyrosinase and laccase are proteins which utilize a binuclear copper active site for a direct interaction with molecular oxygen. Hemocyanin is responsible for reversible oxygenation in the blue blood of various molluscs and arthropods.[1] Tyrosinase, found in a variety of organisms, catalyzes the oxidation of substrates by dioxygen (e.g., Scheme 1).[2] The laccases of Asian lacquer trees and

Scheme 1

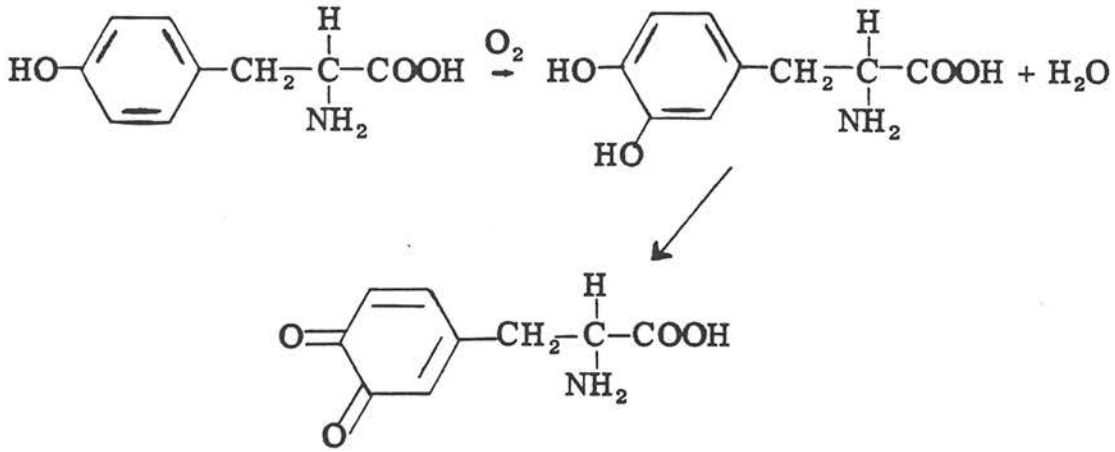

white rot fungi catalyze the reduction of oxygen to water (equation 1)

$$O_2 + 4e^- + 4H^+ \rightarrow 2H_2O \qquad (1)$$

while oxidizing a variety of substrates.[3] In addition to the binuclear copper site, laccase contains two other isolated copper ions ("type I" and "type II") which are also necessary for enzymatic activity.

These binuclear copper protein sites are especially intriguing because they consist of two cupric ions in close proximity which do not exhibit the paramagnetism typical of copper(II) ions.[4-6] This is seen in the diamagnetism and lack of EPR signals at room temperature. (The total EPR intensity of laccase accounts for only 50% of the copper, presumably due to the type I and type II copper present in the protein.)[6] Temperature-dependent magnetic studies indicate that the cupric ions of the binuclear sites in oxyhemocyanin and laccase are antiferromagnetically coupled.[4]

The binuclear cupric site in laccase acts as a two-electron acceptor.[7] Oxidation-reduction titrations indicate that this site is reduced in a one-step, two-electron transfer (n = 2) but reoxidized in two one-electron steps (n = 1). This is rather novel behavior, since the electrochemistry of polynuclear complexes generally shows distinct one-electron processes for interacting metals.[8] In fact, it appears that closer proximity and larger interactions lead to greater separations of the one-electron processes.[9] The potentials found for the reduction of the laccases were +0.43 V for Rhus laccase and +0.78 V for Polyporus laccase.[7] (Potentials are versus the normal hydrogen electrode, nhe). The reduction of both cupric ions of binuclear site in tyrosinase also occurs at a single potential (0.36 V vs. nhe).[5] The reoxidation of tyrosinase has not been reported, nor have electrochemical measurements on hemocyanin been reported.

The reduction potentials measured for these binuclear sites are very positive for copper(II) ions, indicating the stabilization of the

cuprous state relative to the cupric state. On the contrary, the reduction potentials for synthetic Cu(II) complexes with nitrogen and oxygen ligands tend to be quite low, usually well below the potential for the normal hydrogen electrode.[10] Soft donors such as sulfur ligands may be proposed to account for the high reduction potentials exhibited by these copper proteins.[11,12] However, spectroscopic and titration studies indicate the absence of sulfur ligands and the presence of nitrogen ligands such as imidazole.[13]

The above discussion presents several interesting questions about these binuclear copper sites. In addition to the direct study of the proteins, the investigation of appropriate model compounds can yield useful information about the questions posed below.

1) What are the ligands bound to the copper centers? Protein studies have indicated that the majority of ligands may be imidazole nitrogens from histidine.[13] The following structure and ligand environment, 1, was proposed for oxyhemocyanin by Bosnich and

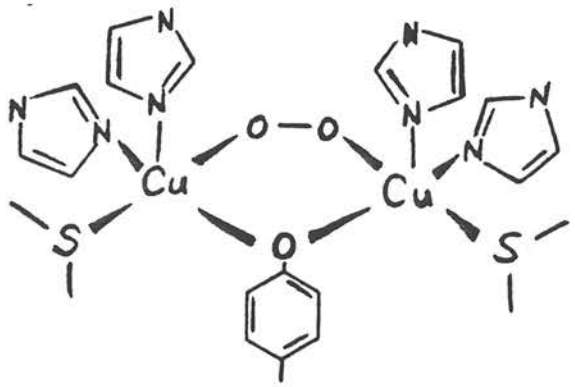

1

coworkers on the basis of electronic spectra.[11] The phenolate oxygen atom, the peroxide ligand, the thioether ligand and an imidazole nitrogen occupy an approximately square-planar array around each copper. This configuration was arrived at by the comparison of the electronic absorption spectra of several synthetic Cu(II) complexes to that of oxyhemocyanin. This model, however, contradicts other evidence against the presence of sulfur atoms.[13]

Similar models have been recently proposed by T. G. Spiro and coworkers for oxyhemocyanin and deoxyhemocyanin (shown below).[14]

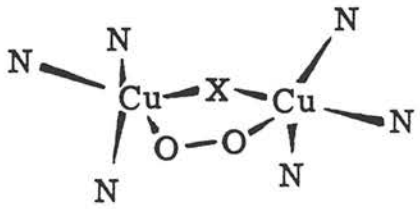

Oxyhemocyanin

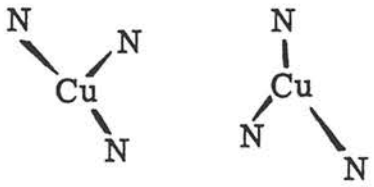

Deoxyhemocyanin

The models are based upon extended X-ray absorption fine structure (EXAFS) and resonance Raman (RR) spectroscopy of hemocyanin. In these models, the nitrogen ligands are from imidazole rings (histidine), and X is suggested to be a phenolate oxygen from tyrosine. The resonance Raman studies imply bridging peroxide, i.e., the transfer of one electron from each Cu(I) upon oxygenation. The above model for oxyhemocyanin is essentially the same as an earlier proposal by Solomon and coworkers, based upon electron paramagnetic resonance

(EPR) and electronic absorption spectroscopy of a series of hemocyanin derivatives.[15]

2) What is the nature of the Cu-Cu interaction? The strong antiferromagnetic coupling between the two cupric ions of oxyhemocyanin is presumably due to superexchange through an endogenous ligand (tyrosine oxygen) and/or the bridging peroxide.[4,15] Strong antiferromagnetic interactions have been observed in a number of binuclear copper(II) complexes.[8,16] For example, compound 2 is diamagnetic,

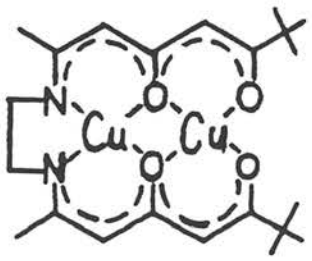

2

exhibiting sharp NMR absorptions and weak EPR signals.[16] Hence, it is not unreasonable to propose strong interactions through a bridging phenolate oxygen in oxyhemocyanin.

3) What is the origin of the unusual electrochemical behavior, including the very high reduction potentials? While the majority of synthetic complexes containing closely interacting metal centers exhibit stepwise reduction and oxidation of the metal centers, compound 2 (above) appears to be an exception. Both coppers in 2 are reported to be reduced and oxidized at a single potential.[16] An investigation of this system is presented in Appendix I. The very

positive reduction potentials exhibited by the binuclear cupric sites in laccase and tyrosinase are still curious. The potentials observed for synthetic copper(II) complexes employing nitrogen and oxygen ligands are usually quite negative, due to the relative stabilization of the oxidized Cu(II) state by these "hard" ligands.[8,10] This dilemma will be addressed in this thesis. That is, what type and geometry of oxygen and nitrogen ligands could lead to the stabilization of the cuprous state and generate these high reduction potentials?

4) What factors are responsible for reversible O_2 binding and O_2 activation? Marginal success has been achieved in obtaining reversible oxygenation of synthetic cuprous complexes. The following complex, 3, isolated by Osborn et al., was found to react with oxygen,

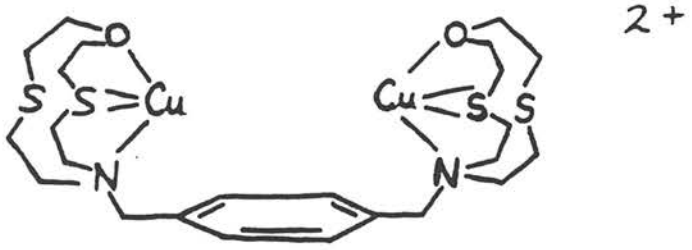

3

possibly leading to reversible oxygenation in the solid state.[17] This reaction has yet to be well characterized by the authors. Reversible oxygenation (in solution) of the mononuclear Cu(I) complex, 4, has been reported by Wilson and coworkers.[18] Only preliminary results

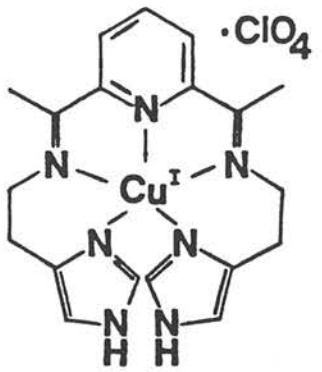

4

have been communicated, but stoichiometry measurements imply a bridging O_2 between two coppers in the oxygenated species.

While a number of reports have appeared describing copper catalyzed autoxidation of organic substrates, the relationships between oxygen activation and coordination environment around the copper ions remains unclear.[19] For this purpose, cuprous complexes containing a well defined ligand environment are desired. Polydentate (including macrocyclic) ligands are useful in this regard. The autoxidation of macrocyclic ligands bound to copper(I) has recently been investigated in our laboratory.[20]

An understanding of oxygen activation is relevant to fuel cell technology.[21] The reduction of oxygen to water (equation 1) is the cathodic reaction involved in a fuel cell. For a fuel cell to become an efficient device for energy conversion, a catalyst must be found for this reduction. By adequately "mimicking" the binuclear copper protein sites, a synthetic catalyst for the reduction of oxygen to water

may eventually emerge.

The work presented in this thesis involves the synthesis, characterization and reactivity of a series of binuclear copper complexes as potential models for the binuclear copper protein sites. Although a large number of binuclear copper complexes are known, most of these have involved the higher (+2) valence state of copper. To understand the inherent stability and dioxygen reactions of the reduced protein sites, binuclear Cu(I) complexes should be investigated. A few binuclear Cu(I) complexes (e.g., $\underset{\frown}{3}$[17] and $\underset{\frown}{5}$[22]) have been recently

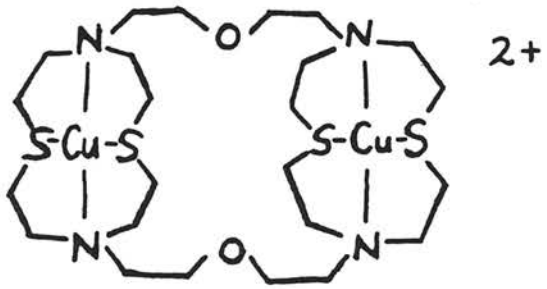

5

reported, but these have employed sulfur ligands for the stabilization of the cuprous centers. Since sulfur ligands are most likely <u>not</u> present in the binuclear copper protein sites,[13] it is desirable to use only nitrogen and oxygen ligands in model compounds.

The problem is, then, to stabilize the +1 oxidation state of copper while utilizing nitrogen and oxygen ligands. The two main factors which appear to be involved in the relative stabilization of Cu(II) and Cu(I) are summarized in Table 1.[8,10,23]

Table 1. Preferences of Copper Valence States

	Cu^{II} (d^9)	Cu^{I} (d^{10})
a)	octahedral (distorted), square-pyramidal or square-planar geometry	tetrahedral, trigonal or digonal geometry
b)	"hard" sigma donors (amines, H_2O, OH^-, NH_3...)	"soft" donors, particularly those capable of π backbonding (CO, CN^-, SR_2, PR_3, aromatic nitrogen...)

Most of the binucleating ligands employed to date are much more conducive to Cu(II) than Cu(I). Inorganic chemists appear to be enamored with amines, imines, alcohols, ethers, ketones and aldehydes for use as ligands. These ligands are to be avoided if stabilization of Cu(I) is desired. Also, macrocyclic ligands are often used because they can promote unusual structural types while minimizing substitution reactions around the metal when the complexes are in solution.[8,24] Yet these macrocycles tend to be unfavorable for Cu(I) due to the square-planar environment of ligands often dictated by the macrocycle.

These factors are demonstrated by the binuclear compound, 6, which has received attention in several laboratories, including ours.[8] This binuclear complex exhibits a two-step reduction at -0.52 V and -0.91 V versus nhe. These very negative potentials indicate the destabilization of Cu(I) relative to Cu(II) in this ligand environment.

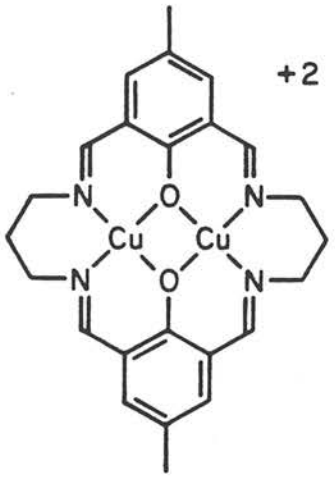

6

In an effort to circumvent the above problems of Cu(I) destabilization, binucleating ligands which contain "softer" aromatic nitrogen ligands in a more flexible framework (to allow tetrahedral geometry around both coppers) were designed. (Also, aromatic type nitrogens begin to approach the ligands (i.e., histidine) suggested for the binuclear copper protein sites.) These modifications on the macrocyclic ligand system of 6 have yielded a very stable copper(I) complex, 7. A tetrahedral array of oxygen and nitrogen ligands around each

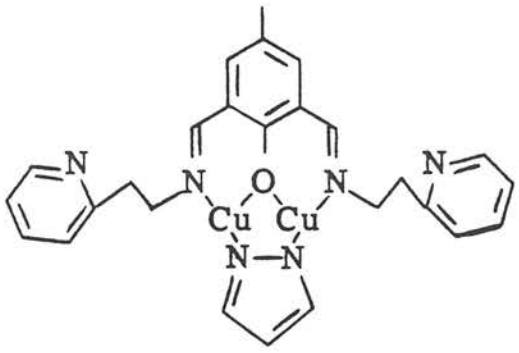

7

copper was expected, but X-ray structural analysis showed only three ligands bound to each copper and in addition, an intermolecular Cu-Cu interaction was observed. This Cu-Cu interaction appears to be associated with an electronic absorption band at 600 nm. The reduction potentials were varied systematically over a wide range by modifications in the ligand system, and the more positive values approach the high potentials exhibited by the copper proteins. These results along with biological implications are presented in Chapter II.

The investigation of binuclear copper(I) complexes was extended to compound 8 and its dicarbonyl adduct 9. Chapter III describes the

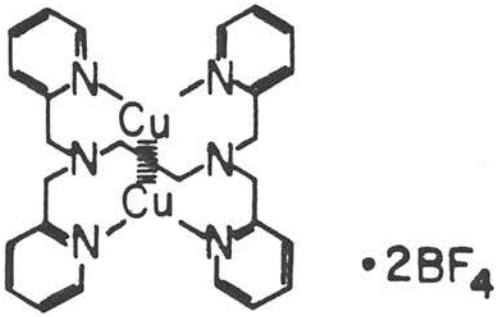

8

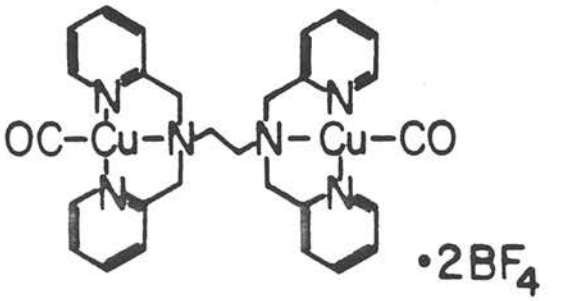

9

synthesis, characterization and X-ray structural analysis of each of these compounds. Again, an unexpected coordination environment was observed for the binuclear cuprous system, 8. Each copper

appears to bind only two nitrogen ligands (from the pyridine rings) in addition to the observed Cu-Cu interaction. The "expected" pseudo-tetrahedral geometry of ligands was observed for 9, but the two copper centers are not equivalent, and this is manifested in two different carbonyl stretching frequencies.

Chapter IV presents an investigation into the dioxygen reactions of binuclear cuprous compounds such as 7. The results led to the design and attempted synthesis of new binuclear three-coordinate copper systems, 10 and 11. Although the ligand syntheses were

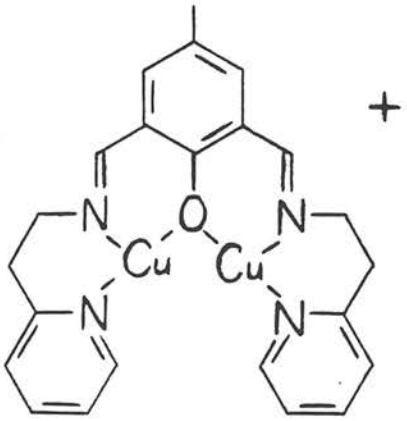

10

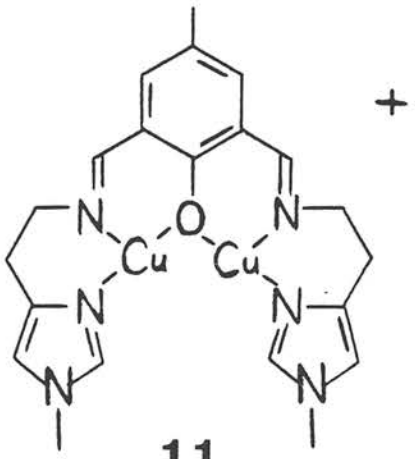

11

accomplished, the copper(I) complexes were not isolated in pure form.

All of the work presented in this thesis was done by this author with the exception of the X-ray structural analyses, and these were performed by John Dodge (7 and 8) and Mike McCool (9).

References and Notes

(1) Lontie, R. in "Inorganic Biochemistry", Eichhorn, G. I. ed.; Elsevier: New York, N.Y., 1973; p. 344.

(2) (a) Mason, H. S. Ann. Rev. Biochem. 1965, 35, 595-634. (b) Vanneste, W. H. and Zuberbühler, A. in "Molecular Mechanisms of Oxygen Activation", Hayaishi, O. ed.; Academic Press: 1974; p. 371.

(3) (a) Fee, J. A. Structure and Bonding 1975, 23, 1-60. (b) Vänngård, T. I. in "Biological Applications of Electron Spin Resonance Spectroscopy", Swartz, H. M.; Bolton, J. R.; and Borg, D. C., eds.: J. Wiley: New York, N.Y., 1972, p. 411.

(4) Solomon, E. I.; Dooley, D. M.; Wang, R.; Gray, H. B.; Cerdonio, M.; Mogno, F.; Romani, G. L. J. Amer. Chem. Soc. 1976, 98, 1029-1031.

(5) Makino, N.; McMahill, P.; Mason, H. S.; Moss, T. H. J. Biol. Chem. 1974, 249, 6062-6066.

(6) Malmstrom, B.G.; Reinhammer, B. R.; Vänngård, T. Biochem. Biophys. Acta 1970, 205, 48.

(7) (a) Reinhammar, B. R. M.; Vänngård, T. Eur. J. Biochem. 1971, 18, 463-468. Reinhammar, B. R. M. Biochem. Biophys. Acta 1972, 275, 245-259. (b) Farver, O. Goldberg, M.; Lancet, D.; Pecht, I. Biochem. Biophys. Res. Commun. 1976, 73, 494-500.

(8) Gagné, R. R.; Koval, C. A.; Smith, T. J. J. Amer. Chem. Soc. 1977, 99, 8367-8368. Gagné, R. R.; Koval, C. A.; Smith, T. J.;

References (continued)

Cimolino, M. C. J. Amer. Chem. Soc. 1979, 101, 4571-4580.

(9) (a) Creutz, C.; Taube, H. J. Amer. Chem. Soc. 1969, 91, 3988-3989. Creutz, C.; Taube, H. J. Amer. Chem. Soc. 1973, 95, 1086-1094. (b) Weaver, T. R.; Meyer, T. J.; Adeyemi, S. A.; Brown, G. M.; Eckberg, R. P.; Hatfield, W. E.; Johnson, E. C.; Murray, R. W.; Untereker, D. J. Amer. Chem. Soc. 1975, 97, 3039-3048. (c) Callahan, R. W.; Keene, F. R.; Meyer, T. J.; Salmon, D. J. J. Amer. Chem. Soc. 1977, 99, 1064-1073.

(10) Patterson, G. S.; Holm, R. H. Bioinorg. Chem. 1975, 4, 257-275.

(11) Admundsen, A. R.; Whelan, J.; Bosnich, B. J. Amer. Chem. Soc. 1977, 99, 6730-6739.

(12) Potentials in the range of +0.3 to +0.9 V (vs. nhe) have been reported for copper(II) complexes of polythiamacrocycles: Dockal, E. R.; Jones, T. E.; Sokol, W. F.; Engerer, R. J.; Rorabacher, D. B.; Ochrymowycz, L. A. J. Amer. Chem. Soc. 1976, 98, 4322-4324.

(13) See Wurzbach, J. A.; Grunthaner, P. J.; Dooley, D. M.; Gray, H. B.; Grunthaner, F. J.; Gay, R. R.; Solomon, E. I. J. Amer. Chem. Soc. 1977, 99, 1257-1258, and references contained therein.

(14) Brown, J. M.; Powers, L.; Kincaid, B.; Larrabee, J. A.; Spiro, T. G. J. Amer. Chem. Soc. 1980, 102, 4210-4216.

References (continued)

Larrabee, J. A.; Spiro, T. G. J. Amer. Chem. Soc. 1980, 102, 4217-4223.

(15) Eickman, N. C.; Himmelwright, R. S.; Solomon, E. I. Proc. Natl. Acad. Sci. USA 1979, 76, 2094-2098.

(16) Lintvedt, R. L.; Tomlonovic, B.; Fenton, D. E.; Glick, M. D. Adv. Chem. Ser. 1975, 150, 407-425.

(17) Bulkowski, J. E.; Burk, P. L.; Ludmann, M. F.; Osborn , J. A. J. Chem. Soc., Chem. Commun. 1977, 498-499.

(18) Simmons, M. G.; Wilson, L. J. J. Chem. Soc., Chem. Commun. 1978, 634-636.

(19) For example, see Brackman, W.; Havinga, E. Recueil, 1955, 74, 1021-1039. Jameson, R. F.; Blackburn, N. J. J. Inorg. Nucl. Chem. 1975, 37, 809-814. Urbach, F. L.; Knopp, U.; Zuberbühler, A. D. Helv. Chim. Acta 1978, 61, 1097-1106. Munakata, M., Nishibayashi, S.; Sakamoto, H. J. Chem. Soc., Chem. Commun. 1980, 219-220.

(20) Lisensky, G. C., Ph.D. Dissertation, California Institute of Technology, 1981.

(21) Bockris, J.; Shrinivasan, S. "Fuel Cells: Their Electrochemistry", McGraw Hill, New York, 1969.

(22) Alberts, A. H.; Annunziata, R.; Lehn, J. M. J. Amer. Chem. Soc. 1977, 99, 8502-8504.

(23) James, B. R.; Williams, R. J. J. Chem. Soc. 1961, 2007-2019.

(24) Gagné, R. R.; Allison, J. L.; Gall, R. S.; Koval, C. A. J. Amer. Chem. Soc. 1977, 99, 7170-7178.

CHAPTER II

Unusual Structural and Reactivity Types for Copper(I): Synthesis, Structural and Redox Properties of Binuclear Copper(I) Complexes which are Probably Three-Coordinate in Solution and Experience Intermolecular Metal-Metal Interactions in the Solid State.

Robert R. Gagné, Robert P. Kreh and John A. Dodge

Contribution No. 5645 from the Division of Chemistry and Chemical Engeineering, California Institute of Technology, Pasadena, California 91125.

Introduction

Protein binuclear copper sites effect remarkable reactions with dioxygen including reversible binding (hemocyanin),[1] activation (tyrosinase)[2] and reduction (laccase).[3] Structural information contrasting these active sites is limited but similarities are notable: sulfur ligands have been proposed but most studies suggest only nitrogen and/or oxygen coordination;[4] in the oxidized forms all three binuclear sites are strongly antiferromagnetically coupled;[5,6] the tyrosinase and laccase binuclear sites exhibit two electron reductions at potentials which are rather high for the proposed all nitrogen/oxygen copper coordination.[6,7]

Model studies have addressed ligand environment(s), redox properties, magnetic interactions and dioxygen binding in these protein active sites.[8-12] To help define protein structure/reactivity relationships we are endeavouring to catalogue fundamental copper(I) coordination chemistry in relatively simple mononuclear and binuclear complexes. As discussed elsewhere, polydentate ligands, including macrocycles, can be utilized to minimize problems associated with both copper(II) and copper(I) substitution lability.[13,14] This approach has resulted in unusual structural and reactivity types for copper including four- and five-coordinate copper(I) species.[13-15] The binuclear complex $\underset{\sim}{1}$ provided an opportunity for meauring intramolecular electron transfer rates between copper centers, but the reduction potentials observed for $\underset{\sim}{1}$ (equations 1 and 2) are significantly more negative than those exhibited by the proteins (e.g., +0.36 V for

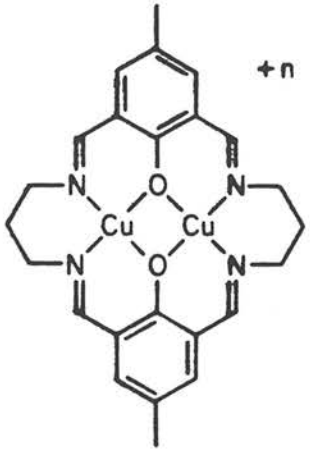

I

$$Cu^{II}Cu^{II}L^{2+} + e^- \xrightarrow{-0.52\,V} Cu^{II}Cu^{I}L^{+} \qquad (1)$$

$$Cu^{II}Cu^{I}L^{+} + e^- \xrightarrow{-0.91\,V} Cu^{I}Cu^{I}L \ . \qquad (2)$$

tyrosinase).[7,14] Modification of the macrocyclic complex, 1, has yielded a series of binuclear complexes 2, in which the R and X groups

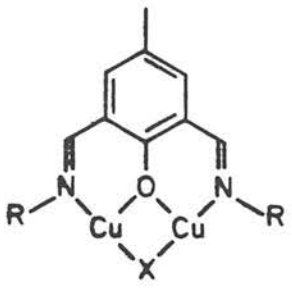

2

X = 

,

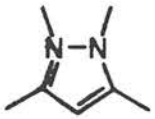

,

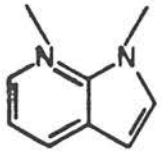

were varied systematically, resulting in a wide range of reduction potentials. In this manner, utilizing only nitrogen and oxygen ligands, high reduction potentials comparable to that of protein binuclear sites have been achieved. The new binuclear copper(I) complexes appear to be only three-coordinate in solution but in some instances experience significant intermolecular copper(I)-copper(I) interactions in the solid state.

Synthesis and Characterization of Complexes

Three copper(II) complexes, 3-5, were prepared by simple condensation of 2-hydroxy-5-methylisophthalaldehyde with primary amines followed by addition of copper(II), Scheme I. The new compounds are blue-green due to weak absorption in the 630-645 nm region (probably ligand field transitions) as listed in Scheme I for methanol solutions. Solid state magnetic susceptibility measurements at 25° C, also listed in Scheme I, suggest that the two copper(II) centers are antiferromagnetically coupled.

Analogous air sensitive copper(I) complexes were prepared in a helium atmosphere in a fashion similar to the synthesis of the copper(II) species. The dialdehyde was condensed with two equivalents of a primary amine, RNH_2, then treated with a bridging bidentate ligand, XH, in the presence of base, followed by addition of $Cu(CH_3CN)_4BF_4$ (Scheme II). The compounds synthesized, along with the abbreviations to be used, are listed in Table I. All of the compounds listed gave satisfactory C, H and N analyses. Selected compounds were also analyzed for copper, giving the expected values. The infrared spectra

Scheme I. Preparation of Binuclear $Cu^{II}Cu^{II}$ Complexes. (Spectra were recorded in methanol solution at 25° C. Magnetic susceptibilities are given in B.M., measured at 25° C, and corrected for diamagnetism, but not for T.I.P.)

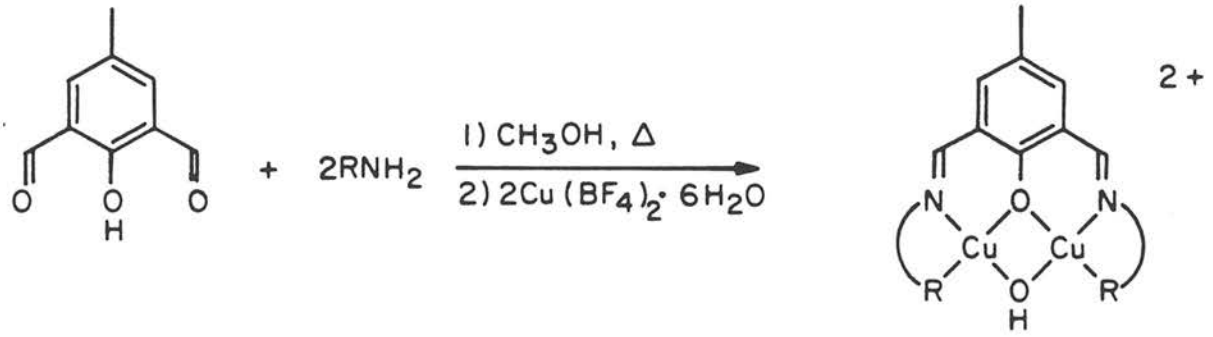

	R	λ (ε)	μ_{eff}/Cu
3	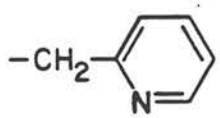	630(160)	1.4
4	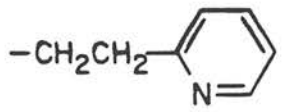	645(120)	1.2
5	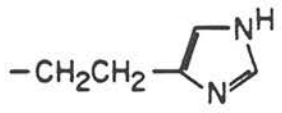	630(100)	0.96

Table I. Binuclear Cu(I)-Cu(I) Complexes, Abbreviations Utilized and NMR Data.

Compound Number	Sidearm (R)	Bridge (X)	Abbreviation	NMR Assignments[a] α_1	α_2	α_3	β_1	β_2	py_1	pz_2	pz_3	aza_2	aza_3	aza_6
6	2-(pyridyl)-methyl	pyrazolate	$Cu(I)_2ISOIM(Mepy)_2(pz)$	2.05	6.66	7.56	4.60	-	8.46	8.02	6.23	-	-	-
7	2-(pyridyl)-methyl	3-5 dimethyl-pyrazolate	$Cu(I)_2ISOIM(Mepy)_2(Me_2pz)$	2.06,s	6.69,s	7.72,s	4.67,s	-	8.37,d	2.13,s/b	6.21	-	-	-
8	2-(pyridyl)-methyl	7-azaindolate	$Cu(I)_2ISOIM(Mepy)_2(aza)$	2.09,s	6.72	7.54	4.70,s	-	8.43,d	-	-	c	c	c
9	2-(2'-pyridyl)-ethyl	pyrazolate	$Cu(I)_2ISOIM(Etpy)_2(pz)$	1.92,s	6.47	7.50	3.82,t	3.29,t	8.42,d	7.87	6.47	-	-	-
10	2-(2'-pyridyl)-ethyl	3-5 dimethyl-pyrazolate	$Cu(I)_2ISOIM(Etpy)_2(Me_2pz)$	1.94,s	6.48,s	7.52,s	3.88,t	3.37,t	8.40,d	2.46,s/b	6.17	-	-	-
11	2-(2'-pyridyl)-ethyl	7-azaindolate	$Cu(I)_2ISOIM(Etpy)_2(aza)$	1.96,s	c	7.60	3.90,t	{3.44, 3.20	8.39	-	-	8.10	c	8.39
12	phenylmethyl	pyrazolate	$Cu(I)_2ISOIM(MePh)_2(pz)$	2.10,s	6.72	7.54	4.26	-	-	8.00	6.26	-	-	-
13	phenylmethyl	3-5 dimethyl-pyrazolate	$Cu(I)_2ISOIM(MePh)_2(Me_2pz)$	2.10,s	6.70	7.57	4.37	-	-	2.06,s/b	c	-	-	-
14	phenylmethyl	7-azaindolate	$Cu(I)_2ISOIM(MePh)_2(aza)$	2.14,s	6.77	c	{4.40, 4.32	-	-	-	-	c	c	c
15	2-phenylethyl	pyrazolate	$Cu(I)_2ISOIM(EtPh)_2(pz)$	1.96,s	6.51	7.37	3.45,t	3.07,t	-	7.93,d	6.51	-	-	-
16	2-phenylethyl	3-5 dimethyl-pyrazolate	$Cu(I)_2ISOIM(EtPh)_2(Me_2pz)$	1.97,s	6.52,s	7.38,s	3.50,t	3.10,t	-	2.61,s/b	6.17	-	-	-
17	2-phenylethyl	7-azaindolate	$Cu(I)_2ISOIM(EtPh)_2(aza)$	1.98,s	6.53,s	7.46,s	3.52,t	{3.18, 2.97	-	-	-	8.13,d	c	8.36,d
18	n-propyl	pyrazolate	$Cu(I)_2ISOIM(1\text{-}Pr)_2(pz)$	2.09,s	6.70,s	7.57,s	3.15,t	1.78,m	-	7.87,d	6.43,t	-	-	-
19	i-propyl	pyrazolate	$Cu(I)_2ISOIM(2\text{-}Pr)_2(pz)$	2.10,s	6.70,s	7.70,s	2.90,m	1.20,d	-	7.87,d	6.45,t	-	-	-
20	t-butyl	pyrazolate	$Cu(I)_2ISOIM(t\text{-}Bu)_2(pz)$	2.13,s	6.85,s	7.91,s	-	1.26,s	-	7.93,d	6.54,t	-	-	-
21	t-butyl	3-5 dimethyl-pyrazolate	$Cu(I)_2ISOIM(t\text{-}Bu)_2(Me_2pz)$	2.10,s	6.81,s	7.85,s	-	1.28,s	-	2.57,s/b	6.10,s	-	-	-
22	t-butyl	7-azaindolate	$Cu(I)_2ISOIM(t\text{-}Bu)_2(aza)$	2.14,s	6.85,s	7.98,s	-	{1.34,e 1.23,s	-	-	-	8.13,d	6.75,d	8.45,d
23	phenyl	pyrazolate	$Cu(I)_2ISOIM(Ph)_2(pz)$	2.04,s	6.67	7.52	-	-	-	7.75,d	6.33	-	-	-
24	p-(dimethylamino)-phenyl	pyrazolate	$Cu(I)_2ISOIM(PhNMe_2)_2(pz)$	2.07	c	7.55	-	-	-	c	c	-	-	-
25	p-acetylphenyl	pyrazolate	$Cu(I)_2ISOIM(PhCOMe)_2(pz)$	c	c	c	-	-	-	c	c	-	-	-

[a]All spectra were obtained in d^6 benzene solution at 34°C. The values listed are given in ppm, δ, relative to TMS. The assignments for the resonances are given in Figure 2 and as follows: α_1 = protons from the methyl group on the aromatic ring arising from 2-hydroxy-5-methylisophthalaldehyde; α_2 = aromatic protons from the 2-hydroxy-5-methyl-isophthalaldehyde ring; α_3 = the imine protons; β_1 = methylene protons (or methine proton) adjacent to the imine nitrogen; β_2 = methylene (or methyl) protons two carbons away from the imine nitrogen; py_1 = the protons on the carbon adjacent to the pyridine nitrogen; pz_2 = protons in the 2 and 4 positions on the pyrazole ring; pz_3 = proton in the 3 position on the pyrazole ring; aza_2, aza_3, aza_6 = the protons on the 2,3 and 6 positions, respectively, on the 7-azaindole bridge. S = singlet, d = doublet, t = triplet, m = multiplet. If not listed in the Table, the multiplicity could not be determined due to broadness or overlapping of the peaks. [b]These peaks are assigned to the methyl groups attached to the pyrazole ring. [c]These peaks could not be discerned because of overlapping peaks and/or limited solubility.

Scheme II.

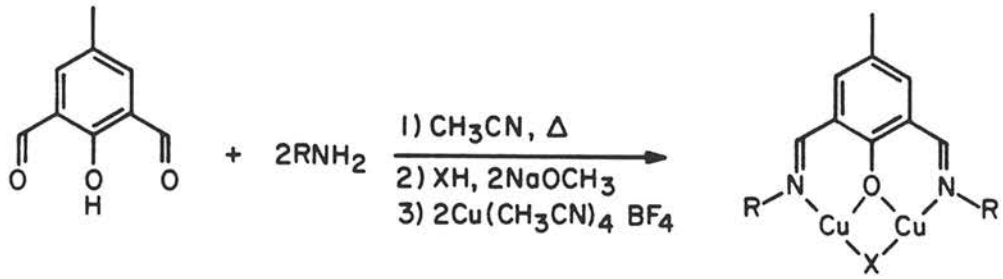

of all compounds showed the absence of aldehydic carbonyl and amine N-H stretches, consistent with complete imine condensation. The multitude of peaks in the region 700 - 1640 cm^{-1} made absolute assignments difficult.

Mass spectra were obtained for compounds 16, 19, 20, 21, and 22, each of which exhibits parent ion peaks in agreement with the formulation given above. The presence of two coppers in these compounds is indicated by three parent peaks due to the presence of both ^{63}Cu and ^{65}Cu. The relative intensities of these three peaks, averaged over all the compounds analyzed were 1:0.90:0.24 for $^{63}Cu_2L$:$^{63}Cu^{65}CuL$:$^{65}Cu_2L$ (theoretical ratio is 1:0.89:0.20).

The electronic absorption spectrum of $Cu_2^{I}ISOIM(EtPh)_2(pz)$, 15, shown in Figure 1 (curve B), is typical of the solution spectrum of all the binuclear copper(I) complexes examined. Spectra obtained in the solid state (nujol mulls) varied. The solid state spectrum of $Cu_2^{I}ISOIM(EtPh)_2(pz)$, 15, shown in Figure 1 (curve A), is typical of

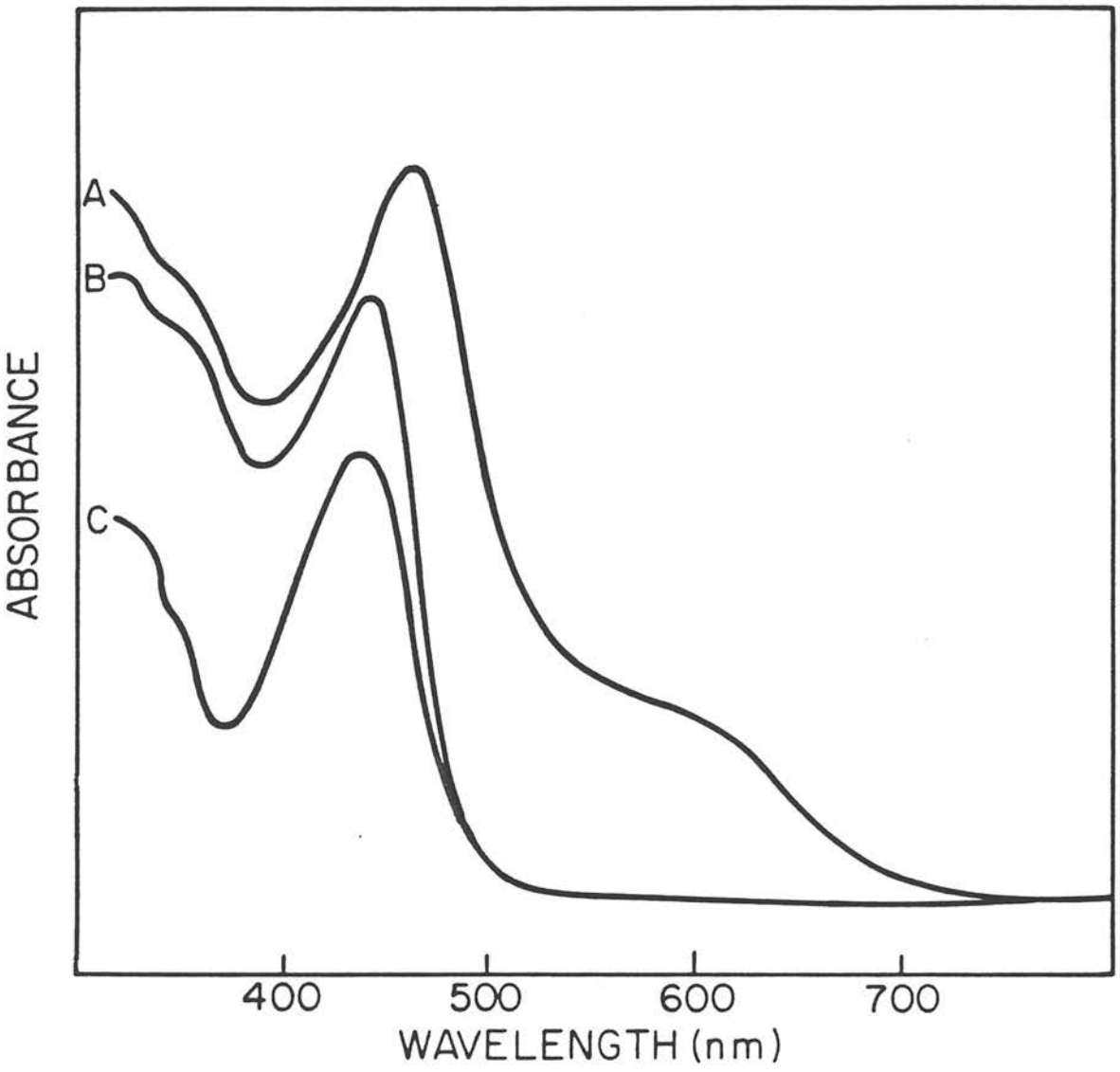

Figure 1. Electronic absorption spectra: (A), Cu^{I}_{2}ISOIM(EtPh)$_2$(pz), 15, in the solid state; (B), Cu^{I}_{2}ISOIM(EtPh)$_2$(pz), 15, in a hexane solution; and (C), Cu^{I}_{2}ISOIM(t-Bu)$_2$(pz), 20, in the solid state.

that for most compounds examined. Note that the absorption present in solution at 444 nm (ϵ = 8600) shifts to lower energies, ca. 464 nm, in the solid state. In addition a new absorption was found in the solid state spectrum at ca. 600 nm. The 600 nm absorption was not found in solution even in spectra of concentrated THF solutions, in which these compounds are considerably soluble.

Not all species examined exhibit the solid state spectrum described above. Compounds 19, 20, 21, and 22 exhibit solid state spectra as shown for $Cu_2^{I}ISOIM(t\text{-}Bu)_2(pz)$, 20, in Figure 1 (curve C), which can be compared to the solution spectra of all complexes. Under no conditions have compounds 19-22 shown notable absorption in the 600 nm region.

All cuprous compounds were shown to be diamagnetic by the presence of very sharp NMR resonances (see Figure 2). Table I lists the peaks observed for each complex. The assignments given were made by cross-comparisons of all the spectra. In each case, the identity of the organic entity is confirmed. Integration values were in agreement with the proposed structures.

Solution Reactivity. All compounds presented here are unreactive towards carbon monoxide. This was shown definitively for CO saturated solutions (CH_2Cl_2) of $Cu_2^{I}ISOIM(Etpy)_2(pz)$, 9, and $Cu_2^{I}ISOIM(1\text{-}Pr)_2(pz)$, 18, both of which show infrared absorptions in the region 1500-1650 cm^{-1}, characteristic of the original complex, 9 or 18, but neither show any bands in the region 1700-2200 cm^{-1} which would be attributable to a carbonyl complex. Also, evaporation of THF solutions of these compounds with a stream of CO gave the original compounds, as identified

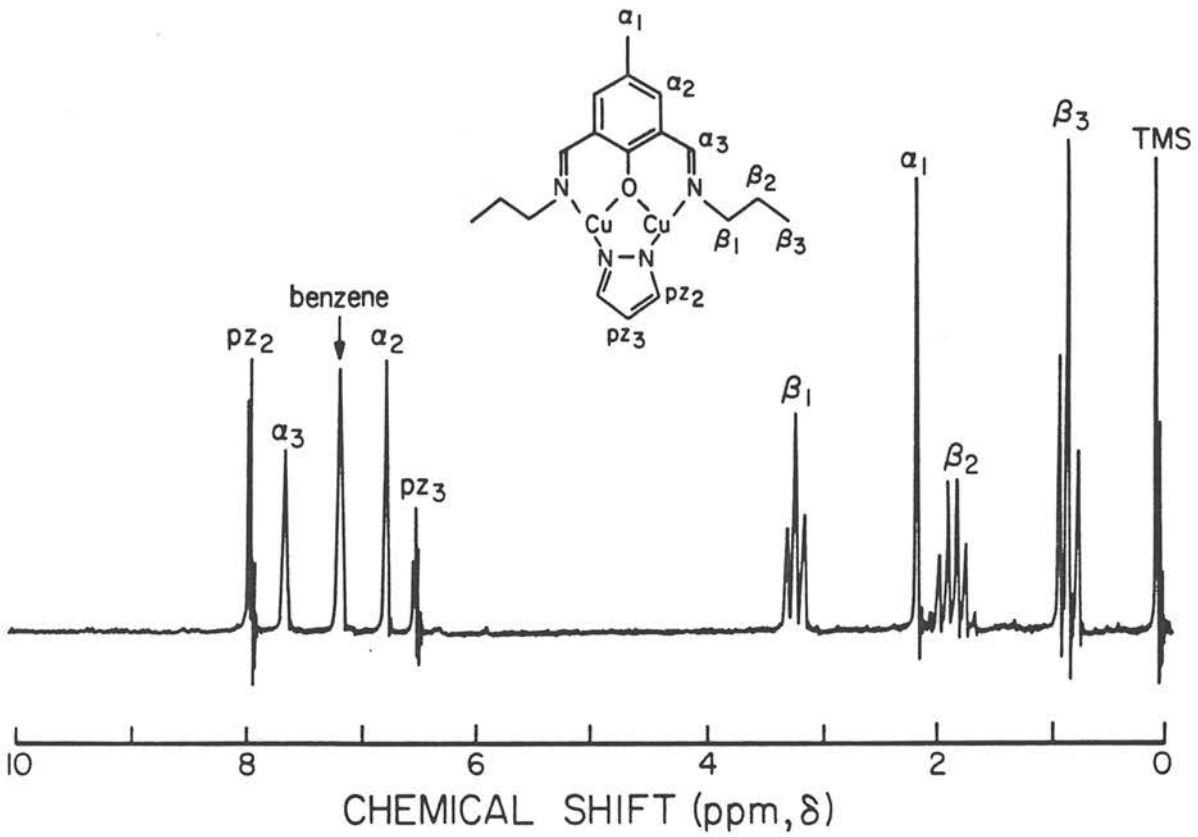

Figure 2. NMR spectrum of Cu^{I}_{2}ISOIM(1-Pr)$_2$(pz), 18, in d^6 benzene at 34° C.

by IR spectra.

All copper(I) compounds react with oxygen at the ambient temperature to form green or brown products from orange DMF solutions. This reaction could not be reversed by subsequent bubbling of argon through the solutions. The air sensitivity of these complexes prevented reliable solution molecular weight measurements.

Electrochemistry. All electrochemical results presented here were obtained in DMF solutions at a platinum indicating electrode. Ferrocene was used as an internal standard and all potentials have been converted to versus nhe using E^f = +0.40 mV vs. nhe for ferrocene.[16] The cyclic voltammograms for the Cu(II) compounds, 3-5, were irreversible as shown in Figure 3 for $Cu_2^{II}ISOIM(Mepy)_2(OH)^{2+}$, 3. Addition of one equivalent of pyrazole to the same solution, however, gave the quasi-reversible electrochemistry also shown in Figure 3.[17] Similar results were observed for $Cu_2^{I}ISOIM(Etpy)_2(OH)^{2+}$, 4. In contrast $Cu_2^{I}ISOIM(hist)_2(OH)^{2+}$, 5, gave very irreversible electrochemistry even with added pyrazole.

Constant potential electrolysis (cpe) of 3 plus an equivalent amount of pyrazole at -0.35 V and -0.70 V indicated that each wave corresponds to a one-electron process. No attempt was made to isolate a mixed valence species, but the binuclear cuprous complex, $Cu_2^{I}ISOIM(Mepy)_2(pz)$, 6, was synthesized by cpe of an acetonitrile solution containing $Cu_2^{II}ISOIM(Mepy)_2(OH)^{2+}$, 3, and an equivalent amount of pyrazole at -0.70 V (n = 2.0).

The cyclic voltammogram for $Cu_2^{I}ISOIM(Mepy)_2(pz)$, 6, was, of course, identical to that shown in Figure 3 for 3 plus one equivalent

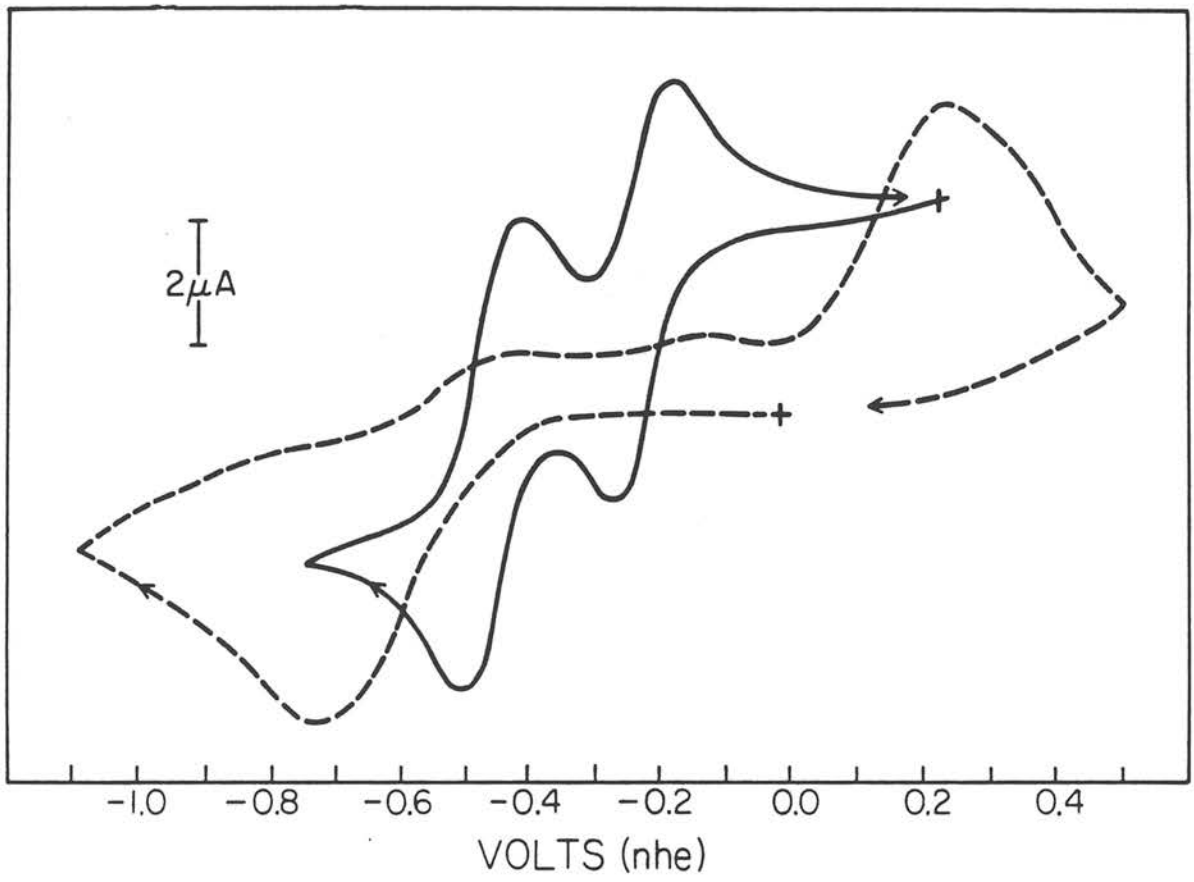

Figure 3. Cyclic voltammograms of DMF solutions: Cu^{II}_2-ISOIM(Mepy)$_2$(OH)$^{2+}$, 3, (----); Cu^{II}_2ISOIM(Mepy)$_2$(OH)$^{2+}$, 3, containing one equivalent of pyrazole (——). Both voltammograms were observed with a platinum electrode, using 0.1M TBAP as the electrolyte at a scan rate of 200 mV/sec.

of pyrazole. All binuclear copper(I) compounds presented in Table II exhibited cyclic voltammetry similar to the solid line in Figure 3; however, large peak separations (Ep_a-Ep_c = 100-150 mV at 50 mV/sec) were observed for many compounds at a platinum electrode.[18] Cyclic voltammetry at a hanging mercury drop electrode (HMDE) gave smaller peak separations (70-90 mV) for most compounds, and the formal potentials (E^f) were identical to those observed using a platinum electrode. The potentials recorded in Table II were determined at a platinum electrode because this electrode allowed direct comparison with the internal standard, ferrocene, on the same scan. It was found that the potentials could be read more accurately using differential pulse voltammetry, and this technique was employed to obtain the values presented in Table II. In all cases, the formal potentials were within 10 mV of the potentials observed by cyclic voltammetry. All compounds containing the 7-azaindole anion as the bridge exhibited irreversible electrochemistry, often showing two anodic waves but only ill-defined cathodic waves, and hence the electrochemistry of these species is not included here.

Constant potential electrolysis at a potential 200 mV more positive than the second oxidation peak was performed on compounds 6, 9, 10, 19, and 20, as typical Cu(I) species, and each gave a two-electron oxidation (n = 2.0 ± 0.1).

The average separation of the two formal potentials (E_1^f-E_2^f) is 194 ± 40 mV for all new compounds listed in Table II. From this value for E_1^f-E_2^f, the average comproportionation constant, K, is calculated to be 1.9×10^3 for the equilibrium in equation 3, where L represents the entire ligand system.[14] Note that all complexes containing a

Table II. Reduction Potentials for Binuclear Copper Complexes.[a]

$$Cu(II)Cu(II)L^{+2} + e^- \overset{E_1^f}{\rightleftharpoons} Cu(II)Cu(I)L^{+}$$

$$Cu(II)Cu(I)L^{+2} + e^- \overset{E_2^f}{\rightleftharpoons} Cu(I)Cu(I)L$$

No.	Compound	E_1^f [b]	E_2^f [b]	n[c]
1	$Cu(II)_2(ISOIM)_2(Pr)_2^{+2}$	-0.52[d]	-0.91[d]	-
6	$Cu(I)_2ISOIM(Mepy)_2(pz)$	-0.211	-0.452	2.0
7	$Cu(I)_2ISOIM(Mepy)_2(Me_2pz)$	-0.190	-0.374	-
9	$Cu(I)_2ISOIM(Etpy)_2(pz)$	-0.110	-0.344	2.0
10	$Cu(I)_2ISOIM(Etpy)_2(Me_2pz)$	-0.113	-0.267	2.0
12	$Cu(I)_2ISOIM(MePh)_2(pz)$	0 146	-0.081	-
13	$Cu(I)_2ISOIM(MePh)_2(Me_2pz)$	0.206	0.005	-
15	$Cu(I)_2ISOIM(EtPh)_2(pz)$	0.128	-0.078	-
16	$Cu(I)_2ISOIM(EtPh)_2(Me_2pz)$	0.205	0.009	-
18	$Cu(I)_2ISOIM(1\text{-}Pr)_2(pz)$	0.146	-0.076	-
19	$Cu(I)_2ISOIM(2\text{-}Pr)_2(pz)$	0.193	0.001	1.9
20	$Cu(I)_2ISOIM(t\text{-}Bu)_2(pz)$	0.240	0.053	2.0
21	$Cu(I)_2ISOIM(t\text{-}Bu)_2(Me_2pz)$	0.239	0.080	-
23	$Cu(I)_2ISOIM(Ph)_2(pz)$	0.144	-0.032	-
24	$Cu(I)_2ISOIM(PhNMe_2)_2(pz)$	0.146	-0.048	-
25	$Cu(I)_2ISOIM(PhCOMe)_2(pz)$	0.152	0.008	-

[a] These values were measured by differential pulse polarography in DMF using a platinum indicating electrode. [b] Potentials are given in volts vs. nhe. Potentials were measured vs. ferrocene as an internal redox couple then corrected to vs. nhe using a value of 0.40V for ferrocene vs. nhe. [c] These values for n were determined by constant potential electrolysis at a potential 200 mV more positive than E_1^f. Values are given for all complexes actually examined by cpe. [d] Reference 13.

$$Cu^{I}Cu^{I}L + Cu^{II}Cu^{II}L^{2+} \overset{K}{\rightleftharpoons} 2Cu^{II}Cu^{I}L^{+} \qquad (3)$$

3,5-dimethylpyrazolate bridge have smaller formal potential separations ($E_1^f - E_2^f$) and correspondingly smaller comproportionation constants than their pyrazolate bridged analogues.

Addition of excess pyridine (up to one hundred-fold excess) to the electrochemical solutions of 6, 12, and 13 did not cause a significant shift (< 10 mV) in the potentials, but merely broadened the peaks. Cyclic voltammetry of 6, 7, 9, and 10 in other solvents such as CH_2Cl_2, CH_3CN and THF, gave similar behavior to that observed in DMF, while the electrochemistry for all other compounds was irreversible in these alternative solvents.

Crystallographic Analysis

The crystal and molecular structure of $Cu_2^{I}ISOIM(Etpy)_2(pz)$, 9, was determined. Basic crystal data are summarized in Table III. Tables IV-VII present the atomic parameters and interatomic distances and angles. The atom labeling scheme is illustrated in Figure 4.

The bonds to the copper atoms are shown in Figure 4. Each copper is bound to three ligand atoms in what is almost a tee geometry, the largest angles being 167.6° (N1-Cu1-N3) and 170.7° (N2-Cu2-N4). The intramolecular copper-copper distance, 3.304 Å, is sufficiently long that any direct interaction is unlikely.

There still remains, however, the possibility of direct intermolecular interaction between copper atoms. The molecules form an

Table III. Basic Crystal Data for $Cu(I)_2ISOIM(Etpy)_2(py)$, 9.

$C_{26}H_{26}Cu_2N_6O$

FW = 565.6	V = 2502.3 (10) Å^3
space group $P2_1/c$ (No. 14)	Z = 4
a = 20.980 (4) Å	ρ_{calc} = 1.50 g cm^{-3}
b = 4.929 (1) Å	μ = 23.8 cm^{-1}
c = 24.773 (6) Å	$\lambda(CuK_\alpha)$ = 1.5418 Å
β = 102.38 (2)°	

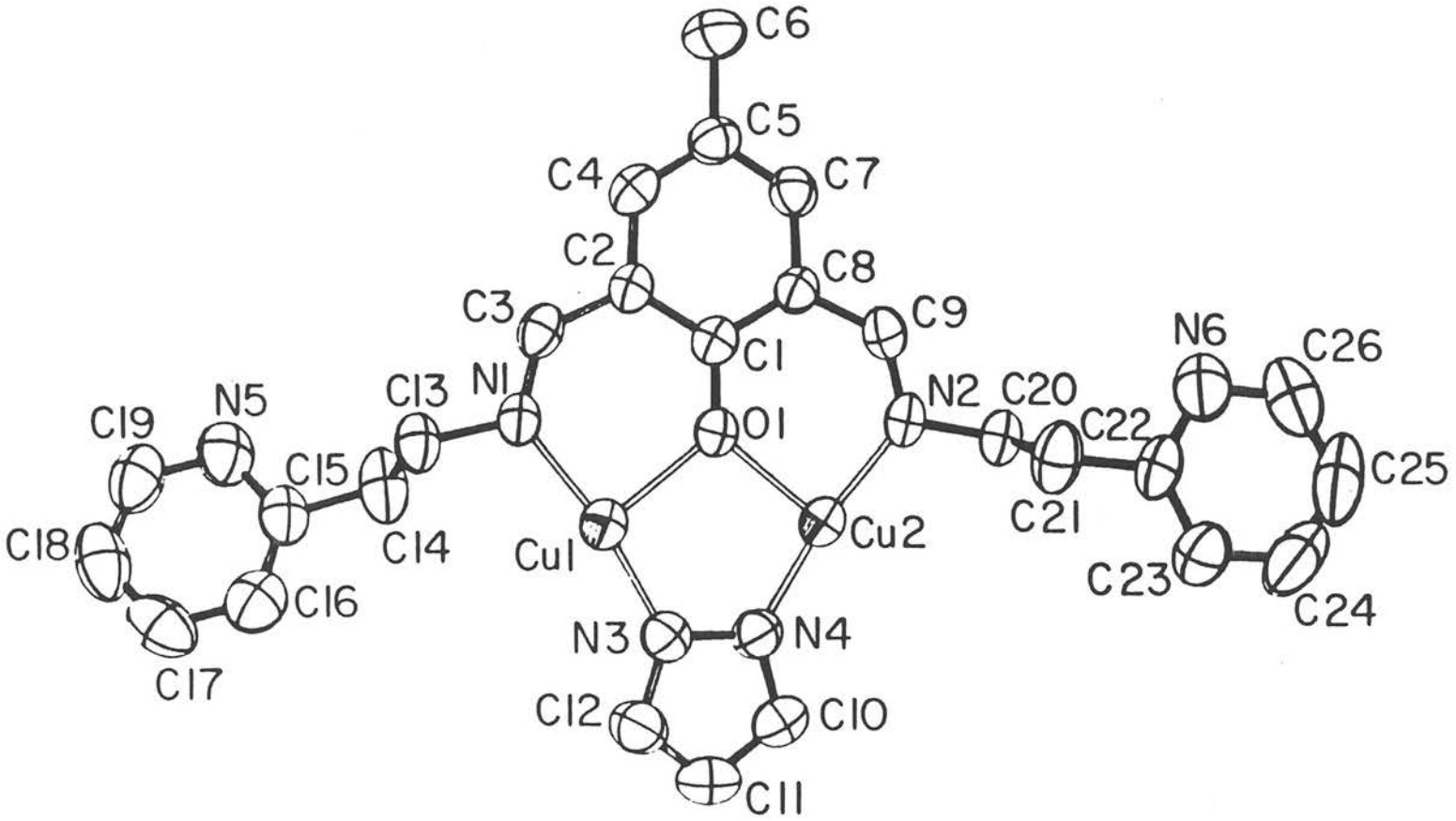

Figure 4. ORTEP drawing of Cu^{I}_{2}ISOIM(Etpy)$_2$(pz), 9, including atomic labeling scheme. Each hydrogen is given the same number as the carbon to which it is bound.

Table IV. Atomic Parameters and ESD's for $Cu(I)_2ISOIM(Etpy)_2(pz)$, 9.

	x[a]	y	z	U_{11}[b]	U_{22}	U_{33}	U_{12}	U_{13}	U_{23}
Cu1	23717(3)	124543(14)	37118(3)	535(4)	554(4)	607(4)	-53(4)	112(3)	54(4)
Cu2	18840(3)	70218(13)	42920(3)	492(4)	575(4)	585(4)	-82(4)	117(3)	26(4)
O1	2624(1)	9960(6)	4407(1)	51(2)	46(2)	51(2)	-8(2)	8(1)	6(2)
N1	3176(2)	14363(7)	3905(1)	56(2)	45(2)	50(2)	-7(2)	18(2)	2(2)
N2	2229(2)	5481(7)	4994(1)	51(2)	41(2)	58(2)	-4(2)	23(2)	3(2)
N3	1614(2)	10565(8)	3366(2)	57(2)	58(3)	63(3)	-3(2)	4(2)	9(2)
N4	1412(2)	8318(7)	3610(1)	51(2)	55(3)	62(2)	-3(2)	7(2)	1(2)
N5	4090(2)	18214(9)	2575(2)	89(3)	79(3)	64(3)	-4(3)	27(2)	-5(3)
N6	1383(2)	1473(10)	6244(2)	94(3)	90(4)	83(3)	-7(3)	31(3)	5(3)
C1	3161(2)	10007(8)	4783(2)	48(2)	41(3)	49(3)	-1(2)	14(2)	-6(2)
C2	3667(2)	11901(8)	4760(2)	47(2)	44(3)	50(2)	-4(2)	16(2)	-3(2)
C3	3633(2)	13920(9)	4330(2)	54(3)	46(3)	57(3)	-9(2)	22(2)	-10(2)
C4	4231(2)	11854(9)	5181(2)	45(2)	54(3)	65(3)	-4(2)	16(2)	-6(3)
C5	4326(2)	10099(10)	5624(2)	45(2)	65(3)	54(3)	-1(2)	10(2)	-7(3)
C6	4942(3)	10164(16)	6072(3)	55(3)	113(5)	78(4)	-5(3)	-2(3)	4(4)
C7	3833(2)	8315(10)	5645(2)	54(3)	61(3)	48(3)	1(2)	15(2)	1(2)
C8	3249(2)	8178(8)	5237(2)	45(2)	47(3)	46(2)	-5(2)	13(2)	-3(2)
C9	2784(2)	6107(9)	5313(2)	57(3)	54(3)	49(3)	3(2)	20(2)	5(2)
C10	868(2)	7395(12)	3265(2)	58(3)	74(4)	74(3)	-13(3)	5(3)	-4(3)
C11	719(3)	8962(12)	2806(2)	61(3)	90(4)	66(3)	1(3)	-7(8)	-6(3)
C12	1187(3)	10881(11)	2876(2)	76(3)	67(4)	67(3)	2(3)	0(3)	6(3)
C13	3289(3)	16574(9)	3531(2)	73(3)	44(3)	57(3)	-8(2)	22(2)	0(2)
C14	3398(3)	15393(11)	2997(2)	124(5)	56(3)	76(4)	-9(3)	47(3)	2(3)
C15	3480(2)	17556(10)	2591(2)	86(3)	55(3)	51(3)	-9(3)	23(3)	-6(3)
C16	2955(3)	18762(13)	2257(2)	83(4)	85(4)	72(4)	-11(3)	22(3)	-14(3)
C17	3054(3)	20797(13)	1894(2)	114(5)	87(4)	53(3)	16(4)	2(3)	-5(3)
C18	3670(4)	21466(12)	1877(2)	148(6)	72(4)	60(3)	-7(4)	43(4)	0(3)
C19	4166(3)	20198(13)	2217(3)	92(4)	85(4)	80(4)	-20(4)	37(3)	-8(4)
C20	1866(2)	3367(9)	5219(2)	56(3)	50(3)	62(3)	-9(2)	22(2)	4(2)
C21	1377(3)	4646(11)	5507(3)	71(3)	63(3)	99(4)	6(3)	45(3)	7(3)
C22	1030(2)	2604(10)	5789(2)	60(3)	62(3)	75(3)	-7(3)	35(3)	-5(3)
C23	392(3)	2021(15)	5593(2)	63(3)	106(5)	87(4)	-4(4)	27(3)	0(4)
C24	98(3)	119(17)	5871(3)	77(4)	147(7)	131(6)	-45(5)	46(4)	-36(6)
C25	443(4)	-1058(15)	6319(3)	136(6)	114(6)	119(6)	-39(5)	85(5)	-11(5)
C26	1070(4)	-366(14)	6499(3)	145(6)	94(5)	77(4)	0(5)	44(4)	14(4)

	x	y	z	B, Å²		x	y	z	B, Å²
H3	401(2)	1530(8)	438(2)	5.00	H14'	378(2)	1416(10)	310(2)	7.20
H4	451(2)	1324(8)	517(2)	5.10	H16	256(2)	1839(9)	228(2)	7.00
H6	502(2)	1180(10)	623(2)	8.00	H17	268(2)	2170(9)	166(2)	7.70
H6'	529(2)	1008(11)	595(2)	8.00	H18	376(2)	2302(9)	166(2)	7.30
H6''	495(2)	864(10)	628(2)	8.00	H19	460(2)	2057(9)	224(2)	7.40
H7	385(2)	693(8)	592(2)	5.00	H20	215(2)	213(8)	548(2)	5.30
H9	291(2)	506(8)	565(2)	5.10	H20'	164(2)	216(8)	493(2)	5.30
H10	69(2)	577(9)	338(2)	6.10	H21	108(2)	554(9)	522(2)	6.30
H11	38(2)	879(9)	253(2)	6.60	H21'	156(2)	587(9)	577(2)	6.30
H12	125(2)	1252(9)	268(2)	6.70	H23	15(2)	295(9)	527(2)	7.00
H13	362(2)	1758(8)	371(2)	5.40	H24	-36(2)	-46(10)	573(2)	9.10
H13'	288(2)	1786(8)	346(2)	5.40	H25	25(2)	-242(10)	652(2)	8.50
H14	298(2)	1442(10)	283(2)	7.20	H26	135(2)	-113(10)	682(2)	9.10

[a] Fractional coordinates have been multiplied by factors of 10^5 for the copper atoms, 10^4 for the remaining nonhydrogen atoms, and 10^3 for the hydrogen atoms. U_{ij} has been multiplied by 10^4 for the copper atoms and 10^3 for the remaining nonhydrogen atoms. [b] The form of the thermal ellipsoid is $\exp[-2\pi^2(U_{11}h^2a^{*2}+\cdots+2U_{23}klb^*c^*)]$ for the anisotropic thermal parameters.

Table V. Bond Distances (Å) for $Cu(I)_2ISOIM(Etpy)_2(pz)$, 9.

Cu1-O1	2.089 (2)	C16-C17	1.391 (8)
Cu1-N1	1.901 (3)	C17-C18	1.344 (8)
Cu1-N3	1.882 (3)	C18-C19	1.345 (9)
Cu2-O1	2.097 (2)	C20-C21	1.508 (7)
Cu2-N2	1.894 (3)	C21-C22	1.499 (7)
Cu2-N4	1.878 (3)	C22-C23	1.354 (7)
O1-C1	1.300 (4)	C23-C24	1.385 (9)
N1-C3	1.281 (5)	C24-C25	1.322 (11)
N1-C13	1.482 (5)	C25-C26	1.339 (10)
N2-C9	1.296 (5)	C3-H3	1.03 (4)
N2-C20	1.469 (5)	C4-H4	0.90 (4)
N3-N4	1.372 (5)	C6-H6	0.90 (5)
N3-C12	1.355 (6)	C6-H6'	0.85 (5)
N4-C10	1.349 (6)	C6-H6''	0.90 (5)
N5-C15	1.330 (6)	C7-H7	0.96 (4)
N5-C19	1.353 (7)	C9-H9	0.96 (4)
N6-C22	1.331 (6)	C10-H10	0.95 (4)
N6-C26	1.354 (8)	C11-H11	0.88 (4)
C1-C2	1.424 (5)	C12-H12	0.96 (4)
C1-C8	1.421 (5)	C13-H13	0.89 (4)
C2-C3	1.449 (5)	C13-H13'	1.05 (4)
C2-C4	1.399 (5)	C14-H14	1.01 (5)
C4-C5	1.378 (6)	C14-H14'	0.99 (5)
C5-C6	1.513 (7)	C16-H16	0.87 (4)
C5-C7	1.366 (6)	C17-H17	0.98 (5)
C7-C8	1.413 (5)	C18-H18	0.98 (4)
C8-C9	1.453 (6)	C19-H19	0.91 (5)
C10-C11	1.355 (7)	C20-H20	0.99 (4)
C11-C12	1.348 (7)	C20-H20'	0.97 (4)
C13-C14	1.507 (7)	C21-H21	0.95 (4)
C14-C15	1.501 (7)	C21-H21'	0.90 (4)
C15-C16	1.363 (7)	C23-H23	0.97 (4)
		C24-H24	0.99 (5)
		C25-H25	0.97 (5)
		C26-H26	0.96 (5)

Table VI. Bond Angles (deg.) for $Cu(I)_2ISOIM(Etpy)_2(pz)$, 9.

O1-Cu1-N1	91. 7 (1)	C4-C5-C6	121. 8 (4)
O1-Cu1-N3	97. 1 (1)	C4-C5-C7	116. 9 (4)
N1-Cu1-N3	167. 6 (2)	C6-C5-C7	121. 3 (4)
O1-Cu2-N2	91. 5 (1)	C5-C7-C8	123. 4 (4)
O1-Cu2-N4	96. 8 (1)	C1-C8-C7	118. 8 (4)
N2-Cu2-N4	170. 7 (2)	C1-C8-C9	124. 8 (4)
Cu1-O1-Cu2	104. 2 (1)	C7-C8-C9	116. 4 (4)
Cu1-O1-C1	127. 5 (3)	N2-C9-C8	129. 0 (4)
Cu2-O1-C1	127. 7 (3)	N4-C10-C11	110. 6 (5)
Cu1-N1-C3	126. 1 (3)	C10-C11-C12	105. 2 (5)
Cu1-N1-C13	117. 3 (3)	N3-C12-C11	110. 0 (5)
C3-N1-C13	116. 6 (4)	N1-C13-C14	109. 8 (4)
Cu2-N2-C9	125. 5 (3)	C13-C14-C15	112. 1 (5)
Cu2-N2-C20	120. 4 (3)	N5-C15-C14	116. 2 (4)
C9-N2-C20	114. 1 (4)	N5-C15-C16	122. 2 (5)
Cu1-N3-N4	120. 6 (3)	C14-C15-C16	121. 5 (5)
Cu1-N3-C12	133. 1 (3)	C15-C16-C17	119. 6 (5)
N4-N3-C12	106. 3 (4)	C16-C17-C18	118. 4 (6)
Cu2-N4-N3	121. 2 (3)	C17-C18-C19	119. 1 (6)
Cu2-N4-C10	131. 8 (3)	N5-C19-C18	124. 3 (6)
N3-N4-C10	107. 0 (4)	N2-C20-C21	110. 1 (4)
C15-N5-C19	116. 4 (4)	C20-C21-C22	112. 8 (4)
C22-N6-C26	115. 9 (5)	N6-C22-C21	116. 0 (4)
O1-C1-C2	121. 5 (4)	N6-C22-C23	123. 0 (5)
O1-C1-C8	120. 2 (4)	C21-C22-C23	121. 1 (5)
C2-C1-C8	118. 4 (4)	C22-C23-C24	118. 4 (6)
C1-C2-C3	124. 0 (4)	C23-C24-C25	119. 5 (7)
C1-C2-C4	118. 6 (4)	C24-C25-C26	119. 3 (7)
C3-C2-C4	117. 4 (4)	N6-C26-C25	123. 8 (7)
N1-C3-C2	129. 2 (4)		
C2-C4-C5	124. 0 (4)		

Table VII. Nonbonding Distances and Associated Angles for $Cu(I)_2ISOIM(Etpy)_2(pz)$, 9.

Cu1-Cu2 ‡	3. 3036 (4)	Cu1-Cu2^{+}	2. 9685(4)
Cu1-H13'‡	2. 64 (4)	Cu2-H20''$^{+}$	3. 09 (4)
O1-Cu1-Cu2^{+}	95. 7 (1)	O1-Cu2-Cu1‡	105. 5 (1)
N1-Cu1-Cu2^{+}	83. 2 (1)	N2-Cu2-Cu1‡	92. 1 (1)
N3-Cu1-Cu2^{+}	104. 5 (1)	N4-Cu2-Cu1‡	89. 6 (1)

$^{+}$ Translated by one unit cell in positive y direction

‡ Translated by one unit cell in negative y direction

infinite stack in the direction of the b axis, a section of which is shown in Figure 5. Although the separation between molecules in the direction of the b axis is 4.929 Å (just the length of the b axis), the molecule is far from perpendicular to this axis, the angle between the axis and the mean molecular plane being 41°. Thus, "overlapping" portions of neighboring molecules come rather close to one another. The average distance of atoms O1, C1, C8, C9, and N2 from the mean plane of atoms N1, C3, C2, C1, and O1 in the neighboring molecule just below is 3.20 Å. This is somewhat shorter than the separation usually observed between stacked π-delocalized molecules.[19] The intermolecular copper-copper distance is shorter yet, at 2.968 Å.

A least squares plane calculation including the atoms of the benzene ring, the methyl carbon, and the phenolic oxygen shows these atoms to be coplanar, with no deviation from the mean plane exceeding 0.009 Å. The deviations of the copper atoms from this plane are 0.04 Å for Cu1 and 0.29 Å for Cu2. In each case the direction of the out-of-plane separation is that which reduces the intermolecular copper-copper distance. Each of the two C=N groups is also twisted slightly out of plane in the direction of the copper atom to which it is bound (deviations: 0.04 Å for C3, 0.05 Å for N1, 0.04 Å for C9 and 0.10 Å for N2).

The atoms of the pyrazolate group are coplanar with no deviation from the mean plane exceeding 0.006 Å. The benzene and pyrazole rings are not quite coplanar, the dihedral angle being 170(3)°.

There is also a slight deviation of each copper atom from the plane defined by the three atoms to which it is bound. These deviations

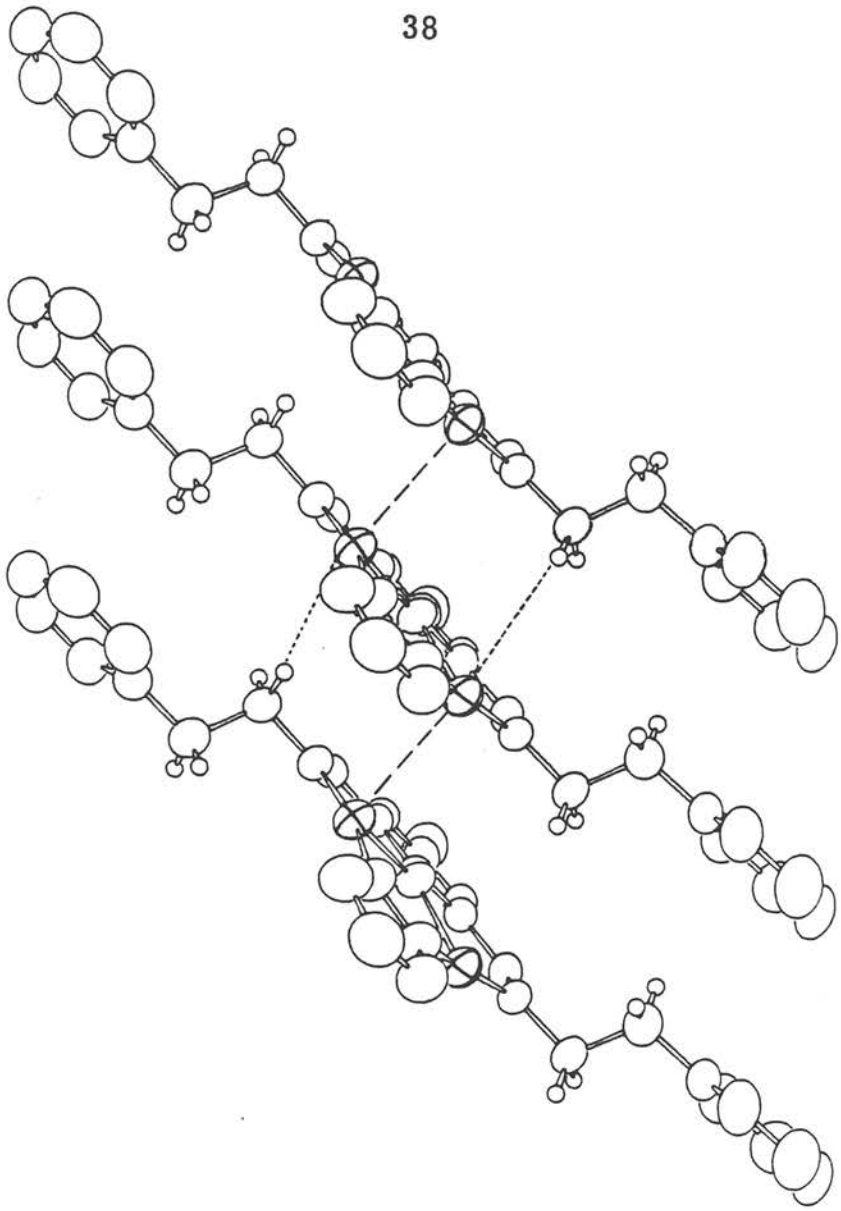

Figure 5. Crystal packing of Cu^{I}_{2}ISOIM(Etpy)$_2$(pz), 9, showing a section of an infinite stack of molecules which forms in the solid state. The three molecules are corresponding ones from three different unit cells, translated along the b axis (which lies in the vertical direction in the orientation of this figure). All copper atoms lie in the same plane, parallel to the page. The pyrazolate groups are directed out of the page, toward the reader. The shortest copper-copper distance, 2.97 Å, occurs between atoms in neighboring molecules, connected by dashed lines in the figure. The two dotted lines correspond to two different intermolecular Cu-H distances, 2.64 Å (Cu1-H13′) and 3.09 Å (Cu2-H20′).

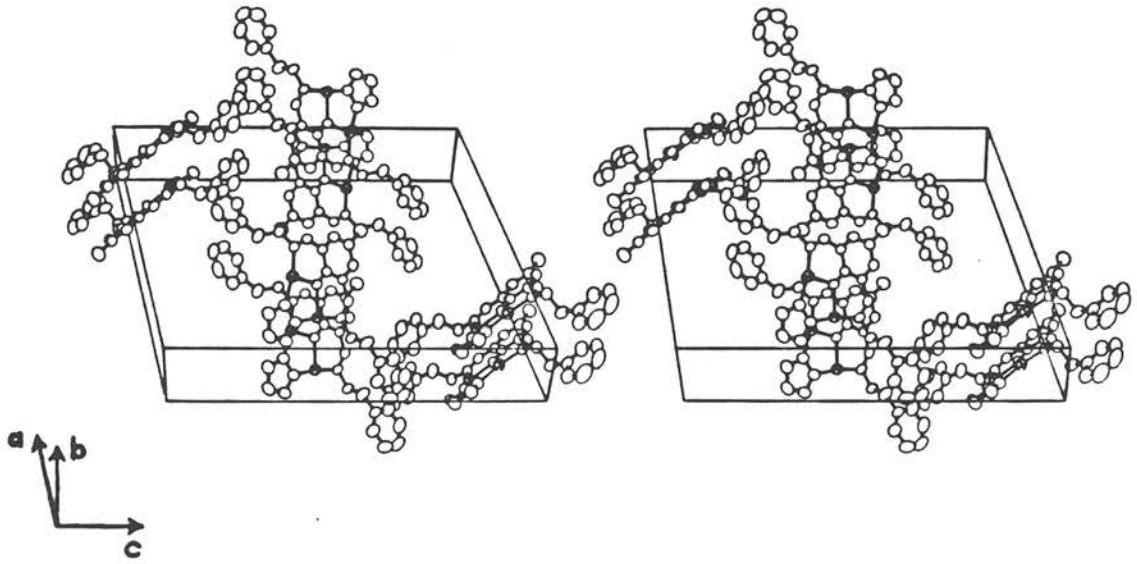

Figure 6. Stereoview illustrating crystal packing of Cu^{I}_{2}ISOIM(Etpy)$_2$(pz), 9. The molecules depicted comprise more than one unit cell, although the edges of only one cell are shown.

are 0.14 Å for Cu1 and 0.06 Å for Cu2. Again, in each case the direction of the out-of-plane separation is that which reduces the intermolecular copper-copper distance.

It should be noted that a possible attraction for another copper atom is not the only factor favoring this direction for the out-of-plane separation. As shown in Figure 5, there is a hydrogen atom on the opposite side of each copper atom, and in the case of Cu1 this hydrogen is at a distance of 2.64 Å. (This is also the copper that is farther out of its donor-atom plane.) Thus, at least for Cu1, copper-hydrogen steric interactions may influence the out-of-plane displacement of the copper ion.

A final point which should be noted concerning the coordination about copper is that the copper-nitrogen bonds are shorter than most which have been reported for Cu(I) complexes with nitrogen donor ligands.[22] The average lengths are 1.88 Å for the copper-pyrazole nitrogen bonds and 1.90 Å for the copper-imine nitrogen bonds. The copper-oxygen distances are substantially longer than this, averaging 2.09 Å. Also, as stated previously, the N-Cu-N bond angles approach 180° (167.6° and 170.7°). These factors may suggest some degree of two-coordinate character, which may be related to the unusual chemical behavior of the compound (e.g., unreactivity toward CO).

Discussion

The rather negative reduction potentials observed for complex 1 (equations 1 and 2) likely result from a square-planar arrangement of "hard" oxygen and nitrogen ligands.[25] The complexes reported here

were designed to stabilize copper(I) in an attempt to better model binuclear copper protein sites. For example, the condensation of 2-hydroxy-5-methylisopthalaldehyde with 2-aminomethylpyridine resulted in the binucleating ligand in 3, which is more flexible than the ligand system in 1 and also presents relatively soft pyridines for coordination. Two additional binucleating ligands providing even greater flexibility were obtained using 2-(2'-aminoethyl)pyridine and histamine, and these ligands reacted readily with copper(II) salts to yield the binuclear copper(II) complexes 4, and 5. Complexes similar to 4 and 5 were reported during the course of the present study.[26]

In all three copper(II) complexes, both copper atoms are presumably bound to an aromatic nitrogen. This has been demonstrated by an X-ray structure determination of $Cu_2^{II}ISOIM(hist)_2(OH)^{2+}$, 5.[27] Each copper(II) is actually five-coordinate with one of the copper atoms bound to the oxygen of a water molecule and the other copper bound to the oxygen of the hydroxy bridge of an adjacent molecule.

The electrochemistry of these non-macrocyclic complexes, 3-5, is irreversible as shown in Figure 3 for $Cu_2^{II}ISOIM(Mepy)_2(OH)^{2+}$, 3. This may be a result of the relatively labile hydroxy bridge, which is a poor ligand for copper(I). The introduction of pyrazole did produce reversible electrochemical behavior, also shown in Figure 3, leading to the isolation of a stable binuclear copper(I) complex, $Cu_2^{I}ISOIM-(Mepy)_2(pz)$, 6, by constant potential electrolysis (n = 2).[17] The reduction potentials observed for $Cu_2^{I}ISOIM(Mepy)_2(pz)$, 6, ($E_1^f$ = -0.21 V, E_2^f = -0.45 V) were appreciably more positive than those observed for the macrocyclic complex, 1, indicating that the binucleating ligand in

6 does indeed provide a better environment for copper(I) relative to copper(II).

The copper(I) compound Cu_2^{I}ISOIM(Mepy)$_2$(pz), 6, was also synthesized directly from cuprous starting materials. Similar reactions with 2-aminomethylpyridine or 2-(2'-aminoethyl)pyridine as sidearms and with pyrazole, 3,5-dimethylpyrazole or 7-azaindole as bridging ligands gave complexes 7-11. The coordination environment around each copper(I) of these complexes was expected to be a tetrahedral arrangement of one oxygen and three nitrogen ligands. The crystallographic results presented herein for Cu_2^{I}ISOIM(Etpy)$_2$(pz), 9, did not yield the expected structure. The sidearm pyridine nitrogen atoms are not coordinated. The overall coordination about copper approximates trigonal pyramidal, with a long, axial, copper-copper interaction with Cu^{I}-Cu^{I} = 2.97 Å. Copper(I)-copper(I) interactions with metal separations as short as 2.45 Å are known, but in all previously characterized species having proposed Cu^{I}-Cu^{I} interactions there is at least one bridging ligand between the two interacting copper atoms.[28] It is reasonable to assume that the structures of the analogous species, 6-11, are similar to this structure found for Cu_2^{I}ISOIM(Etpy)$_2$(pz), 9.

The structure of Cu_2^{I}ISOIM(Etpy)$_2$(pz), 9, suggested the synthesis of a series of compounds which had no donor atoms on the sidearms (R), i.e., complexes 12-25, Table I. These compounds also proved to be crystalline compounds, stable in the absence of dioxygen. Since the polydentate ligand systems employed provide only three-coordination for each copper, these compounds are presumed to be three-coordinate in solution.

All compounds which have non-bulky sidearms are brown in the solid state, this color being due, in part, to a 600 nm band observed in the solid state nujol mull spectrum (Curve A in Figure 1). This band is not present in the spectrum of the complex with t-butyl sidearms, $Cu_2^{I}ISOIM(t\text{-}Bu)_2(pz)$, 20, which is red in the solid state as well as in solution (Curve C, in Figure 1). This 600 nm band may be attributed to the intermolecular copper-copper interaction which may be inhibited by the presence of large t-butyl sidearms. This copper-copper interaction appears to be only a solid state phenomenon, since the 600 nm band was not found in solution spectra, even in very concentrated solutions.

This novel dimerization of d^{10} copper(I) centers may be closely related to the dimerization observed for rhodium(I), d^8, isocyanide complexes.[29] The intermolecular bonding of $Rh(CNPh)_4^+$ monomers results from the mixing of higher energy orbitals with the lower energy (filled) d orbitals, resulting in overall stabilization. These bonding interactions give rise to an electronic absorption at lower energy than the original monomer transition. Similarly, the 600 nm absorption observed in the solid state for $Cu_2^{I}ISOIM(EtPh)_2(pz)$, 15, is lower in energy, compared to the 440 nm absorption observed for the same compound in solution (Figure 1). Note that in the solid state, the higher energy band is at 460 nm. This shift from solution to solid state and the asymmetric nature of the 440 nm solution band suggest that this solution absorption is due to several transitions, one of which may be shifted to lower energy (600 nm) upon interaction with another copper(I). Complexes with apparent copper(I)-copper(I) interactions

have not been reported to exhibit notable electronic absorption spectra. Exact assignments of the electronic absorption spectral bands in the copper(I) complexes reported herein await further studies.

The solution structure of $Cu_2^{I}ISOIM(Etpy)_2(pz)$, 9, appears to be similar to that found in the solid state with the absence of the intermolecular Cu-Cu interaction. The pyridine nitrogens do not appear to be bound in benzene solution, since the NMR resonance for the proton on the carbon adjacent to the pyridine nitrogen (py_1, Table I) of $Cu_2^{I}ISOIM(Etpy)_2(pz)$, 9, occurs at the same position, within experimental error, as the corresponding proton from 2-(2'-aminoethyl)-pyridine (i.e., 8.44 ± 0.02 ppm δ from TMS). In fact, all compounds which contain pyridine on the sidearms exhibit this resonance at the same position within experimental error (i.e., 8.42 ± 0.04 ppm δ from TMS). The resonance of this proton would be expected to shift downfield upon binding to a copper(I) ion. This effect has been observed for the proton in the 2 position of an imidazole ring, which shifts by 0.4 - 0.7 ppm downfield upon binding copper(I) to the imidazole ring.[30] Sharp resonances were observed for the pyrazole protons of these compounds (for instance, the doublet at 7.87 ppm and the triplet at 6.43 ppm in Figure 2). This indicates that there is no equilibrium between bound and unbound pyrazole, and hence the pyrazolate bridge must be totally bound to the copper(I) ions or totally dissociated in benzene solutions (unlikely, at best). The 7-azaindolate bridge also appears to be completely bound to the copper ions in benzene solutions, since the resonances for the β_2 aliphatic hydrogens (on the sidearms) are split by the unsymmetric bridge (for instance, compound 22 in

Table I). Also, the resonances found for the 7-azaindolate protons are very sharp peaks, indicating that no dissociation equilibrium is occurring.

The new copper(I) compounds serve as an interesting series for electrochemical comparisons. Several trends can be observed in Table II. In the following discussion, the formal potentials for the second reduction, (E_2^f), equation 4, will be used since these processes

$$Cu^{II}Cu^{I}L^{+} + e^{-} \overset{E_2^f}{\rightleftharpoons} Cu^{I}Cu^{I}L \qquad (4)$$

were more reversible and slightly more systematic than the E_1^f potentials. The general trends, however, are the same with both processes.

The first point of interest is the effect of possible binding sites (i.e., pyridine) in the sidearms. The following series of potentials (E_2^f) was observed: Cu_2^IISOIM(EtPh)$_2$(pz), 15, (-0.078 V) $\approx$ Cu_2^IISOIM(MePh)$_2$(pz), 12, (-0.081 V) $\gg$ Cu_2^IISOIM(Etpy)$_2$(pz), 9, (-0.344 V) $>$ Cu_2^IISOIM(Mepy)$_2$(pz), 6, (-0.452 V). This indicates that the complexes containing the pyridine rings provide a more favorable environment for copper(II) relative to copper(I) when compared to their benzene ring analogues. Since the pyridine nitrogens do not appear to be bound to the copper(I) ions (in solution or in the solid state), the effect of these pyridine rings must be largely on the oxidized copper(II) sites. Hence, it appears that the pyridines bind to the copper ions upon oxidation, 26, and dissociate from copper(I) upon reduction, 9, Scheme III. Recall that in the similar cupric complex,

$Cu_2^{II}ISOIM(hist)_2(OH)^{2+}$, 5, the imidazole nitrogens were shown to be coordinated in the solid state X-ray structure.[27] It is reasonable that sidearm pyridine nitrogens would also coordinate to copper(II). The above series also indicates that the methyl pyridine sidearm provides a better environment for copper(II) than does the ethyl pyridine sidearm. This may be a result of the geometry of the sidearms and their relative ability to bind to the copper(II) centers.

Scheme III.

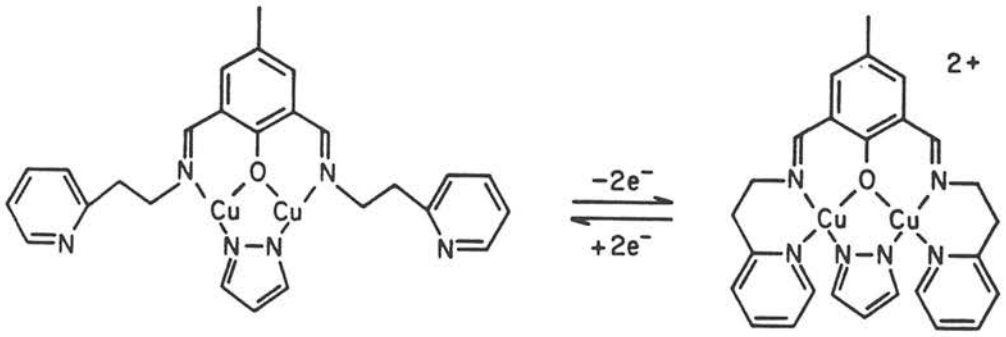

9 26

The introduction of methyl substituents on the pyrazolate bridges causes an increase in the reduction potential (E_2^f) as follows: $Cu_2^{I}ISOIM(Mepy)_2(Me_2pz)$, 7, (-0.374 V) > $Cu_2^{I}ISOIM(Mepy)_2(pz)$, 6, (-0.452 V) and $Cu_2^{I}ISOIM(MePh)_2(Me_2pz)$, 13, (+0.005 V) > $Cu_2^{I}ISOIM(MePh)_2(pz)$, 12, (-0.081 V). An inductive effect of the methyl groups would stabilize copper(II) relative to copper(I), but the reverse trend is actually observed. The steric bulk of the methyl

groups may be responsible for the relative destabilization of copper(II). These methyl groups may inhibit the binding of both pyridine (from the sidearms) and DMF (solvent) to the oxidized copper(II) ions by partially blocking the fourth, square-planar binding site around each copper(II). Also, shielding the copper centers from the solvent molecules with hydrophobic groups (such as these methyls) may not allow the polar DMF molecules to efficiently solvate the charged copper(II) species. Relative stabilization of copper(I) also results from more bulky sidearms, as reflected in the following series (E_2^f): Cu_2^IISOIM($\underline{t}$-Bu)$_2$(pz), 20, (+0.053 V) > Cu_2^IISOIM(2-Pr)$_2$(pz), 19, (+0.001 V) > Cu_2^IISOIM(1-Pr)$_2$(pz), 18, (-0.076 V).

Finally, an electronic effect on E_2^f is observed in the series of compounds which have phenyl rings bonded directly to the imine nitrogens: Cu_2^IISOIM(PhCOMe)$_2$(pz), 25, (+0.008 V) > Cu_2^IISOIM(Ph)$_2$(pz), 23, (-0.032 V) > Cu_2^IISOIM(PhNMe$_2$)$_2$(pz), 24, (-0.048 V). Here, the electron withdrawing carbonyl substituent results in relative copper(II) stabilization. Similar effects of remote substituents have been reported recently for a series of mononuclear copper(II) complexes.[10]

The oxidation/reduction of these compounds in two one-electron steps was the expected behavior for two interacting metal centers.[14,32] This sequential behavior has been observed for the series of binuclear complexes, 27, recently investigated in our laboratories.[33] Stepwise oxidation/reduction was also found for many ruthenium(II) dimers, in which closer proximity and greater interactions between the ruthenium centers correlates with a greater separation of the two redox

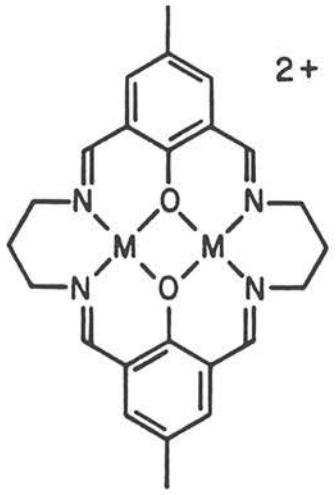

M = Mn, Fe, Co, Ni, Cu

27

processes (and larger comproportionation constants).[34] That all the new complexes exhibit two one-electron redox waves further suggests that the binuclear compounds are monomeric in solution. Oligomerization would probably result in intermolecular copper-copper interactions leading to more complex electrochemical behavior. Even the complexes with t-butyl sidearms, which were designed to inhibit intermolecular interactions, show electrochemical behavior similar to all other compounds. It thus seems likely that all new complexes have comparable solution structures, the most probable having three-coordinate copper(I).

The average comproportionation constant found for the binuclear copper complexes in this study (from Table II) was $K = 1.9 \times 10^3$, which is smaller than that found for the macrocyclic binuclear copper complex, 1 ($K = 4 \times 10^6$).[14] This is reasonable since the lower value was observed for the present copper(I) compounds which contain one

pyrazolate type bridge and one phenoxide bridge, compared to two phenoxide bridges between the coppers in 1. The pyrazolate bridge is expected to result in a larger Cu-Cu distance and smaller intramolecular copper interactions. The oxidized binuclear copper(II) complexes with bridging pyrazolate, such as 26, Scheme III, were not isolated in the present study, but the relative effects of alkoxide vs. pyrazolate bridges on metal interactions have been demonstrated in similar binuclear copper(II) compounds, and the trend was the same as found here.[35]

The non-reactivity of the copper(I) complexes in the present study toward carbon monoxide is an addition to the confusing phenomenon of carbon monoxide binding to copper(I) complexes. In general, copper(I) complexes have been found to bind CO if a fourth coordination site is available.[12,31,36] On the other hand, most four-coordinate copper(I) compounds do not bind CO, with the exception of several square-planar, four-coordinate complexes which bind CO as a fifth ligand.[13-15] Obviously, the geometry and type of ligands around copper(I) affect the CO binding ability for copper(I). The nature of these effects, however, remains obscure.

Biological Implications

It may not be valid to compare exact reduction potentials of simple metal complexes with those of corresponding protein systems due to varying solvation effects.[37] Nonetheless, analysis of trends or comparisons of approximate potentials may be useful. Within this context the high reduction potentials observed for binuclear copper

protein sites have been "mimicked" by the binuclear copper complexes presented in this study. Hence, it is not unreasonable to believe that these proteins utilize only oxygen and/or nitrogen ligands around each copper. Indeed, a three-coordinate copper-ligand environment can be considered for the reduced form of the binuclear site. The non-reactivity of the new compounds towards CO is in contrast to hemocyanin. This does not preclude a three-coordinate reduced binuclear site, since some three-coordinate copper(I) complexes have been shown to bind CO.[12,31,36]

The oxidation/reduction of these compounds in well separated one-electron steps, contrasts with the available electrochemical information on the binuclear protein sites. While no electrochemical data are available on hemocyanin, for both laccase and tyrosinase, a single potential has been associated with the overall two-electron reduction of the binuclear copper site.[6,7,38] Correlations between the electrochemical behavior of the new compounds, 6-25 and of the proteins is difficult due to solvation effects, the different techniques employed, possible non-equilibria in the proteins, etc.[37,38] Nonetheless, the electrochemical behavior reported for the new compounds suggests that the two-electron reduction of laccase and of tyrosinase is probably not a simple reduction of two equivalent copper ions strongly interacting through bridging ligands.

Conclusions

Stable binuclear copper(I) complexes have been prepared using binucleating ligands. Several of the new complexes exhibit copper-copper interactions in the solid state, as suggested by a peculiar visible absorption spectrum. This was confirmed for Cu_2^IISOIM-(Etpy)$_2$(pz), 9, via a complete molecular structure determination. In addition to the copper-copper interaction each copper(I) is bound to one oxygen and two nitrogen ligands. In solution all the new cuprous complexes likely contain three-coordinate copper, which appears to be a quite stable environment for copper(I).

All new complexes exhibit two one-electron redox processes, at well defined potentials. The highest reduction potentials were observed for complex 21 in which the copper(I) centers are somewhat buried within the hydrophobic substituents. With reduction potentials of $E_1^f = 0.239$ V and $E_2^f = 0.080$ V, the ligand environment in 21 represents a substantial improvement on the original square-planar, four-coordinate ligand environment provided by the starting model, 1. The reason for this high (relative) stability of copper(I) within the new molecules is not obvious. While many three-coordinate mononuclear copper(I) complexes have been isolated employing very soft phosphorous or sulfur donors, very few three-coordinate mononuclear (or binuclear) copper(I) complexes have been isolated with nitrogen or oxygen donors.[23,28,39] The binuclear nature of the compounds in this study may be responsible for their stability. Perhaps the second copper serves to anchor the binucleating ligands, promoting a favorable three-

coordinate environment around each copper(I).

Relatively high reduction potentials on the order exhibited by these complexes (and by the binuclear protein site) may be necessary for reversible oxygen binding.[40] Unfortunately these complexes have thus far reacted irreversibly towards oxygen. We are presently investigating modifications on the sidearms and their effect on the nature of the oxygenation reaction.

Acknowledgment. We appreciate helpful discussions from T. J. Smith and financial assistance from the National Institutes of Health (Grant No. PHS AM 18319-04) and the International Copper Research association.

Experimental Section

Materials. All chemicals were reagent grade and were used as received unless otherwise noted. Copper(II) tetrafluoroborate, ground to a powder then dried for several days in vacuo (25° C), was used as $Cu(BF_4)_2 \cdot 6H_2O$. Tetrabutylammonium perchlorate, TBAP, (South-western Analytical Chemicals) was dried exhaustively in vacuo (25° C) before use. Reagent grade N,N-dimethylformamide, DMF, was dried over $MgSO_4$ and 4A molecular sieves for 24 hours and then vacuum distilled. 2-Hydroxy-5-methylisophthalaldehyde was prepared by a modification of the literature method.[41] Tetra(acetonitrile) copper(I) tetrafluoroborate was also prepared by the published method.[42]

$Cu_2^{II}ISOIM(Mepy)_2OH(BF_4)_2 \cdot CH_3OH \cdot H_2O$, 3. Aminomethyl-pyridine (0.44 ml, 4 mmoles) was added to a solution of 2-hydroxy-5-methylisophthalaldehyde (0.33 g, 2 mmoles) in methanol (50 ml). The resulting yellow solution was boiled at reflux for 1 hour, after which, $Cu(BF_4)_2 \cdot 6H_2O$ (1.38 g, 4 mmoles) was added. This resulting blue-green solution was refluxed for 45 minutes. Removal of the solvent (methanol) using a rotary evaporator gave a blue-green solid, which upon recrystallization from methanol yielded blue-green crystals of 3. These crystals were washed with methanol followed by diethylether and dried under vacuum for several hours. Anal. ($C_{22}H_{26}N_4O_4Cu_2B_2F_8$), C, H, N, Cu.

$Cu_2^{II}ISOIM(Etpy)_2OH(BF_4)_2 \cdot CH_3CH_2OH$, 4. 2-(2'-Aminoethyl)-pyridine (0.50 ml, 4 mmoles) was added to a solution of 2-hydroxy-5-methylisophthalaldehyde (0.33 g, 2 mmoles) in ethanol (25 ml). The

resulting yellow solution was boiled at reflux for 5 min., and then $Cu(BF_4)_2 \cdot 6H_2O$ (1.38 g, 4 mmoles) was added to give a green solution. After boiling for 5 min., this solution was allowed to cool slowly to 4° C, and the resulting blue-green solid was collected and recrystallized from ethanol to give blue-green crystals of 4. The product was washed with ethanol, followed by diethyl ether and dried under vacuum for several hours. Anal. ($C_{25}H_{30}N_4O_3Cu_2B_2F_8$) C, H, N; Cu: Calcd, 17.3; Found 18.0.

Cu_2^{II}ISOIM(hist)$_2$OH$(BF_4)_2 \cdot H_2O$, 5. Histamine (0.44 g, 4 mmoles) was added to a solution of 2-hydroxy-5-methylisophthalaldehyde (0.33 g, 2 mmoles) in methanol (50 ml). The resulting yellow-orange solution was boiled at reflux for 15 min., and then $Cu(BF_4)_2 \cdot 6H_2O$ (1.38 g, 4 mmoles) was added to give a green solution. The solution was reduced to a small volume (~10 ml) using a rotary evaporator, and the resulting green solid was collected by vacuum filtration. Recrystallization of this solid from ethanol gave light blue-green needles of 5. The product was collected and washed with ethanol followed by diethylether, and then dried in vacuo for several hours. Anal. ($C_{19}H_{24}N_6O_3Cu_2B_2F_8$) C, H, N; Cu; Calcd 18.6; Found 19.3.

Cuprous Compounds. The series of copper(I) compounds 6-25 were synthesized in the manner described below for Cu_2^{I}ISOIM$(Etpy)_2(pz)$, 9, with the following modifications. The appropriate amine (RNH_2) and bridge (XH) were used to provide the R and X groups listed in Table I. The initial imine condensation is slow for the aromatic amines, and the amine and dialdehyde were allowed to react overnight, in refluxing

acetonitrile, in the synthesis of 23-25. Compounds 7, 10, 13, 16, and 23-25 were recrystallized with DMF instead of CH_3CN. Compounds 20-22 were recrystallized from heptane instead of acetonitrile.

Cu_2^{I}ISOIM(Etpy)$_2$(pz), 9. The following was performed under helium in a Vacuum Atmospheres Dri-Lab inert atmosphere chamber. 2-(2'-Aminoethyl)pyridine (0.24 ml, 2 mmoles) was added to a solution of 2-hydroxy-5-methylisophthalaldehyde (0.16 g, 1 mmole) in acetonitrile (15 ml). The resulting yellow solution was heated at reflux for 15 min., and then cooled to the ambient temperature. Pyrazole (0.07 g, 1 mmole) and sodium methoxide (0.11 g, 2 mmole) were added to the solution, and after stirring briefly $Cu(CH_3CN)_4BF_4$ (0.63 g, 2 mmoles) was added to give a brown solution and a brown precipitate. This mixture was boiled at reflux for 15 min., and then the acetonitrile was removed by evaporation under vacuum. The brown solid was dissolved in hot toluene (30 ml), leaving behind a white solid ($NaBF_4$) upon vacuum filtration. The toluene was then removed from the filtrate by evaporation under vacuum to yield a brown solid. Recrystallization from acetonitrile gave brown needles, 9. The product was collected by vacuum filtration, washed with acetonitrile and dried for several hours in vacuo. Anal. ($C_{26}H_{26}N_6OCu_2$) C, H, N, Cu.

Physical Measurements. Sample preparation for physical studies on the air-sensitive materials was accomplished in a Vacuum Atmospheres Dri-Lab inert atmosphere chamber, under a helium atmosphere. Helium-saturated spectroquality solvents were used for solution studies.

Magnetic susceptibility measurements were done on powdered samples at the ambient temperature using a Cahn Instruments Faraday balance. The calibrant utilized was $HgCo(SCN)_4$, and diamagnetic corrections were made using Pascal's constants.

Electronic spectra were recorded on a Cary 14 spectrophotometer. Solid state spectra were obtained from Nujol mulls on filter paper against a Nujol-saturated filter paper as a blank.

Infrared spectra were recorded on a Beckman IR-12 Infrared Spectrophotometer. Solid state spectra were obtained from Nujol mulls pressed between KBr plates. Solution spectra were obtained using calcium fluoride solution cells (path length of 1 mm).

Proton magnetic resonance spectra were recorded on a Varian EM390 spectrophotometer at 90 MHz (34° C). The solvent utilized was d^6-benzene containing TMS as the reference.

Mass spectra and elemental analyses were performed by the Caltech Microanalytical Laboratory.

Electrochemistry. A Princeton Applied Research (PAR) Model 174A polarographic analyzer was used for cyclic voltammetry and differential pulse voltammetry. For display purposes, a Hewlett-Packard 7004B X-Y recorder was utilized. The apparatus used for constant potential electrolysis (cpe) consisted of a PAR Model 173 potentiostat-galvanostat coupled with a Model 179 digital coulometer.

Cyclic voltammetry was done in a single compartment cell with a volume of ca. 5 ml. In all solvents the supporting electrolyte was 0.1 M TBAP. The working electrode consisted of a platinum button electrode or a hanging mercury drop electrode. In all cases, the

auxiliary electrode was a coiled platinum wire, and the reference electrode consisted of a silver wire immersed in an acetonitrile solution containing $AgNO_3$ (0.01 M) and TBAP (0.1 M), all contained in a 9-mm glass tube fitted on the bottom with a fine porosity sintered glass frit. The apparatus employed for constant potential electrolysis was similar, except a two compartment H-cell was used to isolate the auxiliary electrode from the working compartment. A platinum gauze was used as the working electrode for cpe.

All potentials are reported versus the normal hydrogen electrode, nhe. This was accomplished by the use of an internal reference redox couple, namely ferrocene, for which the formal potential is reported to be +0.400 V versus nhe in water.[16] It has been proposed that the ferrocene reduction potential changes very little in different solvents, and hence it is a good solvent independent redox couple.[16] Experimentally, small amounts (ca. 10^{-3} M) of ferrocene were added to solutions containing the compounds of interest and formal potentials for both couples were measured under the same conditions.

X-Ray Data Collection and Reduction. Acicular crystals of 9 were grown by slow evaporation of an acetonitrile solution under helium. Preliminary oscillation and Weissenberg photographs showed the space group to be $P2_1/c$ (No. 14) uniquely defined by its extinctions.

A crystal of dimensions 0.04 mm × 0.08 mm × 0.33 mm (which had been cut from a larger needle) was mounted on a Syntex $P2_1$ four-circle diffractometer for data collection. No attempt was made to protect the crystal from atmospheric oxygen as no air sensitivity has been exhibited in the solid state. Cell parameters were determined

by a least-squares fit to fifteen automatically centered reflections with $2\theta > 56°$. The resulting parameters are given in Table III. Intensity data were collected from two octants using θ-2θ scans to a maximum 2θ of 130°. The scan range extended from 1° below the CuK_{α_1} 2θ value to 1° above the CuK_{α_2} value, and the scan rate was 1°/min, with the total background counting time equal to the total scan time. Three check reflections were measured after every fifty reflections to monitor the crystal and instrument stability.

Because the check reflections showed an overall drop in intensity of 5% during the course of data collection, the data were scaled in eleven groups according to the average intensity in each group of one of the check reflections (002). Lorentz and polarization corrections were then applied. Standard deviations of intensities were calculated using the formula

$$\sigma^2(I) = [S + (B1 + B2) + (dS)^2]/(Lp)^2,$$

where S, B1, and B2 are the scan and two background counts and d was taken as 0.02.[43] Absorption corrections were calculated by the method of gaussian quadrature.[44] After symmetry-extinct reflections were deleted and equivalent reflections averaged, there remained 4269 unique data ($3390 > 0$; a rather high percentage of the high 2θ data was "unobserved").

Solution and Refinment of the Structure. With the exception of C. K. Johnson's ORTEP program, all computer programs were from the CRYM system of crystallographic programs. Literature values were used for the scattering factors for Cu^+, O, N, and C,[45] the real

part of the anomalous dispersion correction for copper[45] and for the H scattering factors.[46] The function minimized in the least-squares refinement was $\Sigma_w(|F_o|^2 - |k' F_c|^2)^2$, where the weight $w = 1/\sigma^2(F_o^2)$, and F_o and F_c are the observed and calculated structure factors.

The positions of all nonhydrogen atoms were found using standard Patterson-Fourier techniques. Least-squares refinement with these atoms and isotropic temperature factors led to $R = \Sigma||kF_o|-|F_c||/\Sigma|kF_o| = 0.087$ (for those reflections with $F_o^2 > 2\sigma$). Use of anisotropic temperature factors for all nonhydrogen atoms lowered R to 0.062. The 26 hydrogen atoms were located by difference map techniques. Each was assigned a fixed isotropic temperature factor equal to 1.0 $Å^2$ greater than that for the carbon atom to which it was bound. Hydrogen positional parameters were refined. The final refinement was by blocked-matrix least-squares with all positional parameters in one matrix and the anisotropic thermal parameters and scale factor in another. No data were omitted from this refinement. The final R was 0.042 for the 2620 reflections with $F_o^2 > 2\sigma$; R for all data was 0.063. The final goodness of fit, $\Sigma w(k^2F_o^2 - F_c^2)^2/(n-p)$, was 2.85, where n = 4269 is the number of observations and p = 394 is the number of parameters. The largest feature in the final difference Fourier map was a peak of height 0.96 $eÅ^{-3}$, located approximately 0.7 Å from Cu2 in the positive y direction. The second highest peak (0.87 $eÅ^{-3}$) was not in a position of chemical significance (between the pyrazole groups of neighboring molecules). Final parameters and interatomic distances and angles are presented in Tables IV-VII.

References

(1) Lontie, R. in "Inorganic Biochemistry", Eichhorn, G. I. ed.; Elsevier: New York, N.Y., 1973; p. 344.

(2) (a) Mason, H. S. Ann. Rev. Biochem. 1965, 35, 595-634. (b) Vanneste, W. H. and Zuberbühler, A. in "Molecular Mechanisms of Oxygen Activation", Hayaishi, O. ed.; Academic Press: 1974; p. 371.

(3) (a) Fee, J. A. Structure and Bonding 1975, 23, 1-60. (b) Vänngård, T. I. in "Biological Applications of Electron Spin Resonance Spectroscopy", Swartz, H. M.; Bolton, J. R.; and Borg, D. C., eds.: J. Wiley: New York, N.Y., 1972; p. 411.

(4) See Wurzbach, J. A.; Grunthaner, P. J.; Dooley, D. M.; Gray, H. B.; Grunthaner, F. J.; Gay, R. R.; Solomon, E. I. J. Amer. Chem. Soc. 1977, 99, 1257-1258 and references contained therein.

(5) Solomon, E. I.; Dooley, D. M.; Wang, R.; Gray, H. B.; Cerdonio, M.; Mogno, F.; Romani, G. L. J. Amer. Chem. Soc. 1976, 98, 1029-1031.

(6) Makino, N.; McMahill, P.; Mason, H. S.; Moss, T. H. J. Biol. Chem. 1974, 249, 6062-6066.

(7) (a) Reinhammar, B. R. M.; Vänngård, T.I. Eur. J. Biochem. 1971, 18, 463-468. Reinhammar, B. R. M. Biochem. Biophys. Acta 1972, 275, 245-259. (b) Farver, O.; Goldberg, M.; Lancet, D.; Pecht, I. Biochem. Biophys. Res. Commun. 1976, 73, 494-500.

References (continued)

(8) For example see: Amundsen, A. R.; Whelan, J.; Bosnich, B. J. Amer. Chem. Soc. 1977, 99, 6730-6739. Simmons, M. G.; Wilson, L. J. Chem. Commun. 1978, 634-636. Bulkowski, J. E.; Burk, P. L.; Ludmann, M. F.; Osborn , J. A. Chem. Commun. 1977, 498-499. Lehn, J. M.; Pine, S. H.; Watanabe, E.; Willark, A. K. J. Amer. Chem. Soc. 1977, 99, 6766-6768. Alberts, A. H.; Annunziata, R.; Lehn, J. M. J. Amer. Chem. Soc. 1977, 99, 8502-8504.

(9) Arcus, C. S.; Wilkinson, J. L.; Mealli, C.; Marks, T. J.; Ibers, J. A.; J. Amer. Chem. Soc.; 1974, 96, 7564-7565. Mealli, C.; Arcus, C. S.; Wilkinson, J. L.; Marks, T. J.; Ibers, J. A. J. Amer. Chem. Soc. 1976, 98, 711-718.

(10) Yokoi, H.; Addison, A. W. Inorg. Chem. 1977, 16, 1341-1349.

(11) Fenton, D. E.; Lintvedt, R. L. J. Amer. Chem. Soc. 1978, 100, 6367-6375.

(12) Gagné, R. R.; Gall, R. S.; Lisensky, G. C.; Marsh, R. E.; Speltz, L. M. Inorg. Chem. 1979, 18, 771-781.

(13) Gagné, R. R. J. Amer. Chem. Soc. 1976, 98, 6709-6710. Gagné, R. R.; Allison, J. L.; Gall, R. S.; Koval, C. A. J. Amer. Chem. Soc. 1977, 99, 7170-7178.

(14) Gagné, R. R.; Koval, C. A.; Smith, T. J. J. Amer. Chem. Soc. 1977, 99, 8367-8368. Gagné, R. R.; Koval, C. A.; Smith, T. J.; Cimolino, M. C. J. Amer. Chem. Soc. 1979, 10, 4571-4580.

References (continued)

(15) Gagné, R. R.; Allison, J. L.; Lisensky, G. C. Inorg. Chem. 1978, 17, 3563-3571. Gagné, R. R.; Allison, J. L.; Ingle, D. M. J. Amer. Chem. Soc. 1979, 18, 2767-2774.

(16) Bauer, D.; Breant, M. in "Electroanalytical Chemistry", Vol. 8, Bard, A. J. ed., Marcel Dekker, Inc.: New York, N.Y., 1975, pp. 282-344.

(17) Attempts to isolate $Cu_2^{II}ISOIM(Mepy)_2(pz)^{2+}$ directly from Cu^{II} starting materials led only to $Cu_2^{II}ISOIM(Mepy)(OH)^{2+}$, 3.

(18) All electrochemical measurements were made without the use of iR compensation. The cyclic voltammetric peak to peak separations are comparable to those we have observed for other chemically reversible redox couples involving polydentate ligands.[13,14] For comparison purposes, under the cyclic voltammetric conditions utilized ferrocene was observed to give peak to peak separations of 70 - 80 mV.

(19) The separation between planes of carbon atoms in graphite is 3.35 Å, for example.[20] In a recent series of crystal structures of Schiff bases akin to the ligand in the present structure, interplanar distances of 3.42 to 3.50 Å were found.[21] See also: Herbstein, F. H. in "Perspectives in Structural Chemistry", Dunitz, J. D. and Ibers, J. A. eds., Vol. 4, John Wiley and Sons: New York, N.Y., 1972, p. 166.

(20) Cotton, F. A.; Wilkinson, G. "Advanced Inorganic Chemistry", Interscience Publishers: New York, N.Y., 1972, p. 288.

References (continued)

(21) Moustakali-Mavridis, I.; Hadjoudis, E.; Mavridis, A. Acta Cryst. 1978, B34, 3709-3715.

(22) Some of the shorter Cu^{I}-N distances that have been reported are as follows: 1.937 Å to 1.943 Å in [1,1-difluoro-4,5,11,12-tetramethyl-1-bora-3,6,10,13-tetraaza-2,14-dioxacyclotetradeca-3,5,10,12-tetraenato]copper(I), which contains copper in a distorted square-planar geometry;[15] 1.946 Å and 1.948 Å for the non-bridging pyrazole groups in bis[(hydrotris(1-pyrazolyl)-borato)copper(I)], which contains copper in a distorted tetrahedral geometry;[9] 1.97 Å to 2.02 Å in tris-(2-picoline)copper(I)perchlorate, in which copper is three-coordinate, with a distorted trigonal-planar geometry.[23] One structure that does have a Cu^{I}-N bond about as short as some of those in the present structure is the dimer of diazoaminobenzene copper(I). This contains two-coordinate copper, with Cu-N distances of 1.898 Å and 1.939 Å (also a Cu-Cu distance of 2.451 Å).[24]

(23) Lewin, A. H.; Michl, R. J.; Gani, P.; Lepore, U. Chem. Commun. 1972, 661-662.

(24) Brown, I. D.; Dunitz, J. D. Acta Cryst., 1961, 14, 480-485.

(25) Structural and electronic factors influencing copper reduction potentials have been documented: Patterson, G. S.; Holm, R. H. Bioinorg. Chem., 1975, 4, 257-275.

(26) Grzybowski, J. J.; Merrell, P. H.; Urbach, F. L. Inorg. Chem. 1978, 17, 3078-3082.

References (continued)

(27) Gagné, R. R.; McCool, M.; Marsh, R. E. Acta Cryst., in press.

(28) For example see: Camus, A.; Marsich, N.; Nardin, G.; Randaccio, L. Inorg. Chim. Acta 1977, 23, 131-144. Jardine, F. Adv. Inorg. Chem. Radiochem. 1975, 17, 115-163. Mehrotra, P. K.; Hoffmann, R. Inorg. Chem. 1978, 17, 2187-2189, and references contained therein.

(29) Mann, K. R.; Gordon, J. G.; Gray, H. B. J. Amer. Chem. Soc. 1975, 97, 3533-3555. Lewis, N. S.; Mann, K. R.; Gordon, J. G.; Gray, H. B. J. Amer. Chem. Soc. 1976, 98, 7461-7463. Mann, K. R.; Lewis, N. S.; Williams, R. M.; Gray, H. B.; Gordon, J. G. Inorg. Chem. 1978, 17, 828-834.

(30) Suguira, Y. Inorg. Chem. 1978, 17, 2177-2182. We have also observed a 0.13 ppm downfield shift of the proton on the carbon adjacent to the pyridine nitrogen of N,N,N′,N′-tetrakis-(2-pyridylmethyl)-ethylenediamine (TPEN) upon binding of Cu^{I} to this pyridine ring.[31]

(31) Gagné, R. R.; McCool, M.; Marsh, R. E.; Dodge, J. A.; Kreh, R. P., unpublished results.

(32) A curious exception to the stepwise electrochemistry exhibited by interacting metals is that reported for a series of binuclear triketonato copper(II) complexes.[11]

(33) Spiro, C. L., Ph.D. Dissertation, The California Institute of Technology, 1981.

References (continued)

(34) (a) Creutz, C. and Taube, H. J. Amer. Chem. Soc. 1969, 91, 3988-3989. Creutz, C. and Taube, H. J. Amer. Chem. Soc. 1973, 95, 1086-1094. (b) Weaver, T. R.; Meyer, T. J.; Adeyemi, S. A.; Brown, G. M.; Eckberg, R. P.; Hatfield, W. E.; Johnson, E. C.; Murray, R. W.; Untereker, D. J. Amer. Chem. Soc. 1975, 97, 3039-3048. (c) Callahan, R. W.; Keene, F. R.; Meyer, T. J.; Salmon, D. J. J. Amer. Chem. Soc. 1977, 99, 1064-1073.

(35) Robson, R. Inorg. Nucl. Chem. Lett. 1970, 6, 125-128.

(36) Bruce, M. I.; Ostazewski, A. P. J. C. S. Dalton 1973, 2433-2436. Churchill, M. R.; DeBoer, B. G.; Rotella, F. J.; Abu Salah, O. M.; Bruce, M. I. Inorg. Chem. 1975, 14, 2051-2056.

(37) Hill, C. L.; Renaud, J.; Holm, R. H.; Mortenson, L. E. J. Amer. Chem. Soc. 1977, 99, 2549-2557.

(38) Farver, O.; Goldberg, M.; Wherland, S.; Pecht, I. Proc. Natl. Acad. Sci. U.S.A. 1978, 75, 5245-5249.

(39) Ellen, P.; Bradley, D.; Hursthouse, M.; Meek, D. Coord. Chem. Rev. 1977, 24, 1-95.

(40) Reversibility of oxygenation in mononuclear cobalt complexes was shown to be related to reduction potentials: Carter, M. J.; Rillema, D. P.; Basolo, F. J. Amer. Chem. Soc. 1974, 96, 392-400.

(41) Ullmann, F.; Brittner, K. Chem. Ber. 1909, 42, 2539-2548.

(42) Hathaway, B. I.; Holah, D. G.; Postlehtwaite, J. D. J. Chem. Soc. 1961, 3215-3218.

References (continued)

(43) Peterson, S. W.; Levy, H. A. Acta Cryst. 1957, 10, 70-76.

(44) Busing, W. R.; Levy, H. A. Acta Cryst. 1957, 10, 180-182.

(45) "International Tables for X-Ray Crystallography," Vol. III; Kynoch Press: Birmingham, England, 1962.

(46) Stewart, R. F.; Davidson, E. R.; Simpson, W. T. J. Chem. Phys. 1965, 42, 3175-3187.

CHAPTER III

The Synthesis and Structures of (N, N, N′, N′-Tetrakis-(2-Pyridylmethyl)Ethylenediamine) Dicopper(I) and its Dicarbonyl Adduct

Robert R. Gagné, Robert P. Kreh, and John A. Dodge
Richard E. Marsh and Michael McCool

Contribution No. 6294 from the Division of Chemistry and Chemical Engineering, California Institute of Technology, Pasadena, California 91125.

Introduction

Copper(I) complexes show a variety of coordination environments ranging in coordination number from two to five,[1,2] The number of ligands bound to copper(I) seems to be influenced greatly by the imposed geometry and type of ligands. We have recently investigated a series of binuclear copper(I) compounds, including 1,

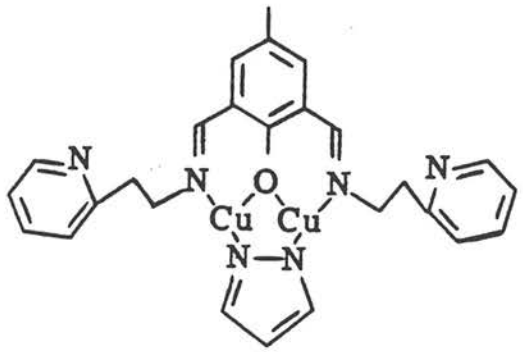

1

which appear to be three coordinate in solution while experiencing significant intermolecular copper-copper interactions in the solid state.[3] Although these compounds contain an "available" (fourth) coordination site on the metal, they are unreactive towards ligands such as pyridine and carbon monoxide.

On the other hand, a stable carbon monoxide adduct is formed by the binuclear Cu(I) complex derived from the ligand, N, N, N′, N′-tetrakis(2-pyridylmethyl)ethylenediamine (TPEN).

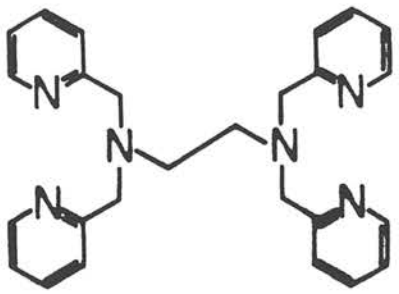

TPEN

In view of the unusual structure and lack of carbon monoxide reactivity for system 1, a complete crystal and molecular structural analysis of both $Cu_2(TPEN)(BF_4)_2$, 2, and its carbonyl adduct 3 have been undertaken for comparative purposes.

Synthesis and Characterization of Complexes

The synthesis of the ligand and the cuprous complexes are presented in Scheme 1. Complex 2 appears slightly green in the solid state, but no absorptions above 450 nm were observed in the visible spectrum of the solid, 2 (Nujol mull, under He). The crystal and molecular structure of 2 has been determined, and the results are presented below.

The binuclear copper(I) complex, 2, is diamagnetic, as expected, showing very sharp signals in the proton NMR (Figure 1). This spectrum confirms the identity of the organic entity. Table I lists the peaks observed for this complex along with the chemical shifts for the free ligand in the same solvent (CD_3CN). The binding of copper(I) to the ligand in complex 2 is evidenced by the rather large changes in chemical shifts,

Scheme 1

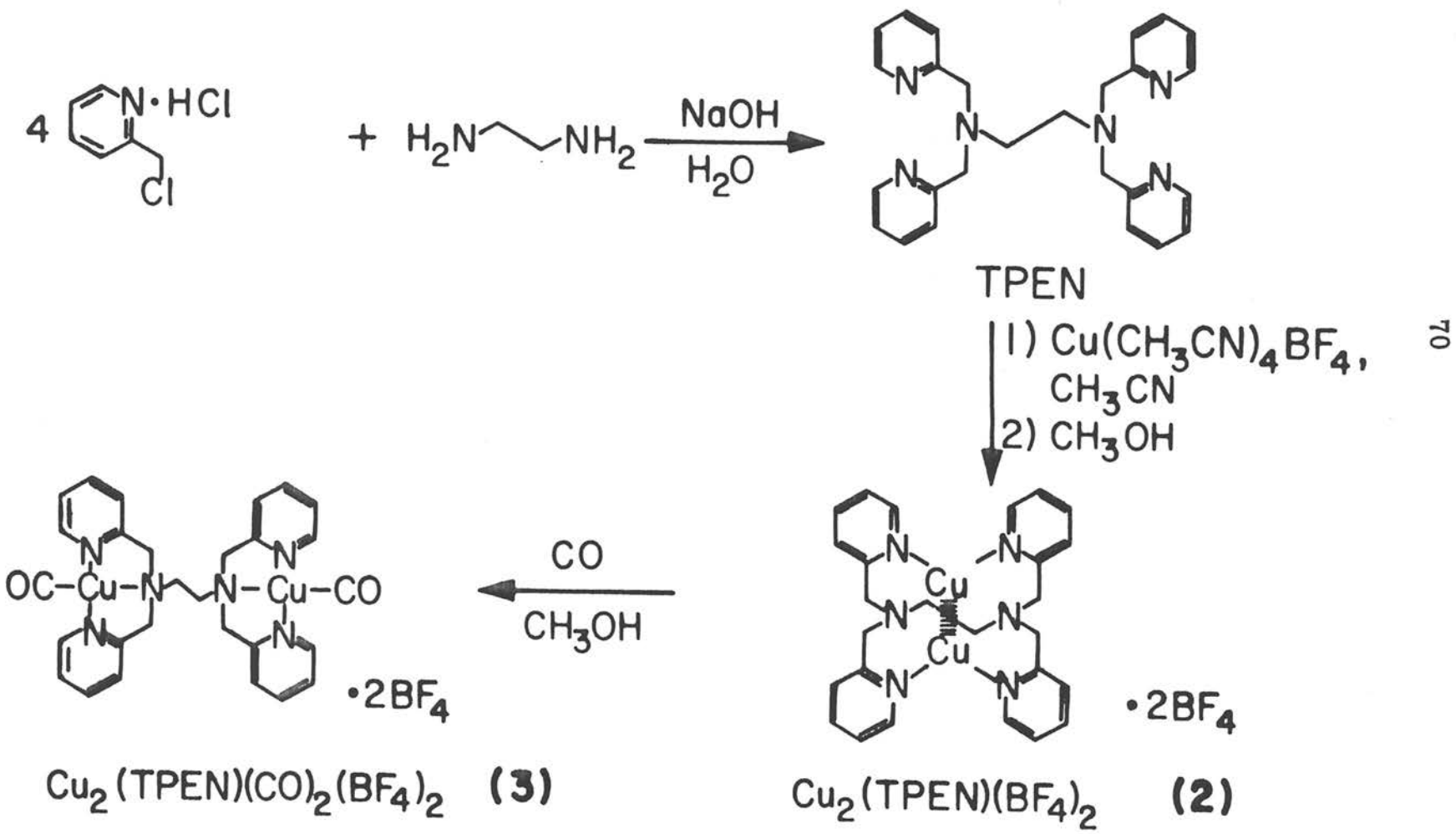
4
N·HCl
Cl
+ H2N NH2
NaOH
H2O
TPEN
1) Cu(CH3CN)4BF4,
CH3CN
2) CH3OH
Cu
Cu
•2BF4
Cu2(TPEN)(BF4)2 (2)
CO
CH3OH
OC–Cu–N
N–Cu–CO
•2BF4
Cu2(TPEN)(CO)2(BF4)2 (3)

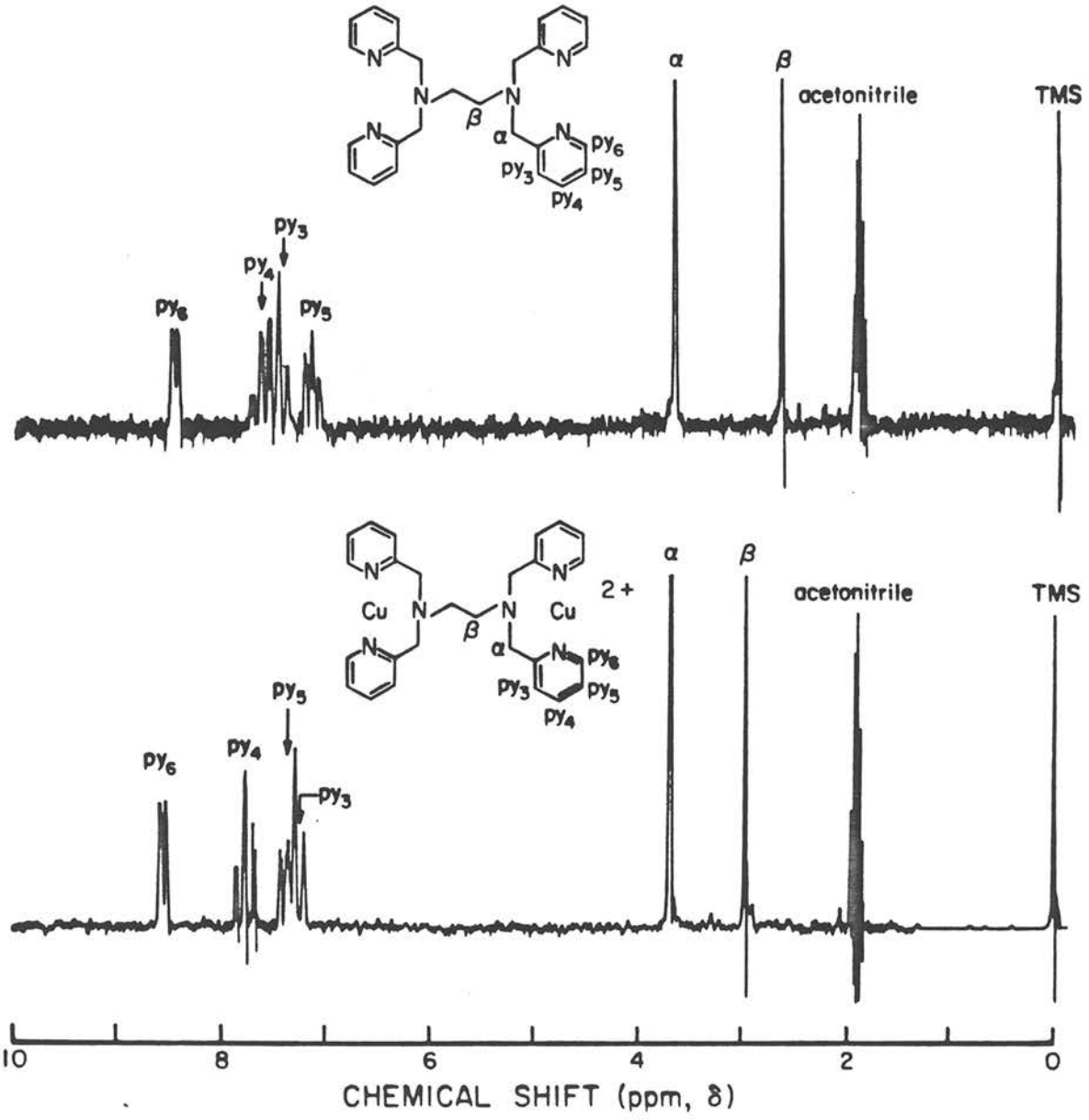

Figure 1. NMR spectrum of the TPEN ligand (top) and $Cu_2(TPEN)(BF_4)_2$, 2 (bottom) in CD_3CN at 34° C.

Table I. Proton NMR Frequencies for TPEN and $Cu_2(TPEN)(BF_4)_2$[a]

Compound	α	β	py_3	py_4	py_5	py_6
TPEN	3.68	2.63	7.39	7.62	7.11	8.44
$Cu_2(TPEN)(BF_4)_2$	3.72	2.98	7.23	7.77	7.34	8.55

[a]All spectra were obtained in CD_3CN solution at 34° C under an atmosphere of helium. The values listed are given in parts per million, δ, relative to Me_4Si. The assignments for the resonances are given in Figure 1.

relative to the free ligand. The resonances due to three of the protons on the pyridine ring (py_4, py_5, py_6) move downfield upon binding to the positive copper(I) ion,[4] while the py_3 resonance shows an anomalous upfield shift. The methylene protons from the ethylenediamine bridge (β) also show a surprising upfield shift in the copper(I) complex. These anomalies could be due to ring current effects from the pyridine rings.

The binuclear complex, 2, is insoluble in most organic solvents (e. g., CH_2Cl_2, CH_3OH), but it is very soluble in acetonitrile, resulting in a deep yellow solution. The solid complex, $Cu_2(TPEN)(BF_4)_2$, 2, is a very faint green color, and this color change upon dissolution is probably indicative of CH_3CN coordination to the cuprous ions. This compound, 2, also dissolved in N, N-dimethylformamide, but the solution turned immediately to blue, and copper metal plated out of solution. However, the disproportionation reaction was reversed entirely by purging the solution with carbon monoxide, presumably resulting in a colorless solution of a copper(I) carbonyl adduct (vida infra).

While complex 2 is only slightly soluble in methanol, saturating a suspension of 2 in methanol (ca. 100 mg of solid in 20 ml of solvent) with carbon monoxide resulted in the dissolution of all of the solid to give a colorless solution. Purging the solution with nitrogen re-precipitated the solid, 2 (identified by I. R.). This process was totally reversible and could be repeated at will. Evaporation of the methanol solvent with a stream of CO resulted in off-white crystals of the dicarbonyl, $Cu_2(TPEN)(CO)_2(BF_4)_2$, 3.

While the solid complexes, 2 and 3, show no apparent reaction with dioxygen, solutions of the dicarbonyl (3 in CH_2Cl_2,CH_3OH or DMF) exhibit a color change from colorless to blue. This reaction could not be reversed by subsequent bubbling of argon through the solutions, and these autoxidation products have not been characterized.

The carbonyl complex, 3, in methylene chloride solution exhibits a single carbonyl stretching frequency, ν_{CO}, at 2110 cm^{-1}. The frequency of this CO stretch is very high compared to that found in other copper(I) carbonyl complexes.[2, 5, 6] The cationic character and "soft" pyridine ligands of complex 3 may result in less π donation from copper(I) into the π^* orbital of CO, thereby raising the frequency of the CO stretch. The solid state I. R. spectrum (Nujol mull) of 3 exhibits ν_{CO} as a strong, sharp doublet at 2097 and 2107 cm^{-1}. To help explain the origin of this phenomenon, a complete structural analysis was performed which confirms the presence of two distinct carbonyls in the solid state.

Crystallographic Analysis of $Cu_2(TPEN)(BF_4)_2$, 2.

Table II summarizes the basis crystal data for the compound. The atomic labeling scheme for $Cu_2(TPEN)^{2+}$ is shown in Figure 2. The molecule lies on a crystallographic two-fold rotation axis, and primes are used to designate symmetry related atoms within the same molecule. The atomic parameters and interatomic distances and angles are given in Tables III-VI.

As seen in Figures 2-4, the binuclear complex is folded into a skewed "face-to-face" configuration. Probably the most significant

Table II. Crystal Data for $Cu_2(TPEN)(BF_4)_2$, 2, and $Cu_2(TPEN)(CO)_2(BF_4)_2$, 3.

Compound	$Cu_2(TPEN)(BF_4)_2$	$Cu_2(TPEN)(CO)_2(BF_4)_2$
Formula (per asymmetric unit)	$BC_{13}CuF_4H_{14}N_3$	$B_2C_{28}Cu_2F_8H_{28}N_6O_2$
Formula weight	362.63	781.27
Space group	C2/c (no. 15)	$P2_1/c$ (no. 14)
a, Å	13.099(4)	17.706(5)
b, Å	15.974(6)	10.372(3)
c, Å	14.472(5)	19.601(5)
β, deg	102.74(2)	112.77(2)
V, $Å^3$	2953.7(17)	3319.2(16)
Z	8	4
ρ_{calcd}, g/cm^3	1.63	1.56
μ, cm^{-1}	15.8	23.7
radiation	MoK_α	CuK_α
λ, Å	0.71069	1.5418

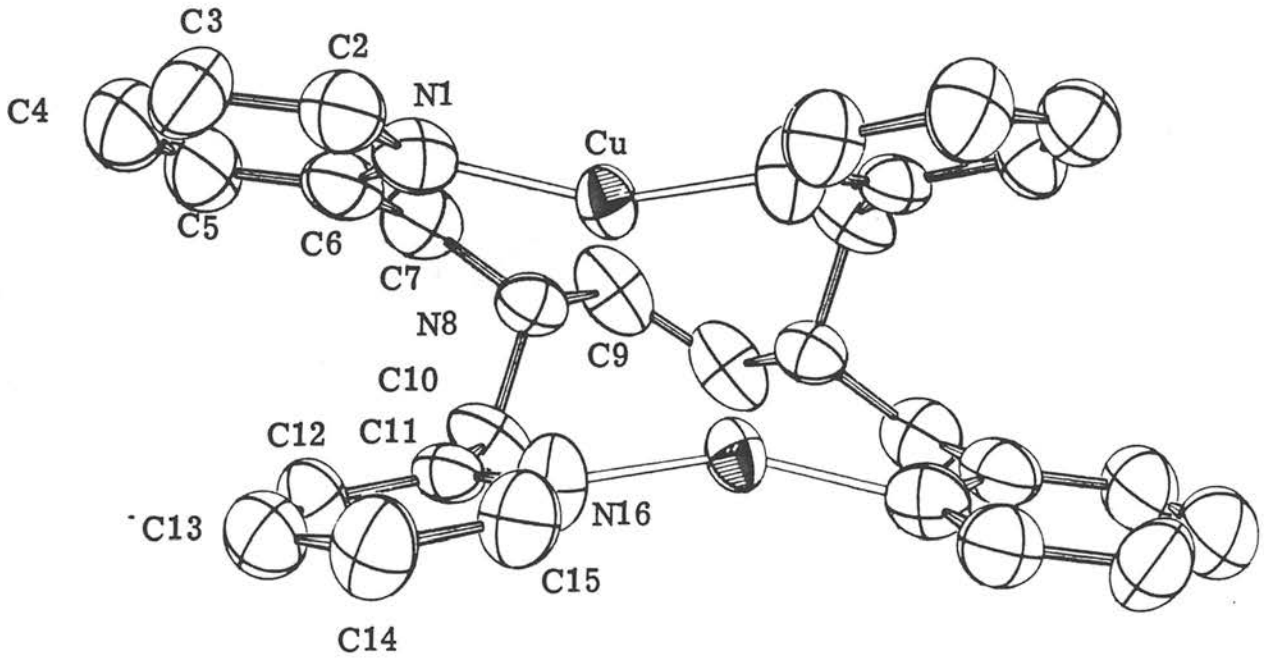

Figure 2. ORTEP drawing showing the nonhydrogen atoms of $Cu_2(TPEN)^{2+}$ as seen along the twofold axis. Forty percent probability ellipsoids are shown. The atomic labeling scheme is given, and each hydrogen is assigned the same number as the carbon to which it is bound. In the discussion of this molecule in the text, primes are used to designate atoms derived by rotation about the axis.

Table III. Atomic Parameters and eds's for the Nonhydrogen Atoms in $Cu_2(TPEN)(BF_4)_2$, 2.

	x[a]	y	z	U_{11}[b]	U_{22}	U_{33}	U_{12}	U_{13}	U_{23}
Cu	3656(9)	3694(8)	16687(9)	470(8)	592(8)	691(9)	-81(10)	59(6)	28(11)
N1	1769(5)	191(5)	1486(5)	87(6)	62(7)	72(6)	-18(5)	10(5)	-17(5)
C2	2163(8)	-550(6)	1290(6)	83(6)	93(10)	77(8)	-3(8)	16(7)	1(7)
C3	3216(9)	-660(7)	1271(7)	95(10)	150(13)	97(10)	33(9)	46(9)	15(9)
C4	3879(8)	1(9)	1469(8)	85(9)	194(17)	99(10)	15(9)	28(8)	36(10)
C5	3508(9)	750(7)	1679(7)	67(8)	166(14)	94(10)	-23(9)	22(8)	33(9)
C6	2448(8)	839(6)	1698(6)	87(9)	90(9)	59(8)	-11(8)	6(7)	9(7)
C7	1956(8)	1664(6)	1873(7)	95(9)	81(9)	82(9)	-29(7)	15(7)	18(7)
N8	1124(5)	1554(4)	2418(5)	76(6)	58(6)	58(6)	-8(5)	8(5)	7(5)
C9	451(7)	2323(5)	2247(7)	91(10)	56(7)	121(11)	-10(6)	-18(8)	9(7)
C10	1601(7)	1426(6)	3447(6)	96(8)	57(7)	71(8)	-5(6)	-15(7)	6(7)
C11	1864(7)	525(6)	3654(5)	71(7)	64(8)	46(6)	8(7)	7(6)	10(6)
C12	2888(7)	248(6)	3909(6)	59(7)	81(8)	86(8)	-11(7)	3(6)	-2(8)
C13	3100(7)	-594(6)	4080(6)	82(8)	93(10)	88(8)	16(7)	17(7)	20(8)
C14	2245(8)	-1129(6)	4034(7)	88(9)	69(8)	119(10)	19(7)	32(8)	22(8)
C15	1246(8)	-793(6)	3802(7)	79(8)	69(8)	103(9)	6(7)	25(7)	-1(7)
N16	1045(6)	14(5)	3621(5)	67(6)	49(6)	122(8)	5(5)	26(5)	13(6)
F1A	4136(6)	2337(5)	390(6)	66(6)	90(7)	176(9)	-4(5)	20(6)	-14(6)
F2A	5526(8)	2097(8)	1446(7)	114(7)	305(13)	66(8)	1(9)	16(6)	-39(8)
F3A	5387(8)	1686(6)	-118(6)	149(9)	111(8)	102(8)	51(7)	20(6)	-35(6)
F4A	5484(10)	3076(7)	218(8)	220(12)	133(10)	186(11)	116(9)	108(9)	-37(8)

Table III. Atomic Parameters and esd's for the Nonhydrogen Atoms in $Cu_2(TPEN)(BF_4)_2$, 2. (cont'd)

	x	y	z	B, Å^2
F1B	473(2)	283(2)	14(2)	13.8(1.2)
F2B	587(2)	251(1)	136(2)	10.3(0.9)
F3B	522(2)	157(2)	53(2)	14.1(1.1)
F4B	627(2)	234(2)	17(2)	11.6(0.9)
BA	513(0)	230(0)	48(0)	8.5(0.7)
BB	552(0)	231(0)	55(0)	6.2(1.4)

[a] Fractional coordinates have been multiplied by 10^5 for the copper atoms and 10^4 otherwise. U_{ij} has been multiplied by 10^4 for the copper atoms and 10^3 otherwise. [b] The form of the thermal ellipsoid is $\exp[-2\pi^2(U_{11}h^2a^{*2} + \cdots + 2U_{23}klb^*c^*)]$ for the anisotropic thermal parameters.

Table IV. Hydrogen Atomic Parameters for $Cu_2(TPEN)(BF_4)_2$, 2.

	x[a]	y	z	B, Å^2
H2	170	-103	116	7.8
H3	348	-120	112	7.8
H4	461	-6	146	8.2
H5	397	123	181	8.0
H7A	165	192	127	7.2
H7B	250	203	222	7.2
H9A	16	237	157	8.0
H9B	89	281	246	8.0
H10A	110	160	382	7.3
H10B	223	176	362	7.3
H12	346	64	397	6.6
H13	381	-80	423	7.4
H14	235	-172	417	6.7
H15	66	-117	377	7.1

[a]Fractional coordinates have been multiplied by 10^3.

Table V. Interatomic Distances (Å) for $Cu_2(TPEN)(BF_4)_2$, 2.[a]

Cu-N1	1.936(7)	BA-F1A	1.284
Cu-N16′	1.890(8)	BA-F2A	1.411
N1-C2	1.346(12)	BA-F3A	1.398
N1-C6	1.355(12)	BA-F4A	1.406
C2-C3	1.398(15)	BB-F1B	1.36
C3-C4	1.356(16)	BB-F2B	1.20
C4-C5	1.353(16)	BB-F3B	1.24
C5-C6	1.402(15)	BB-F4B	1.23
C6-C7	1.513(14)		
C7-N8	1.490(12)		
N8-C9	1.501(11)	Nonbonding Distances	
N8-C10	1.496(11)		
C9-C9′	1.521(13)	Cu-Cu′	2.779(2)
C10-C11	1.495(13)	Cu-N8	2.295(7)
C11-C12	1.383(12)	Cu-N16	2.827(8)
C11-N16	1.339(11)	BA-BB	0.50
C12-C13	1.384(13)		
C13-C14	1.399(14)		
C14-C15	1.386(14)		
C15-N16	1.330(12)		

[a]Primes are used to designate atoms operated upon by the twofold axis (i. e., in the equivalent position $\bar{x}$, y, $\frac{1}{2}$ -z).

Table VI. Interatomic Angles (deg) for $Cu_2(TPEN)(BF_4)_2$, 2.[a]

N16′-Cu-N1	146.8(3)	F3A-BA-F1A	110.0
C2-N1-Cu	125.3(6)	F4A-BA-F1A	108.4
C6-N1-Cu	116.9(6)	F3A-BA-F2A	111.6
C6-N1-C2	117.2(8)	F4A-BA-F2A	113.7
C3-C2-N1	122.7(9)	F4A-BA-F3A	108.1
C4-C3-C2	119.2(10)	F2B-BB-F1B	110.9
C5-C4-C3	119.5(11)	F3B-BB-F1B	110.8
C6-C5-C4	120.0(10)	F4B-BB-F1B	113.2
C5-C6-N1	121.5(9)	F3B-BB-F2B	109.1
C7-C6-N1	114.9(8)	F4B-BB-F2B	105.0
C7-C6-C5	123.5(9)	F4B-BB-F3B	107.6
N8-C7-C6	112.0(8)		
C9-N8-C7	106.7(7)		
C10-N8-C7	110.5(7)	Nonbonding Angles	
C10-N8-C9	112.1(6)		
C9′-C9-N8	114.3(7)	N1-Cu-Cu′	129.6(2)
C11-C10-N8	111.0(7)	N8-Cu-Cu′	77.7(2)
C12-C11-C10	121.9(8)	N16′-Cu-Cu′	71.7(2)
N16-C11-C10	115.6(8)	N8-Cu-N1	82.0(3)
N16-C11-C12	122.5(8)	N16′-Cu-N8	130.8(3)
C13-C12-C11	120.2(8)	C7-N8-Cu	97.9(5)
C14-C13-C12	117.3(9)	C9-N8-Cu	114.8(5)
C15-C14-C13	118.6(9)	C10-N8-Cu	113.6(5)
N16-C15-C14	123.9(9)		
C11-N16-Cu′	124.1(6)		
C15-N16-Cu′	118.4(6)		
C15-N16 C11	117.5(8)		
F2A-BA-F1A	104.9		

[a] See footnote a for Table V.

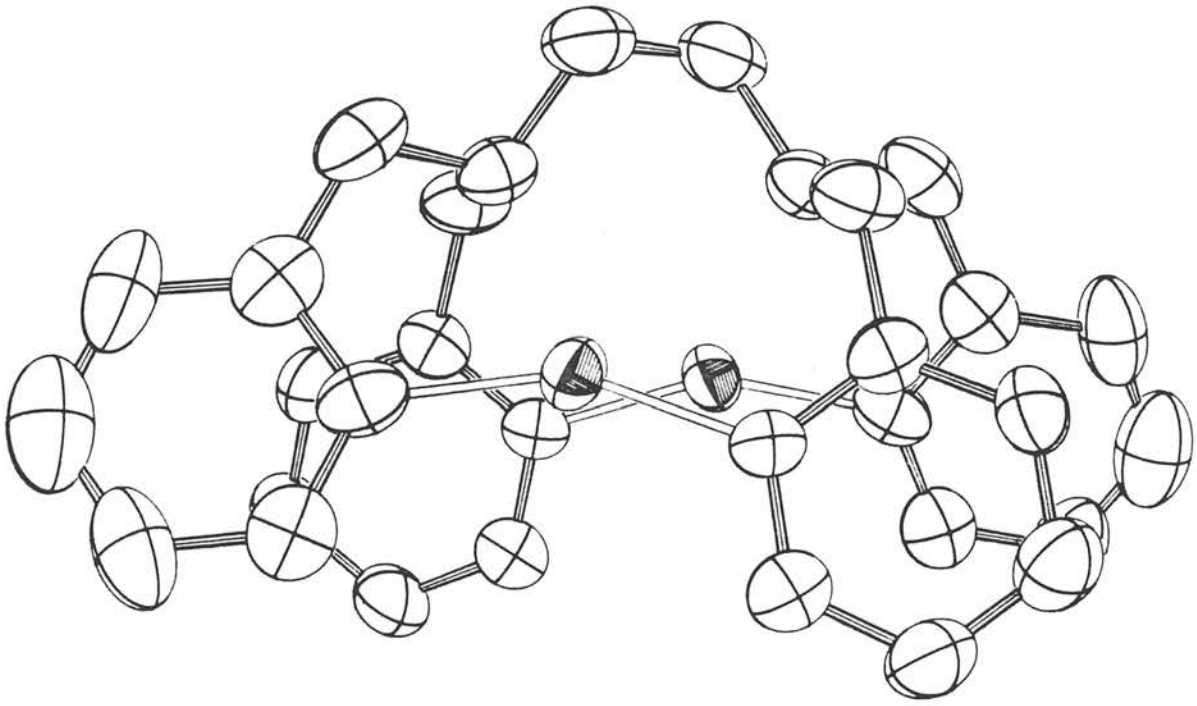

Figure 3. ORTEP drawing showing the nonhydrogen atoms of $Cu_2(TPEN)^{2+}$ as viewed perpendicularly to the twofold axis. Forty percent probability ellipsoids are shown.

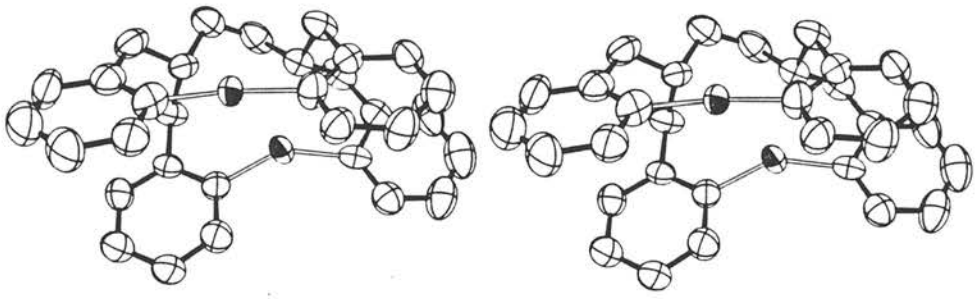

Figure 4. Stereo drawing of $Cu_2(TPEN)^{2+}$.

aspect of this structure is the close intramolecular copper-copper contact which it allows. The separation is only 2.780 Å, even though there are no short ligand bridges as in most other known structures containing close contacts between Cu(I) atoms.[1,7]

The coordination about copper (identical for each of the two atoms) is difficult to place in a specific geometric category. The two bonds to pyridine nitrogens are short (Cu–N1 = 1.94 Å, Cu–N16′ = 1.89 Å), with an N1–Cu–N16′ angle of 146.6°.[8] There is also a relatively close contact between each copper atom and a tertiary amine nitrogen, although this is quite long for a bond (Cu–N8 = 2.30 Å). Finally, there is the close contact between copper atoms themselves. The angles about copper for these various interactions are given in Table VI. (It might also be noted that the distance between Cu and N16 of the pyridine ring below, 2.83 Å, is sufficiently long to preclude anything but a very weak interaction.)

As is suggested by Figures 2-4, each copper atom lies almost in the plane defined by the two bound pyridine nitrogens and the nearest amine nitrogen. The deviation of copper from this plane is 0.07 Å, in the direction that gives the shorter Cu–Cu′ distance. Each copper atom is also nearly coplanar with each of the two pyridine rings to which it is bound. The deviation of Cu from the plane of the ring containing N16′ is only 0.04 Å; for the N1 ring the deviation of Cu is larger (0.20 Å) and in the direction that gives the shorter Cu–Cu′ distance.

Each pyridine ring is nearly planar, the largest deviations from the respective mean planes being 0.014 Å for each of N1 and C6 (in opposite directions) and 0.019 Å for each of C11′ and C12′ (again in opposite directions). The dihedral angle for these two ring planes is 169°.

The reason for the skewed nature of the TPEN ligand is not clear, but some possible explanations can be suggested. First, with the molecule twisted as it is, the lone electron pair of each amine nitrogen is pointed in the direction of the nearest copper atom, as indicated by the following angles about N8: Cu–N8–C7 = 98.0°; Cu–N8–C9 = 114.6°; Cu–N8–C10 = 113.3°. Thus, an affinity of copper for a third ligand could be a contributing factor in the stabilization of this conformation. However, in view of the length of the Cu–N8 separation (2.30 Å) this attraction could not be very strong, and the interaction with another copper atom would seem to be of greater importance.

An examination of CPK molecular models suggests that other steric factors could be responsible for the observed conformation, and that the Cu–N8 proximity could be coincidental. Of course, this structure does prevent the pyridine rings from being perfectly eclipsed. (See Figure 3.) Also, some degree of rotation about the C9-C9′ bond, away from an eclipsed conformation of the ethylenediamine moiety, appears to be necessary to allow the pyridine rings to move sufficiently far apart to accommodate the copper atoms. Rotation about the N8-C9

bond (and the equivalent N8′-C9′ bond), which results in pointing each nitrogen lone pair away from the center of the molecule and toward copper, relieves van der Waals repulsions between hydrogen atoms (e. g., between H7A, H9A, and H10A′).

Molecular models also indicate that, in order for the pyridine rings to be close enough to bind copper, the pyridine nitrogen lone pairs cannot be collinear. This, plus an attraction between copper atoms, would explain the deviation of the N1–Cu–N16′ angle from 180°.

Finally, some mention should be made of the BF_4^- anions. These are distributed uniformly throughout the crystal and are separated by approximately half a unit cell in the direction of each of the crystal axes. The BF_4^- groups are disordered between two positions which differ primarily by rotation of the group with a small degree of translation. The populations of these sites are approximately 0. 65 and 0. 35, respectively. No fluorine atom lies within 3. 5 Å of a copper atom.

Crystallographic Analysis of $Cu_2(TPEN)(CO)_2(BF_4)_2$

The molecular structure and numbering scheme for the cation $Cu_2(TPEN)(CO)_2^{2+}$ are shown in Figure 5. Basic crystal data are listed in Table II. Atomic parameters and interatomic distances and angles are presented in Tables VII-X.

Although the binuclear complex 3 contains two copper ions in identical chemical environments, a center of symmetry was not found

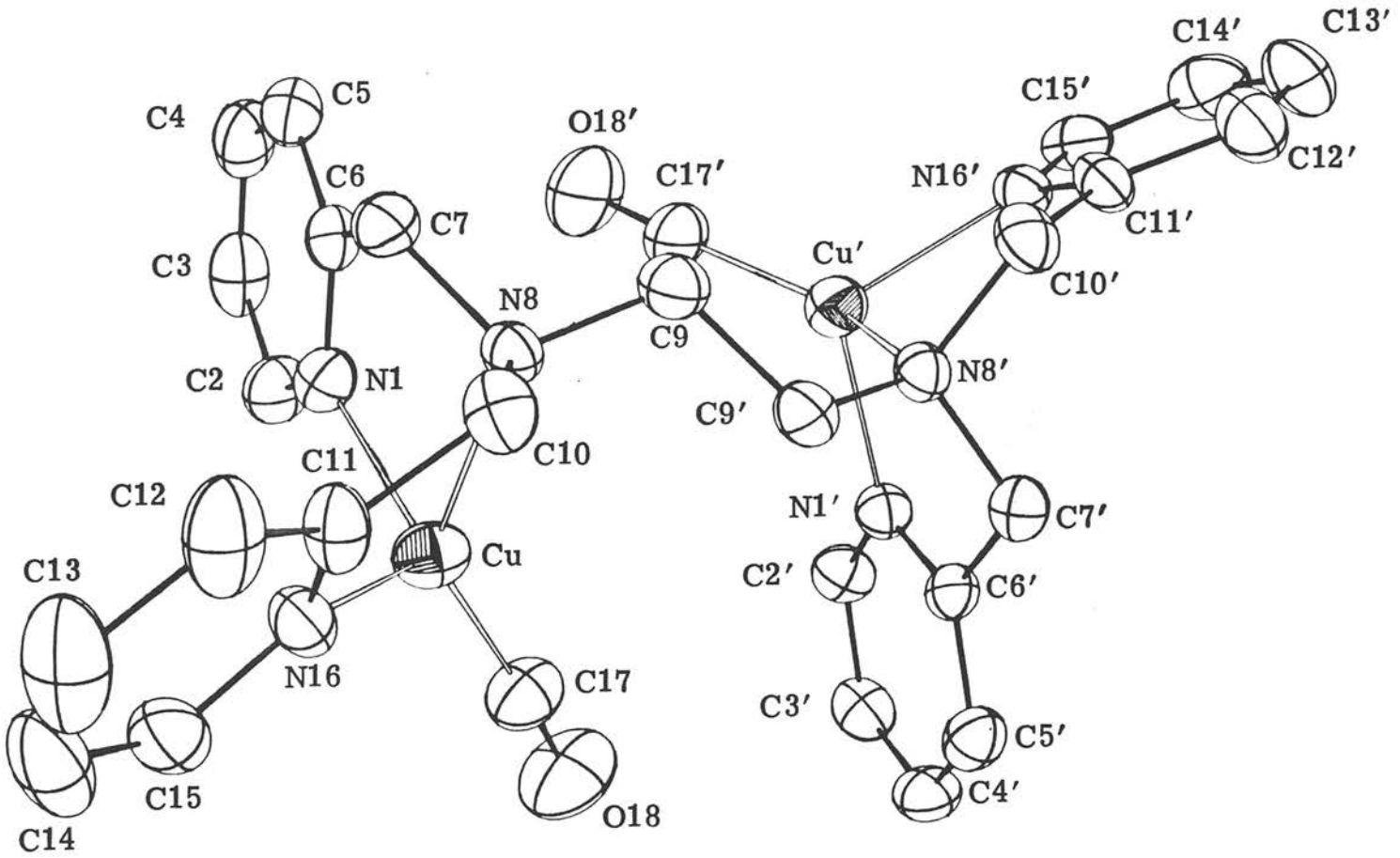

Figure 5. ORTEP drawing showing the nonhydrogen atoms of $Cu_2(TPEN)(CO)_2^{2+}$. The atomic labeling scheme is given, and each hydrogen is assigned the same number as the carbon to which it is bound. Although primes are used here, this molecule does not contain a twofold rotation axis.

Table VII. Atomic Parameters and esd's for the Nonhydrogen Atoms in $Cu_2(TPEN)(CO)_2(BF_4)_2$, 3

	x[a]	y	z	U_{11}[b]	U_{22}	U_{33}	U_{12}	U_{13}	U_{23}
Cu	64488(5)	12678(9)	30151(5)	569(5)	670(6)	633(6)	-7(5)	114(5)	-10(5)
Cu′	81118(5)	27758(8)	17656(5)	574(5)	604(6)	655(6)	4(5)	208(5)	-64(5)
O18	5329(3)	1361(6)	1472(3)	103(4)	138(5)	69(4)	25(4)	-13(3)	-3(4)
O18′	7923(4)	5020(6)	2558(4)	142(5)	107(5)	166(6)	14(4)	62(5)	-62(4)
B1	3857(5)	2529(10)	3087(6)	74(6)	86(8)	96(8)	16(6)	16(6)	-16(6)
B2	553(5)	2391(11)	4120(6)	56(6)	95(9)	122(9)	5(6)	-2(6)	8(8)
F1	4497(3)	2591(7)	2889(4)	128(4)	246(7)	190(6)	16(5)	92(4)	35(5)
F2	3888(3)	3461(6)	3576(3)	131(4)	178(6)	136(4)	21(4)	8(4)	-84(4)
F3	3918(3)	1372(6)	3433(3)	111(4)	139(5)	157(5)	29(3)	34(4)	43(4)
F4	3155(3)	2608(5)	2490(2)	103(3)	117(4)	101(3)	37(3)	-15(3)	-21(3)
F5	-203(4)	2925(7)	3967(6)	116(5)	140(6)	452(14)	-19(4)	25(7)	78(8)
F6	471(3)	1287(5)	4428(3)	147(4)	85(3)	142(4)	-1(3)	45(4)	15(3)
F7	1061(3)	3182(5)	4591(3)	107(4)	158(5)	158(5)	-59(4)	7(3)	-51(4)
F8A	296(8)	2600(11)	3442(5)	205(14)	148(10)	46(6)	-58(10)	13(8)	4(6)
F8B	960(8)	2029(16)	3690(7)	152(11)	336(20)	124(10)	-18(12)	97(9)	-31(12)
N1	6808(3)	3015(5)	3516(3)	63(3)	54(4)	54(3)	-1(3)	23(3)	-2(3)
N16	6321(3)	-39(5)	3734(3)	57(3)	53(4)	78(4)	-8(3)	40(3)	-8(3)
N8	7728(3)	813(5)	3639(2)	43(3)	55(3)	44(3)	-4(3)	20(3)	5(3)
N16′	9140(3)	2526(5)	1556(2)	44(3)	62(4)	46(3)	-8(3)	19(3)	1(3)
N1′	7137(3)	2159(5)	866(2)	44(3)	54(4)	45(3)	3(3)	14(3)	2(3)
N8′	8276(3)	730(4)	1979(2)	44(3)	54(3)	42(3)	3(3)	18(3)	2(3)
C17	5776(4)	1289(7)	2047(4)	66(5)	75(5)	66(5)	12(4)	9(4)	-3(5)
C6	7581(4)	3044(6)	4018(3)	59(4)	69(5)	47(4)	-7(4)	30(4)	-3(4)
C5	7967(4)	4201(7)	4325(4)	73(5)	82(6)	72(5)	-17(4)	40(4)	-22(5)
C4	7542(5)	5315(7)	4115(4)	108(7)	71(6)	96(6)	-23(5)	64(5)	-30(5)
C3	6756(5)	5299(7)	3602(4)	107(6)	63(5)	84(6)	9(5)	61(5)	6(5)
C2	6407(4)	4138(7)	3320(4)	72(5)	60(5)	73(5)	5(4)	28(4)	-5(4)
C11	7005(4)	-660(6)	4159(3)	81(5)	41(4)	66(5)	2(4)	46(4)	5(4)
C12	7049(5)	-1400(7)	4755(4)	126(7)	55(5)	97(6)	12(5)	72(5)	6(4)
C13	6346(6)	-1533(7)	4905(5)	189(10)	49(5)	141(8)	-6(6)	123(8)	7(5)

Table VII. Atomic Parameters and esd's for the Nonhydrogen Atoms in $Cu_2(TPEN)(CO)_2(BF_4)_2$, 3 (cont'd)

C14	5651(6)	-956(8)	4449(5)	138(8)	63(6)	170(9)	-27(5)	119(8)	-21(6)
C15	5637(4)	-208(7)	3869(4)	77(5)	62(5)	117(6)	-18(4)	54(5)	-29(5)
C7	7977(4)	1766(7)	4251(3)	53(4)	84(5)	45(4)	-11(4)	17(3)	-2(4)
C10	7719(4)	-495(6)	3935(3)	63(4)	65(5)	58(4)	11(4)	27(4)	12(4)
C9	8280(3)	914(6)	3246(3)	49(4)	71(5)	54(4)	-3(3)	17(3)	3(4)
C17′	7984(4)	4132(7)	2268(4)	72(5)	77(6)	91(6)	7(4)	26(4)	-28(5)
C6′	9486(3)	1372(6)	1741(3)	38(4)	76(5)	51(4)	2(4)	20(3)	5(4)
C5′	10103(4)	979(7)	1525(4)	64(5)	88(6)	93(6)	-1(4)	40(4)	-2(5)
C4′	10375(4)	1827(9)	1132(5)	69(5)	141(8)	113(7)	-19(5)	63(5)	-12(6)
C3′	10044(5)	3015(8)	965(4)	90(6)	104(7)	80(6)	-42(5)	41(5)	-3(5)
C2′	9423(4)	3332(6)	1186(3)	63(5)	78(5)	51(4)	-21(4)	17(4)	-1(4)
C11′	7083(3)	886(6)	780(3)	51(4)	52(4)	39(4)	-4(4)	21(3)	-1(3)
C12′	6405(4)	313(6)	262(3)	76(5)	52(5)	61(5)	-8(4)	31(4)	-5(4)
C13′	5767(4)	1070(7)	-202(3)	55(4)	86(6)	50(4)	-12(4)	8(4)	-7(4)
C14′	5825(4)	2353(7)	-122(3)	55(4)	78(5)	55(4)	7(4)	18(4)	15(4)
C15′	6518(4)	2875(6)	417(4)	61(4)	49(4)	71(5)	-3(4)	25(4)	6(4)
C7′	9167(3)	539(6)	2192(3)	49(4)	69(5)	59(4)	16(4)	20(3)	8(4)
C10′	7827(3)	129(6)	1242(3)	55(4)	50(4)	54(4)	2(3)	23(3)	-2(3)
C9′	7987(3)	166(6)	2526(3)	51(4)	61(4)	58(4)	-5(3)	26(3)	0(4)

[a]Fractional coordinates have been multiplied by 10^5 for the copper atoms and 10^4 otherwise. U_{ij} has been multiplied by 10^4 for the copper atoms and 10^3 otherwise. [b]The form of the thermal ellipsoid is $\exp[-2\pi^2 (U_{11}h^2 a^{*2} + \cdots + 2\ U_{23}Klb^*c^*)]$ for the anisotropic thermal parameters.

Table VIII. Hydrogen parameters for $Cu_2(TPEN)(CO)_2(BF_4)_2$, 3

	y	z	B, Å^2
H2	414	299	6.1
H3	605	345	6.8
H4	607	431	7.0
H5	422	466	6.4
H7A	146	462	5.5
H7B	187	443	5.5
H9A	175	315	5.4
H9A	62	354	5.4
H10A	-109	359	5.6
H10B	-63	433	5.6
H12	-179	505	7.7
H13	-198	530	8.6
H14	-108	453	8.1
H15	17	357	7.3
H2′	374	47	5.8
H3′	286	-41	6.0
H4′	70	-55	6.3
H5′	-56	22	5.8
H7A′	6	100	5.2
H7B′	-68	131	5.2
H9A′	14	233	5.1
H9B′	-65	262	5.1
H10A′	72	268	5.6
H10B′	-30	213	5.6
H12′	18	164	7.3
H13′	159	98	8.4
H14′	358	72	7.6
H15′	413	108	6.0

[a]The x, y and z fractional coordinates have been multiplied by 10^3.

Table IX. Interatomic Distances for $Cu_2(TPEN)(CO)_2(BF_4)_2$, 3.

Bonding Distances

Cu-N1	2.042(5)	Cu'-N1'	2.036(5)
Cu-N16	2.030(5)	Cu'-N16'	2.032(5)
Cu-N8	2.169(5)	Cu'-N8'	2.160(5)
Cu-C17	1.809(7)	Cu'-C17'	1.781(7)
N1-C6	1.341(8)	N1'-C6'	1.330(8)
N1-C2	1.341(9)	N1'-C2'	1.334(9)
N16-C11	1.340(8)	N16'-C11'	1.329(8)
N16-C15	1.346(9)	N16'-C15'	1.326(8)
N8-C7	1.482(8)	N8'-C7'	1.489(8)
N8-C10	1.479(8)	N8'-C10'	1.481(8)
N8-C9	1.465(8)	N8'-C9'	1.476(8)
C17-O18	1.100(9)	C17'-O18'	1.110(10)
C6-C5	1.396(9)	C6'-C5'	1.372(9)
C6-C7	1.487(9)	C6'-C7'	1.499(9)
C5-C4	1.353(11)	C5'-C4'	1.387(9)
C4-C3	1.366(11)	C4'-C3'	1.340(10)
C3-C2	1.369(11)	C3'-C2'	1.383(10)
C11-C12	1.375(9)	C11'-C12'	1.378(9)
C11-C10	1.500(9)	C11'-C10'	1.494(8)
C12-C13	1.391(11)	C12'-C13'	1.374(11)
C13-C14	1.350(12)	C13'-C14'	1.350(11)
C14-C15	1.369(11)	C14'-C15'	1.368(10)
C9-C9'	1.515(9)	B2-F5	1.369(14)
B1-F1	1.333(13)	B2-F6	1.327(12)
B1-F2	1.347(13)	B2-F7	1.301(12)
B1-F3	1.362(13)	B2-F8A	1.247(16)
B1-F4	1.340(14)	B2-F8B	1.356(19)

Nonbonding Contacts

N1-N16	3.353(8)	N1'-N16'	3.293(7)
N1-N8	2.760(7)	N1'-N8'	2.760(7)
N16-N8	2.717(7)	N16'-N8'	2.735(7)
Cu-Cu'	4.764(1)		

Table X. Interatomic Angles (deg) for $Cu_2(TPEN)(CO)_2(BF_4)_2$, 3.

N16-Cu-N1	110.9(4)	N16'-Cu'-N1'	108.1(4)
N8-Cu-N1	81.9(4)	N8'-Cu'-N1'	82.2(4)
C17-Cu-N1	116.7(4)	C17'-Cu'-N1'	118.7(4)
N8-Cu-N16	80.6(4)	N8'-Cu'-N16'	81.4(4)
C17-Cu-N16	122.1(4)	C17'-Cu'-N16'	121.8(4)
C17-Cu-N8	135.6(4)	C17'-Cu'-N8'	134.9(4)
C6-N1-Cu	114.4(5)	C6'-N1'-Cu'	114.6(5)
C2-N1-Cu	126.9(5)	C2'-N1'-Cu'	126.9(5)
C2-N1-C6	117.9(6)	C2'-N1'-C6	114.4(5)
C11-N16-Cu	115.8(5)	C11'-N16'-Cu'	126.0(5)
C15-N16-Cu	125.0(5)	C15'-C16'-Cu'	126.0(5)
C15-N16-C11	118.7(6)	C15'-C16'-C11'	119.1(6)
C7-N8-Cu	103.3(5)	C7'-N8'-Cu'	104.0(5)
C10-N8-Cu	104.7(5)	C10'-N8'-Cu'	103.6(5)
C9-N8-Cu	116.8(5)	C9'-N8'-Cu'	118.1(5)
C10-N8-C7	109.9(6)	C10'-N8'-C7'	109.3(6)
C9-N8-C7	109.1(6)	C9'-N8'-C7'	109.5(6)
C9-N8-C10	112.5(6)	C9'-N8'-C10'	111.9(6)
O18-C17-Cu	174.7(6)	O18'-C17'-Cu'	176.0(6)
C5-C6-N1	121.7(6)	C5'-C6'-N1'	121.6(6)
C7-C6-N1	115.6(6)	C7'-C6'-N1'	116.1(6)
C7-C6-C5	122.7(6)	C7'-C6'-C5'	122.2(6)
C6-C5-C4	118.8(7)	C6'-C5'-C4'	119.8(6)
C3-C4-C5	120.1(8)	C3'-C4'-C5'	118.7(7)
C2-C3-C4	118.7(8)	C2'-C3'-C4'	118.9(7)
C3-C2-N1	122.8(7)	C3'-C2'-N1'	123.1(7)
C12-C11-N16	122.5(6)	C12'-C11'-N16'	121.3(6)
C10-C11-N16	115.1(6)	C10'-C11'-N16'	116.3(6)
C10-C11-C12	122.4(6)	C10'-C11'-C12'	122.4(6)
C13-C12-C11	118.3(7)	C13'-C12'-C11'	118.3(7)
C14-C13-C12	118.5(8)	C14'-C13'-C12'	120.5(8)
C15-C14-C13	121.3(8)	C15'-C14'-C13'	118.0(7)
C14-C15-N16	120.6(7)	C14'-C15'-N16'	122.8(6)
C6-C7-N8	112.9(6)	C6'-C7'-N8'	112.4(6)
C11-C10-N8	110.9(6)	C11'-C10'-N8'	111.1(6)
C9'-C9-N8	113.4(6)	C9-C9'-N8'	112.6(6)
F2-B1-F1	111.5(9)	F6-B2-F5	100.4(9)
F3-B1-F1	105.9(9)	F7-B2-F5	104.4(9)
F4-B1-F1	110.5(9)	F8A-B2-F5	77.0(11)
F3-B1-F2	107.7(9)	F8B-B2-F5	133.2(12)

Table X. Interatomic Angles (deg) for $Cu_2(TPEN)(CO)_2(BF_4)_2$, 3. (cont'd)

F4-B1-F1	110.3(9)	F7-B2-F6	112.8(8)
F4-B1-F3	110.9(9)	F8A-B2-F6	125.1(10)
		F8B-B2-F6	102.7(11)
Nonbonding Angles		F8A-B2-F7	121.0(10)
		F8B-B2-F7	103.16(11)
N16-N1-N8	51.7(5)	F8B-B2-F8A	56.5(12)
N1-N8-N16	75.5(5)	F8B-F8A-B2	66.3(26)
N8-N16-N1	52.8(5)	F8A-F8B-B2	57.3(27)
N16'-N1'-N8'	52.8(5)		
N1'-N8'-N16'	73.7(5)		
N8'-N16'-N1'	53.5(5)		

in the crystal structure. This is evidenced by the slightly different bond lengths and angles for each half of the molecule, which are listed in Tables IX and X. The origin of this asymmetry is not obvious, especially since no intermolecular interactions less than 3.6 Å were observed.

The stereoview of $\underset{\sim}{3}$ shown in Figure 6 depicts a distorted tetrahedral geometry around the copper ions. Each copper is bound to three ligand nitrogens, with two short Cu–N distances of ca. 2.04 Å (between copper and the pyridine nitrogens) and one long Cu–N distance of ca. 2.17 Å (between copper and the tertiary amine nitrogen). While the shorter Cu–N bond lengths are within the expected range for Cu^{I}–N bonds,[2, 3, 5, 6] the Cu^{I}–N (tertiary amine) is rather long, possibly indicating a lower affinity between the cuprous ion and the "hard" tertiary amine ligand. The Cu–C bond lengths average 1.80 Å, and the C–O bond lengths average 1.11 Å with a Cu–C–O angle of 176°. These values are in agreement with other previously reported four- and five-coordinate copper(I) carbonyls.[2, 5, 6]

The distorted environment around each copper is also evident in the observed bond angles. Two of the N–Cu–N bond angles around each copper average 82° (between either short Cu–N bond and the long Cu–N bond), and the remaining N–Cu–N angle averages 110° (between the short Cu–N bonds). Each copper atom is ca. 1.14 Å above the basal plane defined by the three nitrogen ligands, with carbon monoxide occupying an apical position. The three dihedral angles between the planes formed by the atoms of the inner coordination sphere (N1, N8, N16, C17 and the copper atom) are listed in Table XI.

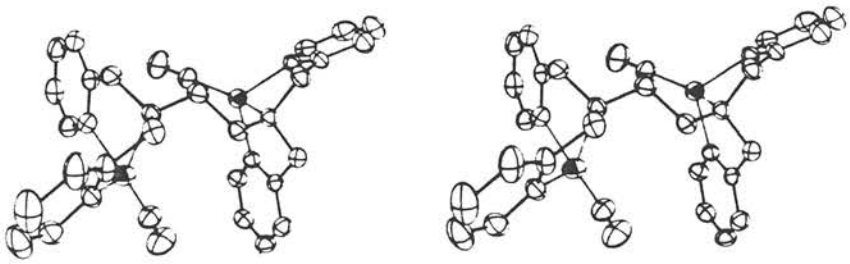

Figure 6. Stereoview illustrating the distorted tetrahedral ligand environment around each copper in $Cu_2(TPEN)(CO)_2^{2+}$.

Table XI. Plane Calculations for $Cu_2(TPEN)(BF_4)_2$, 3.

Plane	Atoms in plane	Dihedral angle between planes	equation of plane (Ax + By + Cz = D) A	B	C	D
1	N1, N8, N16		0.0266	0.1148	0.9054	6.919
2	N1′, N8′, N16′		0.3610	-0.6378	-0.7671	1.833
3	Cu, N8, N16	} 68.0°	0.2111	0.7365	0.6743	2.542
4	Cu, N1, C17		0.9675	-0.0104	0.6075	7.446
5	Cu, N1, N16	} 89.9°	0.9247	-0.2665	-0.1073	9.576
6	Cu, N8, C17		0.2914	0.9545	-0.1718	3.567
7	Cu, N1, N8	} 67.0°	0.5637	0.3041	-0.9263	1.364
8	Cu, N16, C17		0.7530	-0.6254	-0.4801	4.941
9	Cu′, N1′, N8′	} 69.7°	0.8486	-0.0441	0.8146	9.245
10	Cu′, N16′, C17′		0.0968	-0.5098	0.7508	2.521
11	Cu′, N16′, N1′	} 90.1°	0.0956	0.9194	-0.3779	1.994
12	Cu′, N8′, C17′		0.9050	0.1286	0.0237	6.018
13	Cu′, N16′, N8′	} 70.4°	0.2081	0.1868	0.8046	6.312
14	Cu′, N1′, C17′		0.5373	0.6085	-0.7465	6.888

Deviations from Plane

Plane	Cu	C17	Cu′	C17′
1	-1.1141	-2.8618	--	--
2	--	--	-1.1377	-2.8714

Deviations from 90° (expected for a perfect tetrahedron) indicate a distorted environment. These distortions are probably the result of constraints from the polydentate ligand, and these constraints are due to the presence of only two carbon atoms between each ligating nitrogen. A lower affinity of these cuprous ions toward the "hard" tertiary amine nitrogens may also contribute to the unusual geometry.

Only the outer atoms (oxygen of carbon monoxide and the outer carbons of the pyridines) of the dication are undergoing any significant thermal vibrations, but both tetrafluoroborate anions have significant anisotropic motions. One anion is well ordered, the boron atom (B1) remaining positionally fixed (as indicated by its small temperature parameters) with the four fluorines (F1-F4) undergoing thermal vibrations. The second anion is positionally disordered at the boron (B2) and at two fluorines. One of these fluorines, (F8) is clearly disordered with a 50% occupancy at each of two positions separated by 1.3 Å. Another fluorine (F7) is similarly disordered with a 0.5 Å positional separation. The center boron atom (B2) also occupies two positions, but the separation is less than 0.5 Å. As a result, anisotropic temperature factors adequately described the electron distribution of the boron atom (B2) and the small positional disorder of one fluorine (F7), while two positions (F8A and F8B) with anisotropic temperature parameters were required for the other disordered fluorine. The two remaining fluorines of this anion are positionally settled and are not significantly involved in the disorder of the other atoms.

Discussion

The apparent preference of cuprous ions for lower coordination numbers (i. e., two, three, and four)[1, 3] suggested the possibility of the hexadentate TPEN ligand performing as a bridging ligand between two copper(I) ions. Indeed, a binuclear cuprous complex employing the TPEN ligand was isolated. The structure of $Cu_2(TPEN)(BF_4)_2$ (2), however, was somewhat surprising. Rather than the expected three or four (including BF_4 as a ligand) coordination, each copper appears to bind only two nitrogen ligands. In fact, the nitrogen ligands originate from pyridine rings on opposite ends of the ethylenediamine bridge (Figures 1 and 2). Apparently the molecule adopts this conformation in order to maximize the Cu-Cu interaction and minimize the Cu–N (tertiary amine) interaction. (Molecular models corroborate this explanation.)

The structure presented herein for 2 as well as the structure reported for 1[3] indicate a preference of copper(I) toward a somewhat linear arrangement of two nitrogen ligands.[9, 12] (This was observed in 1 by very short Cu-N distances and rather long Cu–O distances.) Note, however, that in both cases, the potential third ligand (i. e., tertiary nitrogen or phenolate oxygen) is rather "hard" and hence unfavorable for copper(I). Therefore, the observed two coordinate character of these compounds may simply be an avoidance of undesirable ligands. Both systems (1 and 2) apparently foster a direct Cu-Cu interaction.[9, 13]

$Cu_2(TPEN)(BF_4)_2$ (2) undergoes an extensive ligand rearrange-

ment in the presence of carbon monoxide to form the dicarbonyl, 3. The crystal structure of this complex exhibited the "expected" pseudotetrahedral geometry. In 3, all nitrogen ligands originate from the same side of the ethylenediamine bridge. In the present system (i. e., 2 and 3) the preferred coordination about copper depends on the presence or absence of a potential fourth ligand (CO or CH_3CN). On the contrary, the previously examined system (1) showed no tendency to bind CO or pyridine as a fourth ligand. The reason for this difference is not clear since molecular models indicate that complexes such as 1 could form a pseudotetrahedral geometry with the addition of a fourth ligand. Thus, there appears to be a special stabilization for cuprous ions in 1 such that significant energy would be lost upon the binding of a fourth ligand.[12] The origin of such stabilization, however, remains obscure.

The structures reported in this paper, as well as the structures found for other cuprous systems,[1-3] demonstrate that a wide variety of coordination environments can be assumed by copper(I) ions. Obviously, the number and geometry of ligands preferred by copper(I) are extremely sensitive to minor ligand alterations. These effects have not been well defined, and as a result, one must exercise caution in the prediction of structures for cuprous compounds.

A few final points about the structure of $Cu_2(TPEN)(CO)_2^{2+}$ deserve mention. This structure bears a close resemblance to the

structure recently reported for $Cu_2(en)_3(CO)_2^{2+}$ (en = ethylenediamine).[5, 14] In this latter complex, the two centrosymmetric copper ions are bridged by an ethylenediamine, and a chelating en and a CO complete a pseudotetrahedral geometry around each copper. Although the atoms of the carbonyl group were found to be distributed over two positions (with C–O bond distances differing by 0.01 Å and the Cu–C bond distances differing by 0.02 Å), only one CO stretching frequency was observed (ν_{CO} = 2078 cm^{-1}).[15] This is most likely due to a dynamic equilibrium between the two carbonyl sites, with a rate faster than the I.R. time scale (~10^{12} sec^{-1} for $\Delta \nu_{CO}$ of 10 cm^{-1}). This contrasts with $Cu_2(TPEN)(CO)_2(BF_4)_2$ which exhibits two CO stretching frequencies (ν_{CO} = 2097, 2107 cm^{-1}), which apparently arise from two distinctly different copper centers (not in equilibrium in the solid state). This system (3) demonstrates that minor alterations in bond lengths and angles of metal carbonyls can be manifested by different CO stretching frequencies.[16]

Experimental Section

Materials. All chemicals were reagent grade and were used as received unless otherwise noted. N, N, N′, N′-tetrakis-(2-pyridylmethyl)-ethylenediamine (TPEN) was prepared by a modification of the literature method.[17] Tetra(acetonitrile) copper(I) tetrafluoroborate was also prepared by the published procedure.[18]

$Cu_2(TPEN)(BF_4)_2$ (2). The following was performed under helium in a Vacuum Atmospheres Dri-Lab inert atmosphere chamber. $Cu(CH_3CN)_4BF_4$ (0.315 g, 1 mmol) was added to a solution of TPEN (0.21 g, 0.5 mmoles) in 25 ml of acetonitrile. After stirring for 10 min at ambient temperature, the solvent was removed under vacuum. Addition of methanol (25 ml) to the resulting orange oil yielded slightly yellow-green crystalline product. The product was collected by vacuum filtration, washed with methanol, and dried for several hours in vacuo. Anal. ($C_{26}H_{28}N_6Cu_2B_2F_8$) C, H, N.

$Cu_2(TPEN)(CO)_2(BF_4)_2$ (3). A suspension of 2 (ca. 100 mg) in 20 ml of methanol (under helium) was placed in an Erlenmeyer flask and covered with a rubber septum. Purging the system with CO caused dissolution of the solid. Evaporation of the solvent with a slow stream of CO yielded off-white crystals of 3. Anal. ($C_{28}H_{28}N_6O_2Cu_2B_2F_8$) C, H, N; Cu: calcd, 16.3; found, 16.8.

Physical Measurements. Sample preparation for physical studies on the air-sensitive materials was accomplished in a Vacuum Atmospheres Dri-Lab inert atmosphere chamber, under a helium

atmosphere. Helium saturated spectroquality solvents were used for solution studies.

Electronic spectra were recorded on a Cary 14 spectrophotometer. Solid state spectra were obtained from Nujol mulls on filter paper (under He) against a Nujol-saturated filter paper as a blank.

Infrared spectra were recorded on a Beckman IR-12 Infrared Spectrophotometer. Solid state spectra were obtained from Nujol mulls pressed between KBr plates. Solution spectra were obtained using calcium fluoride solution cells (path length of 1 mm).

Proton magnetic resonance spectra were recorded on a Varian EM390 spectrophotometer at 90 MHz (34°C). The solvent utilized was CD_3CN containing TMS as the reference.

Elemental analyses were performed by the Caltech Microanalytical Laboratory.

Collection and Reduction of X-Ray Intensity Data for $Cu_2(TPEN)(BF_4)_2$. Yellow needles of $Cu_2(TPEN)(BF_4)_2$, 2, were grown by slow evaporation (under helium) of a solution of 2 in acetonitrile/bis(2-methoxyethyl)ether (ca. 1:1). Preliminary Weissenberg and precession photographs showed the crystals to be monoclinic with the z axis parallel to the needle axis. Two alternatives for the space group, Cc (no. 9) or C2/c (no. 15) were indicated by systematic absence of the following reflections: hkl, $h + k = 2n + 1$; h0l, $l = 2n + 1$. The space group was shown to be C2/c by satisfactory solution and refinement of the structure.

A crystal of dimensions 0.31 mm × 0.12 mm × 0.07 mm which had been cut from a longer needle, was mounted for data collection on a Syntex $P2_1$ four-circle diffractometer using graphite-monochromatized MoK_α radiation. Cell parameters were determined by a least-squares fit to 15 automatically centered reflections with $18° < 2\theta < 25°$. The resulting parameters are given in Table II. Intensity data were collected from four octants (excluding reflections for which $k + l = 2n + 1$) using $\theta - 2\theta$ scans. The maximum 2θ value was 45° for data in the hkl and -hkl octants, and 25° for data in the h-kl and -h-kl octants. The scan range extended from 1° below the MoK_{α_1} 2θ value to 1° above the MoK_{α_2} value, and the scan rate was 1°/min., with the total background counting time equal to the total scan time. Three check reflections were measured after every 60 reflections to monitor the crystal and instrument stability. These showed no systematic variations throughout the course of data collection.

The data were prepared for solution of the structure by first applying Lorentz and polarization corrections. Standard deviations of intensities were calculated using the formula

$$\sigma^2(F_o^2) = [S + (B1 + B2) + (dS)^2]/(Lp)^2$$

where S, B1, and B2 are the scan and two background counts and d was taken as 0.02.[19] Absorption corrections were calculated by the method of Gaussian quadrature.[20] After symmetry-extinct reflections were deleted, data from the hkl and -hkl octants were averaged with

those from the h-kl and -h-kl octants, respectively. There remained 1941 unique data, with 1598 of these greater than zero.

Solution and Refinement of the Structure for $Cu_2(TPEN)(BF_4)_2$. With the exception of C. K. Johnson's ORTEP program, all computer programs were from the CRYM system. All scattering factors (Cu^+, F, N, C, B) with the exception of those for hydrogen[21] were taken from the International Tables,[22] as was the real part of the anomalous dispersion correction for copper. The function minimized in the least-squares refinement was $\Sigma w(F_o^2 - F_c^2)^2$, where the weight $w = 1/\sigma^2(F_o^2)$.

The position of the copper atom was determined by means of a three-dimensional Patterson synthesis. Under the assumption that the correct space group was C2/c, this atom was used as a phasing model for a three-dimensional Fourier map. This map revealed the positions of most of the carbon and nitrogen atoms. A cycle of least-squares, followed by another Fourier map, gave the positions of the remaining nonhydrogen atoms. Full matrix least-squares refinement including all of these atoms with isotropic temperature factors led to $R = \Sigma||F_o| - |F_c||/\Sigma|F_o| = 0.111$, for those reflections with $F_o^2 > 3\sigma$. Use of anisotropic temperature factors lowered R to 0.067. Hydrogen atom positions were calculated assuming a carbon-hydrogen distance of 0.97 Å. All of these positions corresponded to regions of positive electron density in a difference Fourier map. Hydrogen atoms were included in the least-squares with the isotropic temperature factor for

each fixed at 1.0 $Å^2$ greater than that previously determined for the bound carbon atom. The hydrogen positional parameters were not refined but were recalculated periodically.

The large and highly anisotropic temperature factors which had been determined at this point for the fluorine and boron atoms indicated a probability of disordering of the BF_4^- anion. A detailed Fourier map of the anion showed that the fluorine atoms occupied two different sets of positions, although one of these sets had a much lower occupancy than the other. Consequently, two partial BF_4^- groups were included in the least-squares along with a single population factor. The fluorine atoms in the more and less heavily occupied positions were refined with anisotropic and isotropic temperature factors, respectively. The boron atom for each of these BF_4^- groups was placed at coordinates calculated by averaging the corresponding fluorine coordinates. These coordinates were not refined but were recalculated periodically (final boron-boron separation = 0.50 Å). The isotropic temperature factors for the boron atoms were refined. The final, refined populations of the more and less heavily occupied positions were 0.71 and 0.29, respectively.

The final refinement of the structure was done by block-diagonal least-squares with two matrices. All nonhydrogen positional parameters were included in one matrix; the second contained all nonhydrogen thermal parameters, the BF_4^- population factor, and the scale factor. No reflections were omitted from this refinement. The

final R was 0.051 for the 665 reflections with $F_o^2 > 3\sigma$, and 0.143 for all data. The goodness of fit, $[\Sigma w(F_o^2 - F_c^2)^2/(m-s)]^{\frac{1}{2}}$ was 1.18, where m = 1941 is the number of observations and s = 209 is the number of parameters. Features on a final difference map were between -1.4 e/Å^3 (at the position of Cu) and 1.2 e/Å^3 (near F4A). Final atomic parameters are given in Table III and IV.

Collection and Reduction of X-Ray Intensity Data for $Cu_2(TPEN)(CO)_2(BF_4)_2$. An approximately cubic crystal, 0.2 mm on an edge, was sealed in epoxy to prevent decomposition and was used for all X-ray diffraction measurements. Preliminary oscillation and Weissenberg photographs showed Laue symmetry 2/m with systematic absences h0l with l odd and 0k0 with k odd, indicating the monoclinic space group $P2_1/c$; the crystal was then transferred to a Syntex $P2_1$ diffractometer operating with Ni-filtered CuK_α radiation. Unit-cell dimensions were obtained by centering 15 well-scattered reflections with 2θ values ranging from 23° to 48°. Intensities were measured using a θ-2θ scan at a rate of 2°/minute with an equal amount of time spent on backgrounds; three check reflections, monitored every 100 measurements, showed no intensity decay nor abnormal fluctuations. All reflections out to 2θ = 100° were measured in two different quadrants (h, k, l and h, -k, -l) and were averaged to yield 3538 net intensities, of which 2998 were greater than zero.

The initial attempt at solving the structure was by manual application of direct methods based on 95 reflections with $|E|$ greater

than 1.85, three origin-fixing signs and two symbolic signs. The resulting E map was not structurally reasonable because, as it turned out, one of the early sign entries was reversed. A three-dimensional Patterson map was then calculated, and quickly led to the positions of the Cu atoms. The C, N, O, B and F atoms were recovered from F_o and difference maps; the positions of the hydrogen atoms were calculated using a C–H bond length of 0.9 Å. In the least-squares refinement the same quantity was minimized as in the preceding structure, with weights calculated in the same manner.

A late difference map indicated rather severe disorder for one of the BF_4^- groups: while three of the fluorine atoms could be adequately represented by large, anisotropic B's, the fourth could not and accordingly was split into two half-occupied sites separated by about 1.2 Å.

In the final least-squares cycles, three matrices were collected, each of order between 140 and 150; the coordinates of the 49 nonhydrogen atoms in one, anisotropic B's for one-half the cation and one of the BF_4 groups in a second, and anisotropic B's of the remaining atoms, a scale factor, and an extinction parameter in the third. The final value of the goodness-of-fit was 1.76 for the 3538 measured reflections; the R factors were 0.062 for the 2998 reflections with net intensity greater than zero and 0.042 for the 2271 reflections with intensities greater than 3 esd's above background. Features on a difference map were between -0.8 and 0.6 e/Å^3, in generally uninteresting places.

All calculations were carried out on the CRYM system of programs. Final atomic parameters are given in Tables VII and VIII, based on the numbering scheme shown in Figure 5.

Acknowledgment. We appreciate helpful discussions with Grant A. Mauk and financial assistance from the National Institutes of Health (Grant No. PHS AM18319), and the International Copper Research Association.

References and Notes

(1) Jardine, F. H. Adv. Inorg. Chem. Radiochem. 1975, 17, 115-163; Eller, P. G.; Bradley, D. C.; Hursthouse, M. B.; Meek, D. W. Coord. Chem. Rev. 1977, 24, 1-95; Camus, A.; Marsich, N.; Nardin, G.; Randaccio, L. Inorg. Chim. Acta 1977, 23, 131-144.

(2) Gagné, R. R.; Allison, J. L.; Gall, R. S.; Koval, C. A. J. Amer. Chem. Soc. 1977, 99, 7170-7178.

(3) Gagné, R. R.; Kreh, R. P.; Dodge, J. A. J. Amer. Chem. Soc. 1979, 101, 6917-6927.

(4) Similar downfield shifts have been observed for imidazole protons upon binding of the imidazole nitrogen to a cuprous ion: Auguira, Y. Inorg. Chem. 1978, 17, 2177-2182.

(5) Pasquali, M.; Floriani, C.; Gaetani-Manfredotti, A. Inorg. Chem. 1980, 19, 1191-1197.

(6) Bruce, M. I.; Ostazewski, A. P. J. Chem. Soc. Dalton Trans. 1973, 2433-2436; Churchill, M. R.; DeBoer, B. G.; Rotella, F. J.; Abu Salah, O. M.; Bruce, M. I. Inorg. Chem. 1975, 14, 2051-2056.

(7) Mehrotra, P. K.; Hoffmann, R. Inorg. Chem. 1978, 17, 2187-2189, and references cited therein.

(8) The short Cu^{I}-N bond lengths found here are reminiscent of the short Cu^{I}-N bond lengths (1.88-1.90) which were found for 1. These are shorter than most Cu^{I}-N bond lengths which have

been reported and may be characteristic of two coordinate copper(I).[3, 9]

(9) Somewhat similar structures were observed for tetrakis-[1, 3-dimethyltriazenocopper(I)][10] and bis-[diazoaminobenzene-copper(I)][11] in which each copper is bound linearly to two nitrogens, and in addition, close Cu-Cu contacts were observed.

(10) O'Connor, J. E.; Janusonis, G. A.; Corey, E. R. J. Chem. Soc. Chem. Commun. 1968, 445-446.

(11) Brown, I. D.; Dunitz, J. D. Acta Cryst. 1961, 14, 480-485.

(12) In general, two coordinate copper(I) complexes are found with strong σ-donor nitrogen ligands (e. g., $Cu(NH_3)_2^+$) while four coordination appears to be favored with π-acceptor nitrogen ligands (e. g., $Cu(pyridine)_4^+$): James, B. R.; Williams, R. J. P. J. Chem. Soc. 1961, 2007-2019.

(13) Mehrotra and Hoffman have reported molecular orbital calculations which indicate a positive attraction between Cu^I (d^{10}) centers through the mixing in of metal s and p orbitals.[7]

(14) A similar structure was also found for $Cu_2(histamine)_3(CO)_2^{2+}$, but here each copper has a different ligand environment, resulting in different bond lengths and angles for each carbonyl, and two CO stretching frequencies were observed (ν_{CO} = 2055, 2066 cm^{-1}): Pasquali, M; Floriani, C.; Gaetani-Manfredotti, A.; Guastini, C. J. Chem. Soc., Chem. Commun. 1979, 197-199.

(15) It should be noted, however, that the differences in bond lengths do not exceed the standard deviations given. The differences in bond angles for the two carbonyl sites are more significant.

(16) Two different molecules were found in the crystal structure of [hydrotris(1-pyrazolyl)borato]copper(I) carbonyl, and while the Cu-C bond lengths differ by 0.02, the C-O bond lengths are equivalent, and only one CO stretching frequency was observed (ν_{CO} = 2083 cm^{-1}).[6]

(17) Anderegg, G.; Wenk, F. Helv. Chim. Acta 1967, 50, 2330-2332.

(18) Hathaway, B. I.; Holah, D. G.; Postlethwaite, J. D. J. Chem. Soc. 1961, 3215-3218.

(19) Peterson, S. W.; Levy, H. A. Acta Cryst. 1957, 10, 70-76.

(20) Busing, W. R.; Levy, H. A. Acta Cryst. 1957, 10, 180-182.

(21) Stewart, R. F.; Davidson, E. R.; Simpson, W. T. J. Chem. Phys. 1965, 42, 3175-3187.

(22) "International Tables for X-ray Crystallography", Vol. III; Kynoch Press: Birmingham, England, 1962.

CHAPTER IV

Dioxygen Reactions of Three-Coordinate Binuclear Copper(I) Complexes, Leading to the Design and Attempted Synthesis of Improved Models for Copper Proteins

The synthesis and characterization of an extensive series of binuclear copper(I) complexes, 1, are presented in Chapter II (Table I).

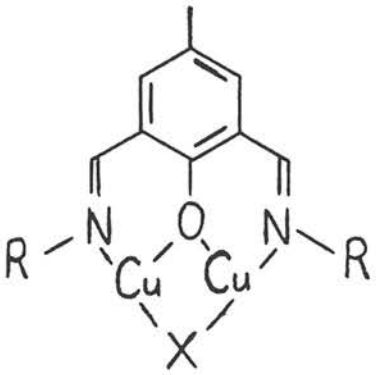

1

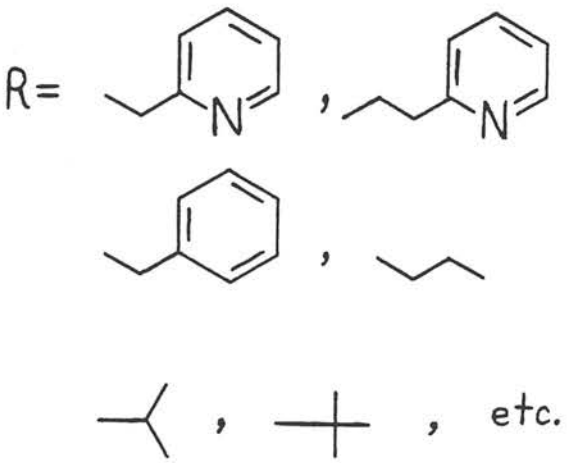

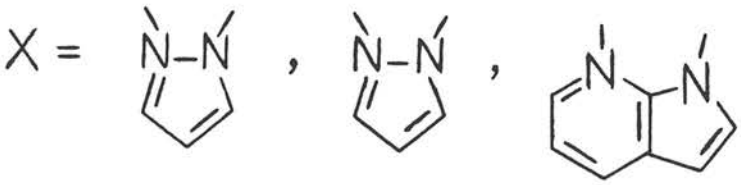

The compounds were synthesized as potential models for the binuclear copper protein sites in hemocyanin, tyrosinase and laccase. These proteins are responsible for reversible dioxygen binding (hemocyanin),[1] dioxygen activation (tyrosinase)[2] and the reduction of dioxygen to water (laccase).[3] Hence, it was of interest to investigate the dioxygen

Table I. Binuclear $Cu^{I}Cu^{I}$ Complexes and Abbreviations Utilized.

Compound Number	Sidearm (R)	Bridge (X)	Abbreviation
2	2-(pyridyl)-methyl	pyrazolate	Cu_2^IISOIM(Mepy)$_2$(pz)
3	2-(pyridyl)-methyl	3-5 dimethyl-pyrazolate	Cu_2^IISOIM(Mepy)$_2$(Me$_2$pz)
4	2-(pyridyl)-methyl	7-azaindolate	Cu_2^IISOIM(Mepy)$_2$(aza)
5	2-(2'-pyridyl)-ethyl	pyrazolate	Cu_2^IISOIM(Etpy)$_2$(pz)
6	2-(2'-pyridyl)-ethyl	3-5 dimethyl-pyrazolate	Cu_2^IISOIM(Etpy)$_2$(Me$_2$pz)
7	2-(2'-pyridyl)-ethyl	7-azaindolate	Cu_2^IISOIM(Etpy)$_2$(aza)
8	phenylmethyl	pyrazolate	Cu_2^IISOIM(MePh)$_2$(pz)
9	phenylmethyl	3-5 dimethyl-pyrazolate	Cu_2^IISOIM(MePh)$_2$(Me$_2$pz)
10	phenylmethyl	7-azaindolate	Cu_2^IISOIM(MePh)$_2$(aza)
11	2-phenylethyl	pyrazolate	Cu_2^IISOIM(EtPh)$_2$(pz)
12	2-phenylethyl	3-5 dimethyl-pyrazolate	Cu_2^IISOIM(EtPh)$_2$(Me$_2$pz)
13	2-phenylethyl	7-azaindolate	Cu_2^IISOIM(EtPh)$_2$(aza)
14	1-propyl	pyrazolate	Cu_2^IISOIM(1-Pr)$_2$(pz)
15	2-propyl	pyrazolate	Cu_2^IISOIM(2-Pr)$_2$(pz)
16	t-butyl	pyrazolate	Cu_2^IISOIM(t-Bu)$_2$(pz)
17	t-butyl	3-5 dimethyl-pyrazolate	Cu_2^IISOIM(t-Bu)$_2$(Me$_2$pz)
18	t-butyl	7-azaindolate	Cu_2^IISOIM(t-Bu)$_2$(aza)
19	phenyl	pyrazolate	Cu_2^IISOIM(Ph)$_2$(pz)
20	p-(dimethylamino)-phenyl	pyrazolate	Cu_2^IISOIM(PhNMe$_2$)$_2$(pz)
21	p-acetylphenyl	pyrazolate	Cu_2^IISOIM(PhCOMe)$_2$(pz)
22	bis-(2-pyridyl)-methyl	pyrazolate	Cu_2^IISOIM(Mepy$_2$)$_2$(pz)
23	1-adamantyl	pyrazolate	Cu_2^IISOIM(ada)$_2$(pz)

reactivity of these synthetic binuclear cuprous systems, 1. All compounds listed in Table I are unreactive towards dioxygen in the solid state, but they are oxidized by dioxygen in DMF solution (as evidenced by an orange → green color change). The lack of solid state reactivity may be due to the necessity for pyrazole dissociation prior to reaction with O_2 (vide infra). The rate of reaction is (qualitatively) much slower for compounds which do not contain potential ligands (i.e., pyridine nitrogens) on the "sidearms" (R). This is not surprising, since the presence of these pyridine nitrogens was found to stabilize the oxidized Cu(II) species (see Chapter II). Attempts to reverse the O_2 reaction by purging with argon were unsuccessful at ambient temperature and at -50° C.

In most cases the products from the oxygen reactions have not been characterized, but oxygen uptake measurements were performed on a series of the cuprous complexes and the results are shown in Figure 1. The reactions were run at both -79° C and at ambient temperatures (20-25° C), but the temperature did not affect the amount of dioxygen consumed. A stoichiometry of 0.5 O_2/Cu_2L (where L is the entire ligand system) corresponds to the complete reduction of dioxygen to water (or hydroxide or oxide) by four copper(I) ions from two binuclear species. This uptake was found for 5, which contains 2-(2′-pyridyl)ethyl groups on the "sidearms" (R). In contrast, compounds 2 and 22 exhibit a stoichiometry of 1.5 O_2/Cu_2L. This high value is indicative of ligand oxidation, and the likely targets are the methylene and methine groups of the ligands in 2 and 22, respectively. The activation of these positions by both the imine nitrogen and the

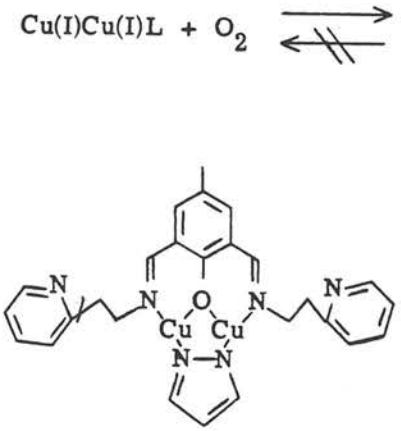

	O_2 : Cu(I)Cu(I)L
5	0.5
2	1.5
22	1.5

Figure 1. Oxygen uptake measurements in CH_2Cl_2/ solutions. The values given here were observed at both -79°C and ambient temperatures.

pyridine rings may lead to oxidation by dioxygen.[4]

The binding of dioxygen to the cuprous ions is apparently necessary for this ligand oxidation since no ligand oxidation is observed for the analogous copper(II) complex, 24, even in the presence of excess

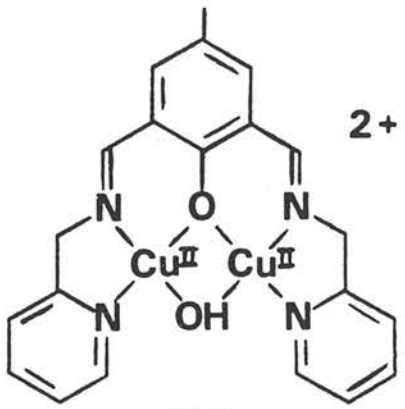

24

pyrazole. The mechanisms and products of these reactions have not been investigated, but hydroxylations of the carbons adjacent to the imine nitrogens are plausible.[5] This would account for the uptake of 1.0 O_2/Cu_2L in addition to the 0.5 O_2/Cu_2L required for the four-electron reduction of dioxygen by four Cu^I ions (as was observed for 5). The formation of a ketone on one side of 2 is also consistent with the stoichiometry,[4,6] but this is not possible for the methine carbons in 22.

Other explanations for these results are certainly possible, and further work would be necessary to advance any explanation beyond mere speculation. The dioxygen reactions were not investigated further, since ligand oxidation was not desired in the present study, nor was the four-electron reduction of dioxygen by two binuclear cuprous compounds of particular interest. However, these results

suggested the avoidance of "activated" positions in the ligand, and this factor was taken into account in the design of additional copper(I) complexes (vide infra).

The large adamantyl groups on the "sidearms" of 23 were introduced in an effort to inhibit a bimolecular reaction between 23 and a dioxygen adduct of 23, which could ultimately lead to the (undesired) four-electron reduction of dioxygen. In this manner, the formation of a stable dioxygen adduct was envisioned. This rationale proved unsuccessful, however, as shown in equation 1. The isolated product

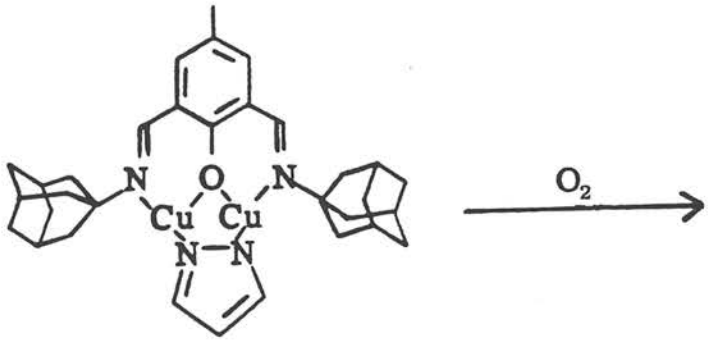

23

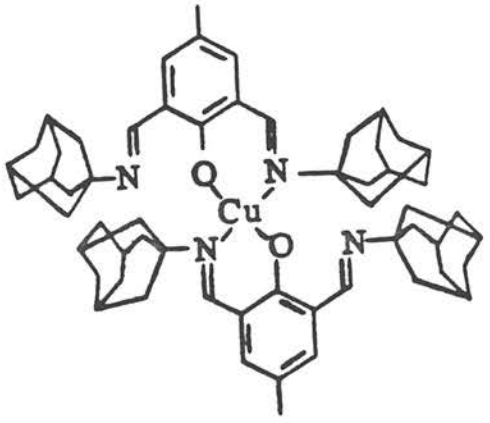

24

\+ other products (1)

indicates major ligand dissociation during the dioxygen reaction. Although other (uncharacterized) products were present, 25 appeared to be a major product. The identity of 25 was confirmed by direct synthesis from copper(II) starting materials. These results are discouraging, and they suggest that the pyrazole may have dissociated during many of these dioxygen reactions.

The preliminary results on the dioxygen reactivity of the binuclear cuprous systems, 2-23 (Table 1) indicate that the processes were not simple binding of dioxygen to copper. Possible problems appear to be activated ligand positions and dissociable ligands. These factors were taken into account in the design of 26 and 27, which were

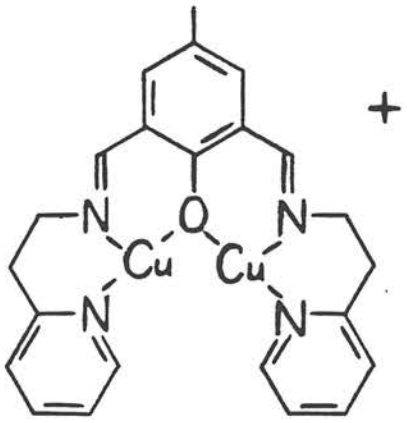

26

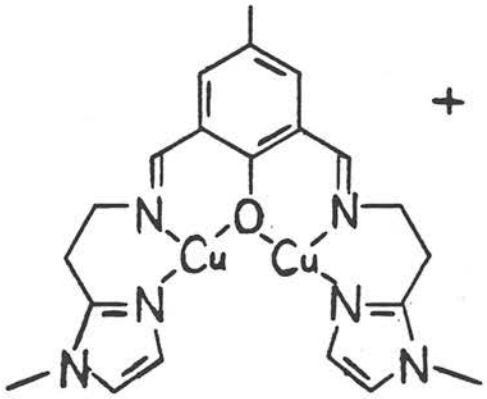

27

desired for investigation of their dioxygen reactivity. The three-coordinate environments of nitrogen and oxygen ligands in 26 and 27 were predicted to be stable configurations for Cu^{I} on the basis of the results presented in Chapter I on three-coordinate copper(I). Complex 27 was of particular interest since it closely approximates the proposed ligands in hemocyanin.[7]

— The synthesis of 26 was unsuccessful, leading instead to a product with a Cu:ligand ratio of 3:2 (e.g., 28, equation 2). The

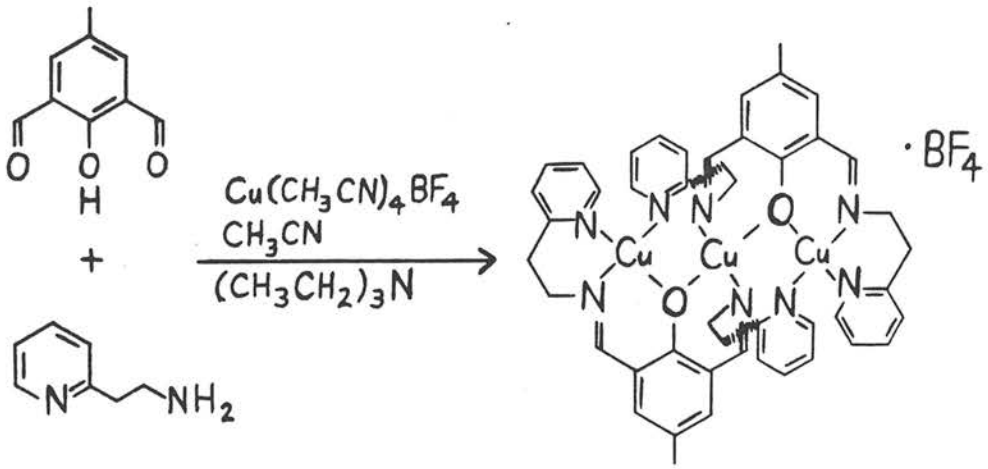

28 (2)

actual structure of 28 is not known, but the structure proposed in equation 2 is in agreement with the elemental analysis and allows for four ligands around each copper(I). A mononuclear Cu^{I} complex, 29, was isolated in the absence of base (equation 3). Here again, the

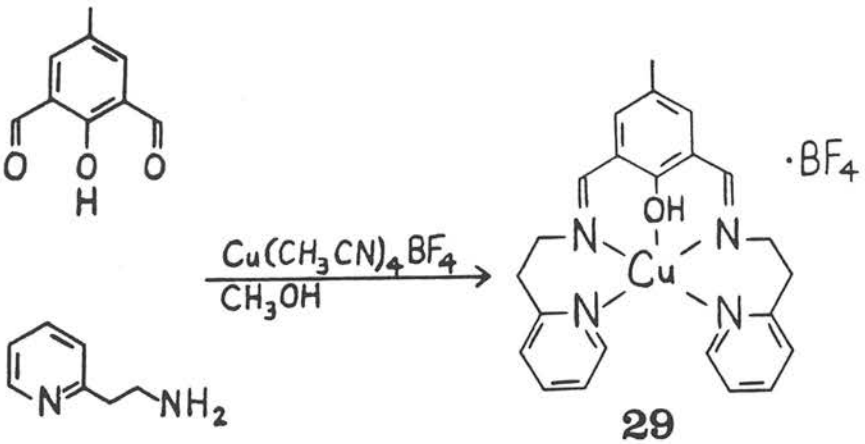

29 (3)

actual structure of 29 is unknown, but the ligand can provide four nitrogen ligands for one copper(I). These results suggest that the desired three-coordinate environment of these ligands in 26 may not be most favorable for Cu^{I}, and hence alternative structures such as 28 and 29 are formed.

It was hoped, however, that the use of imidazole ligands in 27 (rather than the pyridine ligands in 26) would stabilize Cu^{I} in this three-coordinate geometry. Synthesis of 27 required the prior synthesis of 2-(2'aminoethyl)-1-methylimidazole dihydrochloride, 30. The literature synthesis of this compound proved unsuccessful,[8,9] but the procedure shown in Scheme 1 yielded the desired product in fair yield.

The primary amine, 30, condensed readily with 2-hydroxy-5-methyl-isophthalaldehyde and yielded the binuclear copper(II) complex, 31 (equation 4). However, the desired copper(I) complex (27), proved

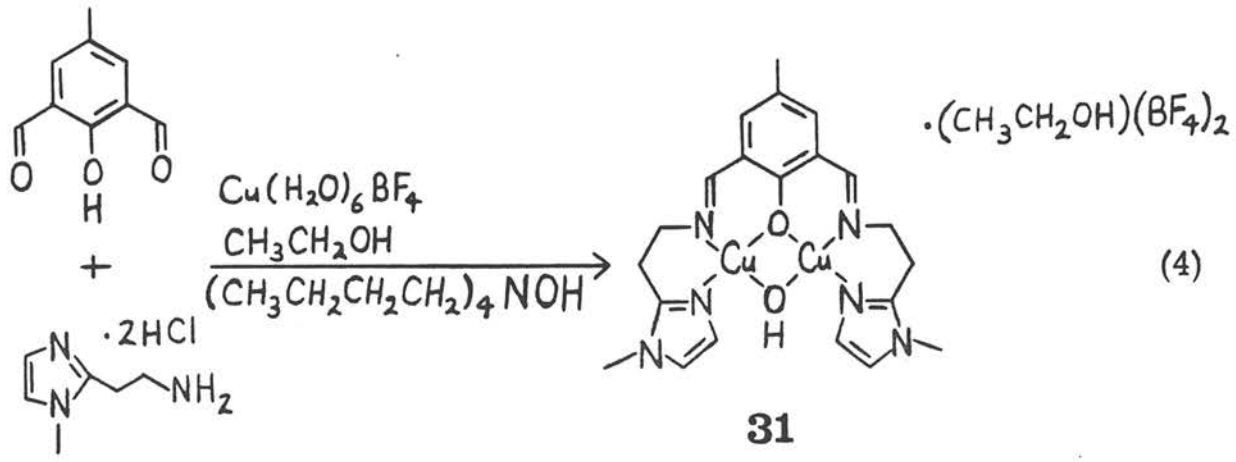

30 31 (4)

elusive, despite numerous attempts (equation 5). A variety of solvents were employed including acetonitrile, methanol, ethanol and acetone.

Scheme 1

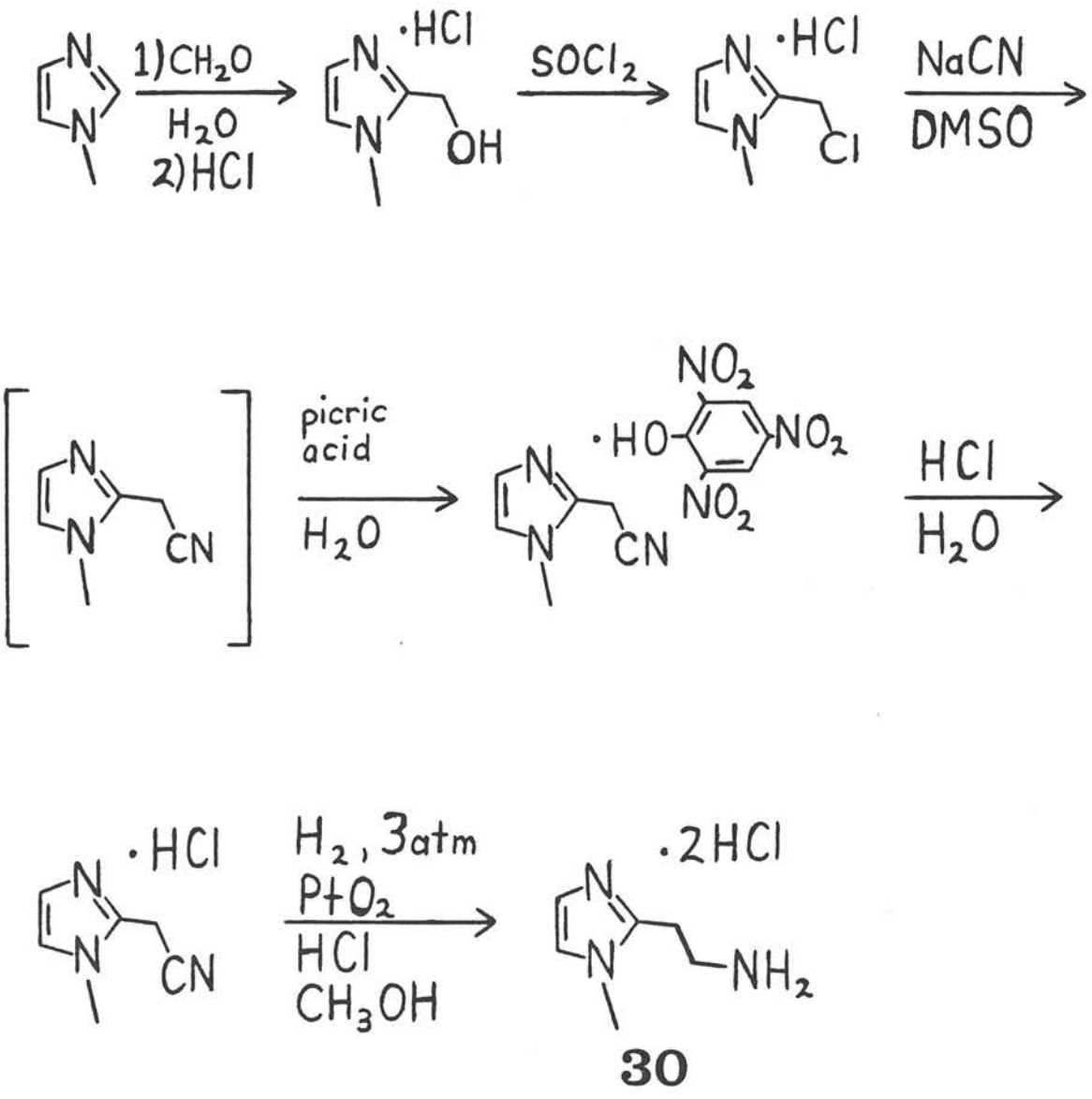
1) CH2O
H2O
2) HCl
·HCl
OH
SOCl2
·HCl
Cl
NaCN
DMSO
CN
picric acid
H2O
NO2
·HO
NO2
NO2
CN
HCl
H2O
·HCl
CN
H2, 3atm
PtO2
HCl
CH3OH
·2HCl
NH2

30

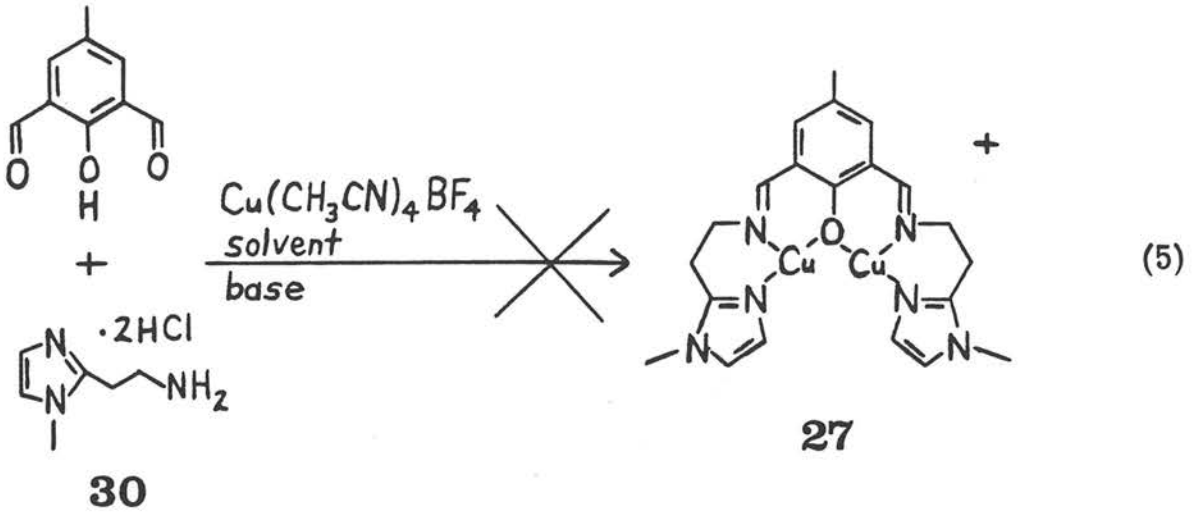

30 27 (5)

Triethylamine, sodium methoxide and tetrabutylammonium hydroxide were tried as bases, and the reactions were run at both reflux and ambient temperatures. In all cases, impure products (based on I.R. and elemental analysis) were isolated, with most reactions leading to some disproportionation of Cu^{I} to Cu^{0} and Cu^{II}. This was observed by a copper mirror on the reaction flask, and the proton magnetic resonance spectra exhibited only very broad peaks. (Pure copper(I) complexes should be diamagnetic.)

Similar results were obtained using 1-benzyl-2-(2′-aminoethyl)-imidazole, 32, which was synthesized in a manner analogous to 30.[9] This amine (32) was investigated because of possible solubility enhancement from the benzyl groups. Again, copper(II) species were straightforwardly synthesized (equations 6 and 7), but attempts to synthesize analogous copper(I) compounds led to disproportionation and impure products.

The synthesis of cuprous analogues of 31, 33 and 34 could, in

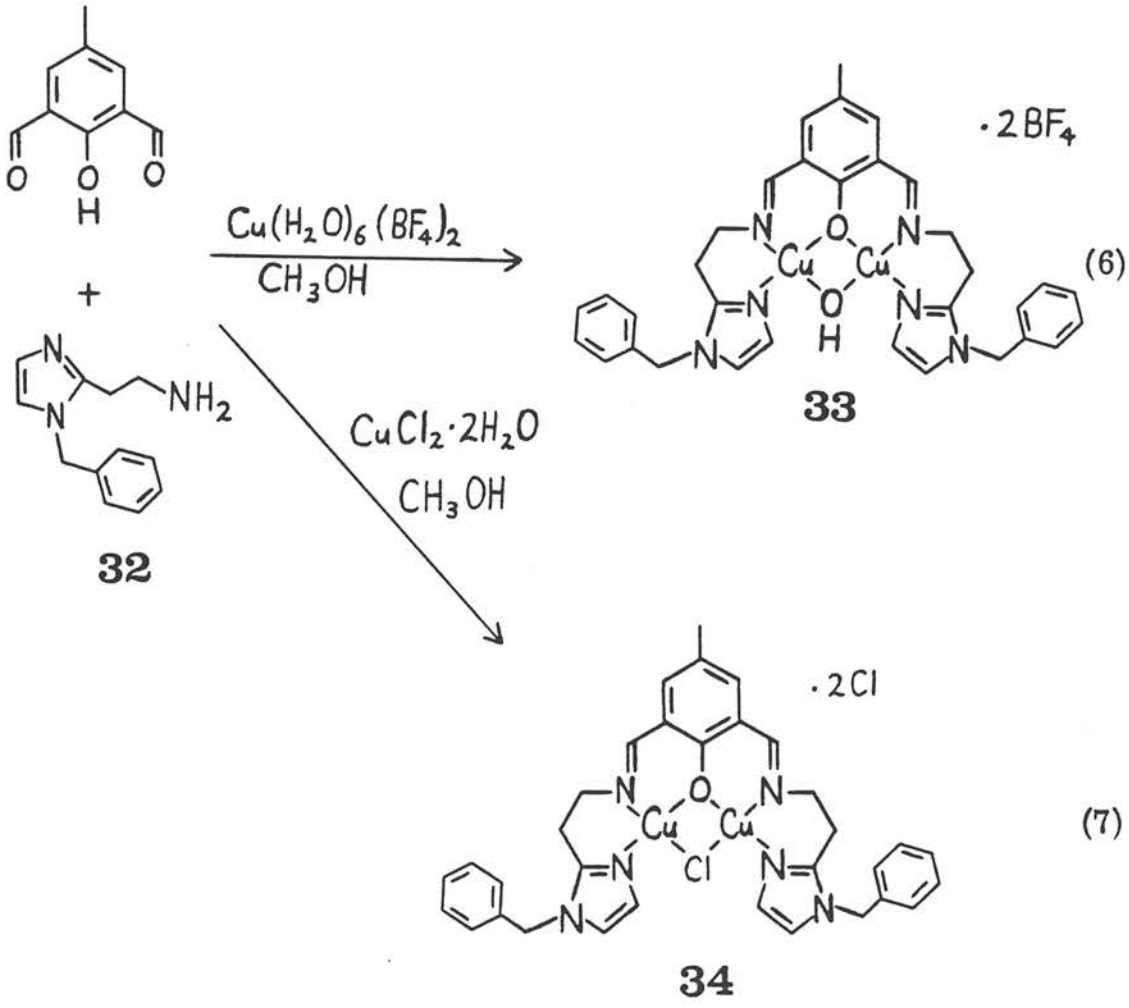

theory, be accomplished by electrochemical reduction of these Cu^{II} compounds. Unfortunately, only very broad, irreversible reduction waves were observed in the cyclic voltammograms of these compounds (at Pt or Hg electrodes). Hence, clean electrochemical reduction of these compounds does not seem tenable.

Addition of excess pyrazole to a solution of 31 in DMF, gave the quasi-reversible electrochemical behavior shown in Figure 2. This

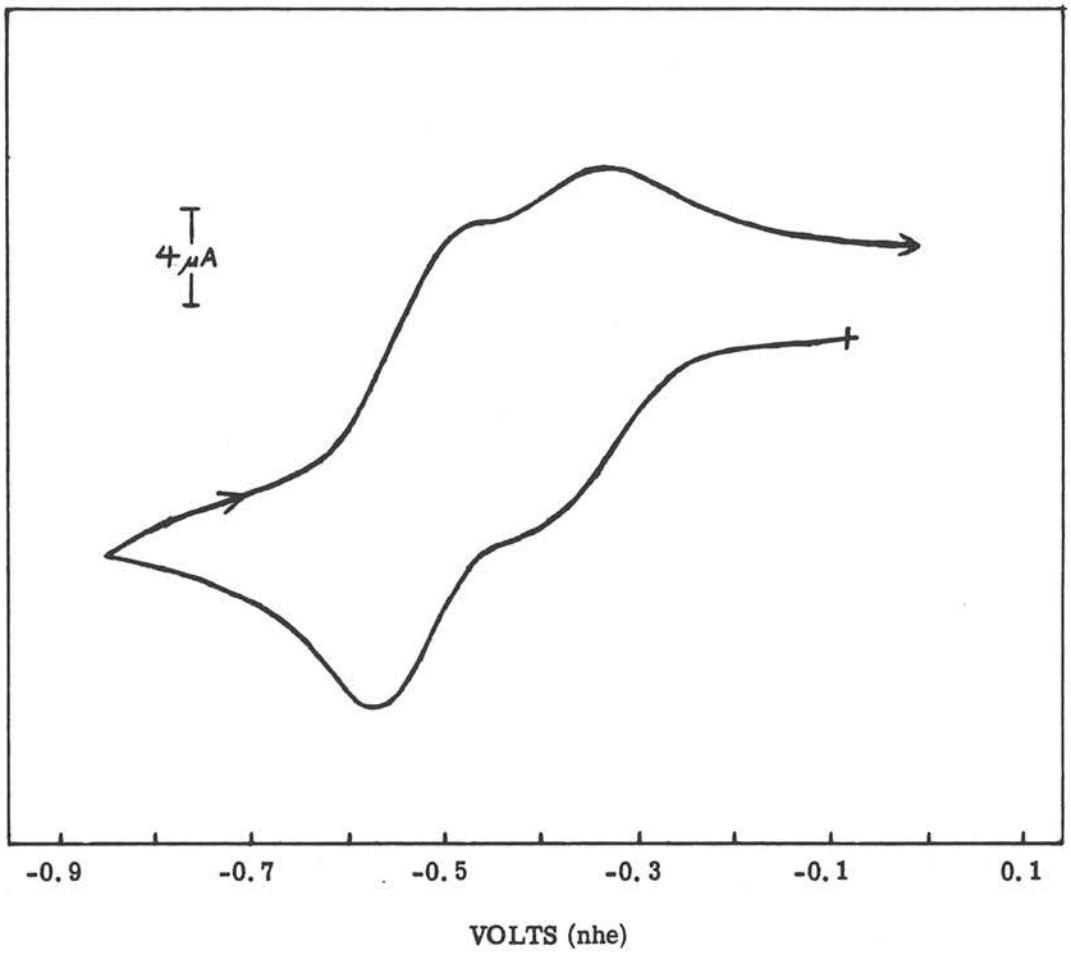

Figure 2. Cyclic voltammogram of Cu^{II}_2ISOIM(EtMim)$_2$(OH)$^{2+}$ (31, containing excess pyrazole) in DMF solution with 0.1 M TBAP as the electrolyte. A platinum indicating electrode was used, and the scan rate was 200 mV/sec.

cyclic voltammogram is similar to those observed for the three-coordinate cuprous compounds presented in Table 1 (see Chapter II). This suggested the synthesis of the binuclear Cu^I complex, 35 (equation 8). By analogy to compounds 2-7, each Cu^I in complex 35

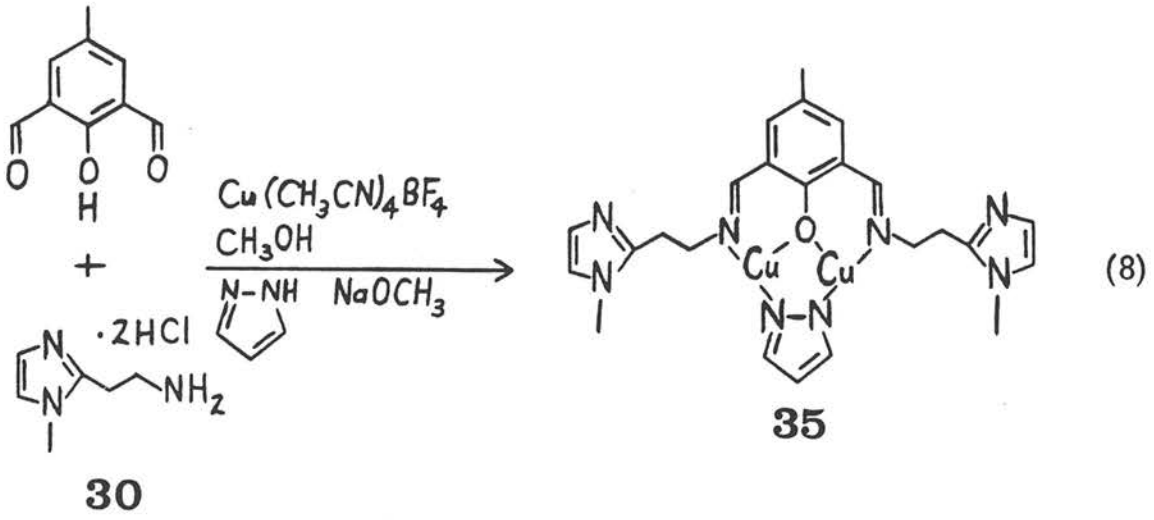

(8)

is assumed to be three-coordinate in solution (with the imidazole nitrogens not bound to the copper centers). An intermolecular Cu-Cu interaction is likely in the solid state, and indeed, a visible absorption at ca. 580 nm is observed for 35 in the solid state (again, see Chapter II).

The cyclic voltammogram of 35 is essentially identical to that shown in Figure 2. The reduction potentials are E_1^f = -0.34 V (for $Cu^{II}Cu^{II}L^{2+} \rightleftharpoons Cu^{II}Cu^{I}L^{+}$) and E_2^f = -0.53 V (for $Cu^{II}Cu^{I}L^{+} \rightleftharpoons Cu^{I}Cu^{I}L$). These potentials compare to E_1^f = -0.11 V and E_2^f = -0.34 V for the analogous compound with pyridines on the sidearms (5). The more negative potentials of 35 indicate a relative stabilization of Cu^{II} vs. Cu^{I}, and this is probably due to a stronger binding of the imidazole nitrogens to the oxidized cupric ions (compared to the pyridine nitrogens).

This is in agreement with the stronger σ-donating ability of the imidazole nitrogens. Presumably, the imidazole nitrogens bind to the cupric ions upon oxidation and dissociate from the cuprous ions upon reduction (equation 9).

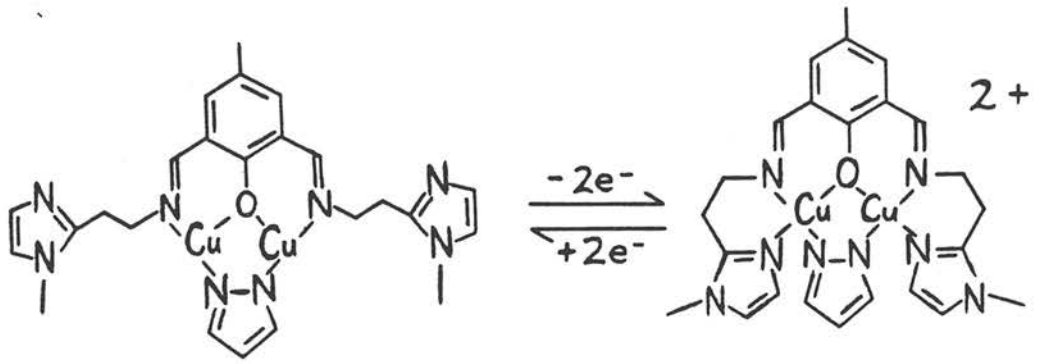

(9)

35

The results presented herein would seem to suggest that complexes 2-23 and 35 provide a stable three-coordinate geometry for Cu^{I} while the proposed complexes 26 and 27 do not. Of course, this is not a valid assumption, since the failure to produce 26 and 27 may be a result of the synthesis methods employed. For example, unstable intermediates may have led to disproportionation and impure products. Also, a mixture of unwanted products may have been preferentially insoluble. However, the paucity of reported three-coordinate cuprous complexes with nitrogen ligands[10] suggests that this is not the most favorable environment for copper(I). Recall that the crystal structure found for Cu_2^{I}ISOIM(Etpy)(pz), 5, indicated some degree of two coordinate character due to the short Cu-N distances and long Cu-O distances (see Chapter II).

The possible stabilization of 26 and 27 by the addition of a fourth

ligand was considered. Attempts were made to introduce a bridging chloride, but no pure compounds were obtained. An effort was also made to synthesize a carbonyl complex by repeating the synthesis shown in equation 5 under an atmosphere of CO. Once again, disproportionation and impure products resulted. Thus, we have not yet been able to stabilize the system by the addition of these potential ligands, but further work in this direction may be desirable. Toward this end, an approach to the synthesis of polydentate ligands which can encompass two copper ions in tetrahedral geometries is presented in Appendix II.

Experimental

Materials. All chemicals were reagent grade and were used as received unless otherwise noted. Copper(II)tetrafluoroborate, ground to a powder then dried for several days in vacuo (25 °C), was used as $Cu(BF_4)_2 \cdot 6H_2O$. Tetrabutylammonium perchlorate, TBAP, (Southwestern Analytical Chemicals) was dried exhaustively in vacuo (25 °C) before use. Reagent grade N,N-dimethylformamide, DMF, was dried over $MgSO_4$ and 4A molecular sieves for 24 hours and then vacuum distilled. 2-Hydroxy-5-methylisophthalaldehyde was prepared by a modification of the literature method.[11,12] Tetra(acetonitrile) copper(I) tetrafluoroborate[13] and bis-(2-pyridyl) methylamine[14] were also prepared by published methods. The preparation of compounds 2-21 (which are numbered 6-25 in Chapter II) is described in Chapter II and 22 and 23 were synthesized analogously. The syntheses of all cuprous compounds were performed under helium in a Vacuum Atmospheres Dri-Lab inert atmosphere chamber. The synthesis of the cupric complex, 24 (given the number 3 in Chapter II), is also presented in Chapter II.

Dioxygen Reaction of Cu_2^{I}ISOIM(ada)$_2$(pz), 23. A solution of 23 (0.079 g) in 10 ml of DMF was exposes to dioxygen for several hours, yielding green crystalline product. The product, $Cu^{II}[ISOIM(ada)_2]_2$ (25), was collected by filtration, washed with acetone and dried under vacuum for several hours. Anal. Calcd. for $C_{58}H_{74}N_4O_2Cu$: C, 75.53; H, 8.03; N, 6.07. Found: C, 73.93; H, 7.95; N, 6.46.

$Cu^{II}[ISOIM(ada)_2]_2$ (25). 1-aminoadamantane (0.60 g, 4 mmoles) was added to a solution of 2-hydroxy-5-methylisophthalaldehyde

(0.33 g, 2 mmoles) in acetonitrile (20 ml). This mixture was heated at reflux for 15 min., after which, a hot solution of cupric acetate (0.20 g, 1 mmole) in 10 ml of acetonitrile was added. The resulting mixture (brown-green) was heated at reflux for 15 min., and the solution volume was reduced to 10 ml by rotary evaporation. The solid product was collected by filtration and washed with acetonitrile and acetone. Dissolution of this solid in CH_2Cl_2 (20 ml), followed by slow addition of acetonitrile, gave brown-green crystalline product, 25, which was collected by filtration, washed with acetone and dried under vacuum for several hours. Anal. Calcd. for $C_{58}H_{74}N_4O_2Cu$: C, 75.53; H, 8.03; N, 6.07; Cu, 6.89. Found: C, 73.73; H, 8.43; N, 5.87; Cu, 7.3.

$Cu^I_3[ISOIM(Etpy)_2]_2BF_4$ (28). 2-(2'-aminoethyl)pyridine (0.24 ml, 2 mmoles) was added to a mixture of 2-hydroxy-5-methylisophthalaldehyde (0.16 g, 1 mmole) in 10 ml of acetonitrile in an oxygen-free (helium) glove box. The mixture was heated briefly to dissolve all of the dialdehyde. Addition of triethylamine (0.14 ml, 1 mmole) followed by $Cu(CH_3CN)_4BF_4$ (0.62 g, 2 mmoles) yielded a crystalline orange solid. The mixture was heated to reflux and filtered. The orange product was washed twice with ethanol, then acetone and dried for 3 hrs under vacuum. Anal. Calcd. for $C_{46}H_{46}N_8O_2Cu_3BF_4$: C, 54.15; H, 4.51; N, 10.98; Cu, 18.69. Found: C, 53.68; H, 4.54; N, 11.46; Cu, 18.6.

$Cu^I[(H)ISOIM(Etpy)_2]BF_4$ (29). 2-(2'-aminoethyl)pyridine (0.24 ml, 2mmoles) was added to a solution of 2-hydroxy-5-methylisophthalaldehyde (0.16 g, 1 mmole) in 10 ml of methanol in an oxygen

free glove box. This solution was heated to reflux, and a hot solution of $Cu(CH_3CN)_4BF_4$ (0.31 g, 1 mmole) in 10 ml of methanol was added, resulting in an orange solution. Upon cooling to the ambient temperature, orange crystals of 29 formed. The product was collected by filtration, washed with ethanol and diethylether and dried under vacuum for several hours. Anal. Calcd. for $C_{23}H_{24}N_4OCuBF_4$: C, 52.84; H, 4.60; N, 10.72; Cu, 12.16. Found: C, 52.22; H, 4.64; N, 10.45; Cu, 12.4.

2-hydroxymethyl-1-methylimidazole hydrochloride.[8,9] 1-methylimidazole (26 g, 0.34 moles) was mixed with 47 g of 37% formaldehyde in water and sealed in a glass, high-pressure reaction vessel. The solution was heated to 115°C for 15 hrs, then allowed to cool to room temperature. The residual pressure was released, and the solvent was removed by rotary evaporation. To the resulting oil was added 100 ml of ethanol and 25 ml of conc. HCl. The solvent was again removed by rotary evaporation to give an oil, which crystallized upon cooling with an ice bath. Recrystallization from 2-propanol yielded white crystals of 2-hydroxymethyl-1-methylimidazole (28 g, 51% yield). Anal. Calcd. for $C_5H_9N_2OCl$: C, 40.42; H, 6.06; N, 18.86. Found: C, 40.50; H, 6.17; N, 18.97.

2-chloromethyl-1-methylimidazole hydrochloride.[9] 2-hydroxymethyl-1-methylimidazole (20 g, 0.135 moles) was added over a 10 min. period to 20 ml of thionyl chloride which was cooled by an external ice bath. The solution was heated at reflux for 20 min. Removal of the solvent using a rotary evaporator (cleaned thoroughly afterwards) gave a white, crystalline solid which was washed with diethyl ether and

recrystallized from isopropanol. The product was collected by filtration, washed with diethyl ether and dried under vacuum overnight to yield 19 g (84%) of 2-chloromethyl-1-methylimidazole hydrochloride. Anal. Calcd. for $C_5H_8N_2Cl_2$: C, 35.93; H, 4.79; N, 16.77. Found: C, 36.21; H, 4.68; N, 17.04.

2-cyanomethyl-1-methylimidazole hydrochloride.[9] Dry, powdered NaCN (8 g, 0.16 moles) was added to a stirred solution of 150 ml of dimethylsulfoxide. To this solution was added 2-chloromethyl-1-methylimidazole (13.4 g, 0.08 moles) over a 5 min period while cooling with an external ice bath to keep the temperature below 45°C. The mixture was stirred and heated to keep the temperature at ca. 40°C for one hour. The dark-brown suspension was then added dropwise, with stirring, to a hot (85°C) mixture of 24.4 g (0.08 moles) of 75% picric acid (25% water) suspended in 300 ml of water. The resulting brown solution was cooled to 5°C, yielding a brownish-yellow precipitate which was collected by filtration and washed twice with water.

The crude picrate from above was suspended in 80 ml of nitrobenzene, and 20 ml of conc. HCl was added. After mixing in a separatory funnel, the nitrobenzene (lower) layer was drawn off, and the aqueous phase was washed with 2 × 20 ml of chloroform. These washes were combined with the nitrobenzene solution, and this combined organic phase was extracted with 20 ml of conc. HCl. The combined aqueous extracts were washed with 20 ml of $CHCl_3$. The solvent was then removed from the aqueous solution by rotary evaporation. The resulting brown solid was recrystallized twice from ethanol to yield slightly brown crystals of 2-cyanomethyl-1-methylimidazole hydro-

chloride (5g, 40% overall yield). Anal. Calcd. for $C_6H_8N_3Cl$: C, 45.71; H, 5.08; N, 26.67. Found: C, 45.64; H, 5.26; N, 26.80.

2-(2′-aminoethyl)-1-methylimidazole dihydrochloride (30).[15] A mixture of 2-cyanomethyl-1-methylimidazole hydrochloride (4 g, 0.025 moles), platinum oxide (0.25 g), conc HCl (10 ml) and methanol (250 ml) was subjected to 3 atm of hydrogen pressure for 12 hrs. The catalyst was removed by filtration, and the solvent was removed by rotary evaporation. Ethanol (200 ml) was added, and the solvent was again removed by rotary evaporation. The resulting oil was immediately transferred into the glove box (under He) due to the hygroscopic nature of the product. The oil soon crystallized and was recrystallized from ethanol to yield slightly brown crystals of 2-(2′-aminoethyl)-1-methylimidazole (3.2 g, 64% yield). Anal. Calcd. for $C_6H_{13}N_3Cl_2$: C, 36.36; H, 6.56; N, 21.21. Found: C, 36.37; H, 6.47; N, 20.84.

Cu_2^{II}ISOIM(EtMim)$_2$OH$(BF_4)_2 \cdot CH_3CH_2OH$ (31). Tetrabutylammonium hydroxide (2.08 g of a 25% methanol solution, 2 mmoles) was added to a suspension of 2-(2′-aminoethyl)-1-methylimidazole dihydrochloride (0.2 g, 1 mmole) in 25 ml of ethanol. To the resulting solution was added 2-hydroxy-5-methylisophthalaldehyde (0.08 g, 0.5 mmoles) to give an orange-yellow solution. This solution was heated at reflux for 15 min. then allowed to cool to the ambient temperature. Tetrabutylammonium hydroxide (0.52 g of a 25% methanol solution, 0.5 mmole) was added with stirring, followed by the addition of $Cu(H_2O)_6(BF_4)_2$. The mixture was heated at reflux for 30 min. and filtered while hot. Allowing the filtrate to cool slowly to

0°C gave microcrystalline blue-green solid (31), which was collected by filtration, washed with ethanol and dried under vacuum overnight. Anal. Calcd. for $C_{23}H_{32}N_6O_2Cu_2B_2F_8$: C, 38.09; H, 4.42; N, 11.59. Found: C, 37.70; H, 4.49; N, 11.89.

1-benzyl-2-(2'aminoethyl)imidazole (32).[9] The literature method was employed for the synthesis of 32, but the dihydrochloride of 32 could not be crystallized, and therefore, the free base was isolated as an oil and used directly in further syntheses.

Cu_2^{II}ISOIM(EtBim)$_2$OH$(BF_4)_2$ (33). 1-benzyl-2-(2'-aminoethyl)-imidazole (0.2 g, 1 mmole) was added to a suspension of 2-hydroxy-5-methylisophthalaldehyde in 15 ml of methanol. The resulting orange-yellow solution was heated at reflux for 10 min., followed by the addition of $Cu(H_2O)_6(BF_4)_2$ (0.35 g, 1 mmole), which yielded a blue-green solution. After heating this solution at reflux for 15 min., a small amount of white solid was removed by filtration, and the solvent was removed from the filtrate by rotary evaporation. The resulting green solid was dissolved in 25 ml of acetone, and a light-blue, micro-cyrstalline solid (33) came out of solution. This product was collected by filtration, washed with boiling acetone and dried under vacuum for several hours. Anal. Calcd. for $C_{33}H_{34}N_6O_2Cu_2B_2F_8$: C, 46.78; H, 4.02, N, 9.92. Found: C, 46.11; H, 3.95; N, 9.81.

Cu_2^{II}ISOIM(EtBim)$_2$(Cl)$_3$ (34). 1-benzyl-2-(2'-aminoethyl)-imidazole (0.2 g, 1 mmole) was added to a suspension of 2-hydroxy-5-methylisophthalaldehyde in 15 ml of methanol. The resulting orange-yellow solution was heated at reflux for 10 min., followed by the addition of $CuCl_2 \cdot 2H_2O$ (0.17 g, 1 mmole) which yielded a green

solution. After heating this solution at reflux for 15 min., the solvent was removed by rotary evaporation. Recrystallization of the resulting solid from ethanol gave an olive-green microcrystalline product, 34, which was collected by filtration, washed with ethanol and acetone, and dried overnight under vacuum. Anal. Calcd. for $C_{33}H_{33}N_6OCu_2Cl_3$: C, 51.93; H, 4.33; N, 11.02. Found: C, 51.60; H, 4.23; N, 11.01.

Cu_2^{I}ISOIM(EtMim)$_2$(pz) (35). 2-(2'-aminoethyl)-1-methylimidazole dihydrochloride (0.2 g, 1 mmole) was added to a solution of 2-hydroxy-5-methylisophthalaldehyde in 20 ml of methanol (in an oxygen-free glove box). To this solution was added sodium methoxide (0.11 g, 2 mmoles), which resulted in a yellow-orange solution. This solution was heated at reflux for 15 min., then allowed to come to ambient temperature over the next 15 min. Pyrazole (0.034 g, 0.5 mmole) and sodium methoxide (0.055 g, 1 mmole) were added and the solution was stirred for 5 min. Addition of a solution of $Cu(CH_3CN)_4BF_4$ in 15 ml of hot methanol yielded an immediate orange-brown solid. The mixture was cooled to ambient temperature, and the solid was collected by filtration. The orange-brown solid was dissolved in hot toluene and a white precipitate was removed by filtration. Removal of the solvent from the filtrate by evaporation under vacuum yielded solid product, which was recrystallized from methanol to give orange-brown needles of 35. This product was collected by filtration, washed with ethanol and dried under vacuum for several hours. Anal. Calcd. for $C_{24}H_{28}N_8OCu_2$: C, 50.44; H, 4.90; N, 19.61. Found: C, 49.01; H, 4.85; N, 19.43.

Oxygen Uptake Measurements. An accurately weighed sample (ca. 0.1 mmole) was placed in a 10 ml round-bottom flask along with a magnetic stir bar. This flask was connected to an 8 ml calibrated volume apparatus on the vacuum line, and the system was evacuated. Dry methylene chloride (stored over CaH_2) was vacuum transferred onto the sample to give a solution volume of ca. 7 ml. The sample chamber was isolated, and the calibrated volume was filled with a measured pressure of dioxygen (ca. 600 Torr) and then closed off. The temperature was also recorded. For the low temperature reactions, a dry ice-acetone bath was then placed around the reaction flask to keep the temperature at -79°C. The calibrated volume of O_2 was then exposed to the sample, and the solution was stirred for 6 hrs. The remaining dioxygen was then collected with a Toepler pump, with the methylene chloride being caught by three intervening liquid nitrogen traps. The gas was collected in a calibrated volume (13.76 ml), and the pressure and temperature were measured. The amount of dioxygen consumed was then calculated by difference.

Physical Measurements. Sample preparation for physical studies on the air-sensitive materials was accomplished in a Vacuum Atmospheres Dri-Lab inert atmosphere chamber, under a helium atmosphere. Helium saturated spectroquality solvents were used for solution studies.

Electronic spectra were recorded on a Cary 14 spectrophotometer. Solid state spectra were obtained from Nujol mulls on filter paper against a Nujol saturated filter paper as a blank. Infrared spectra were recorded on a Beckman IR-12 Infrared spectrophotometer. Solid

state spectra were obtained from Nujol mulls pressed between KBr plates. Proton magnetic resonance spectra were recorded on a Varian EM390 spectrophotometer at 90 MHz (34° C). The solvent utilized was CD_3CN containing TMS as the reference.

Elemental analyses were performed by the Caltech Microanalytical Laboratory.

Electrochemistry. A Princeton Applied Research (PAR) Model 174A polarographic analyzer was used for cyclic voltammetry and differential pulse voltammetry. For display purposes, a Hewlett-Packard 7004B X-Y recorder was utilized.

Cyclic voltammetry was done in a single compartment cell with a volume of ca. 5 ml. of DMF. The supporting electrolyte was 0.1 M TBAP. The working electrode consisted of a platinum button electrode or a hanging mercury drop electrode. In all cases, the auxiliary electrode was a coiled platinum wire, and the reference electrode consisted of a silver wire immersed in an acetonitrile solution containing $AgNO_3$ (0.01 M) and TBAP (0.1 M), all contained in a 9 mm glass tube fitted on the bottom with a fine porosity sintered glass frit.

All potentials are reported versus the normal hydrogen electrode, nhe. This was accomplished by the use of an internal reference redox couple, namely ferrocene, for which the formal potential is reported to be +0.400 V versus nhe in water.[16] It has been proposed that the ferrocene reduction potential changes very little in different solvents, and hence it is a good solvent independent redox couple.[16,17] Experimentally, small amounts (ca. 10^{-3} M) of ferrocene were added to solutions containing the compounds of interest and formal potentials for both couples were measured under the same conditions.

References and Notes

(1) Lontie, R. in "Inorganic Biochemistry", Eichhorn, G. I. ed.; Elsevier: New York, N.Y., 1973; p. 344.

(2) (a) Mason, H. S. Ann. Rev. Biochem. 1965, 35, 595-634.
(b) Vanneste, W. H. and Zuberbühler, A. in "Molecular Mechanisms of Oxygen Activation", Hayaishi, O. ed.; Academic Press: 1974; p. 371.

(3) (a) Fee, J. A. Structure and Bonding 1975, 23, 1-60.
(b) Vänngård, T. I. in "Biological Applications of Electron Spin Resonance Spectroscopy", Swartz, H. M.; Bolton, J. R.; and Borg, D. C., eds.: J. Wiley: New York, N.Y., 1972; p. 411.

(4) Metal-catalyzed autoxidations of similar activated positions have been reported. See: Sprecher, C. A.; Zuberbühler, A. D. Angew. Chem. Int. Ed. Engl. 1977, 16, 189. Urbach, F. L.; Knopp, U.; Zuberbühler, A. D. Helv. Chim. Acta 1978, 61, 1097-1106.

(5) There appears to be little, if any, precedent for this alkyl carbon hydroxylation. For a discussion of metal-catalyzed autoxidation of organic substrates, see: Sheldon, R. A.; Kochi, J. K. Adv. Cat. 1976, 25, 272-413.

(6) For a discussion of related ligand "ketonations" see: Lisensky, G. C., Ph.D. Dissertation, California Institute of Technology, 1981, and references cited therein.

(7) Eickman, N. C.; Himmelwright, R. S.; Solomon, E. I. Proc. Natl. Acad. Sci. USA, 1979, 76, 2094-2098. Brown,

References (continued)

J. M.; Powers, L.; Kincaid, B.; Larrabee, J. A.; Spiro, T. G. J. Amer. Chem. Soc. 1980, 102, 4210-4216. Larrabee, J. A.; Spiro, T. G. J. Amer. Chem. Soc. 1980, 102, 4217-4223.

(8) Jocelyn, P. C. J. Chem. Soc. 1957, 3305-3307.

(9) Kornfeld, E. C.; Wolf, L.; Lin, T. M.; Slater, I. H. J. Med. Chem. 1968, 11, 1028-1031.

(10) Ellen, P.; Braldey, D.; Hursthouse, M.; Meek, D. Coord. Chem. Rev. 1977, 24, 1-95. Jardine, F. Adv. Inorg. Chem. Radiochem. 1975, 17, 115-163.

(11) Ullmann, F.; Brittner, K. Chem. Ber. 1909, 42, 2539-2548.

(12) Spiro, C. L.; Ph.D. Dissertation, California Institute of Technology, 1981, p. 86.

(13) Hathaway, B. I.; Holah, D. G.; Postlethwaite, J. D. J. Chem. Soc. 1961, 3215-3218.

(14) Niemers, E.; Hiltmann, R. Synthesis 1976, 593-595.

(15) Secrist, J. A.; Logue, M. W. J. Org. Chem. 1972, 37, 335-336.

(16) Koepp, H. M.; Wendt, H.; Strehlow, H. Z. Electrochem. 1960, 64, 483-491.

(17) Gagné, R. R.; Koval, C. A.; Lisensky, G. C. Inorg. Chem. 1980, 19, in press.

CHAPTER V

Summary and Conclusions

This thesis has presented the design and synthesis of a number of binuclear copper(I) complexes as potential models for binuclear copper protein sites. Indeed, system 1 may represent the best synthetic "models" available for the reduced protein site. The most

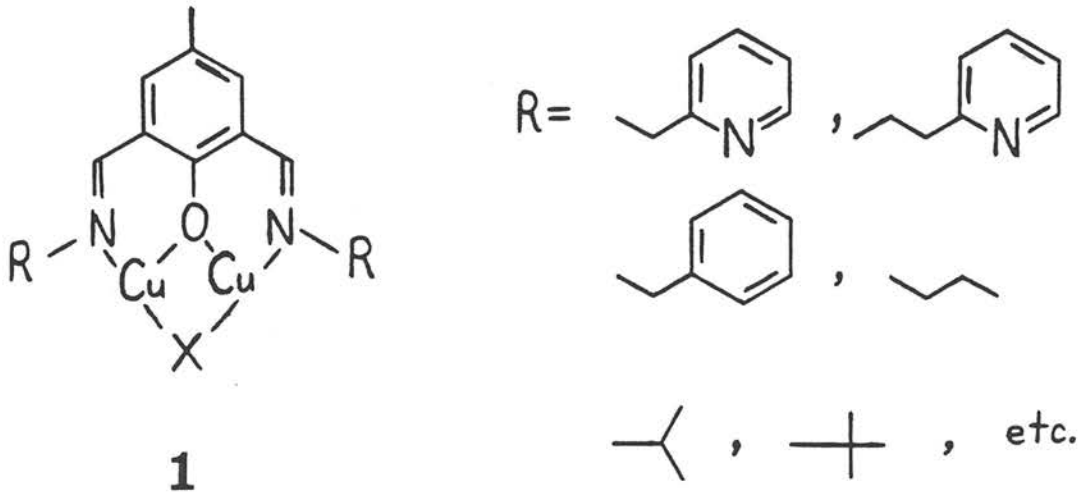

1

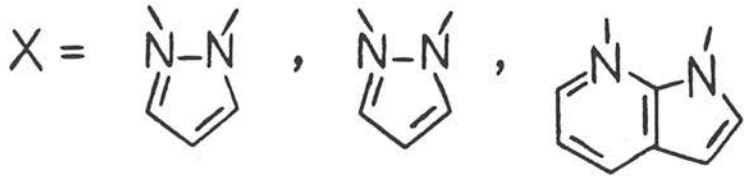

recent physical studies on hemocyanin point to two or three coordinate copper(I) ions bound to imidazole ligands.[1] Also, a bridging ligand such as a tyrosine oxygen appears to be present in oxyhemocyanin.[1,2] Thus, the series of complexes, 1, presented in Chapter II, closely

approximates the proposed ligand environment for hemocyanin. The positive reduction potentials exhibited by the compounds (ca. 0 V vs. nhe) approach the value recorded for tyrosine (+0.36 V). This system fails, however, to mimic the dioxygen and carbon monoxide reactivity of these proteins. Reversible oxygenation was not observed, and this may have been due to the presence of dissociable ligands and activated positions (toward oxidation) as well as the lack of steric hindrance to prevent the four-electron reduction of oxygen to water. While hemocyanin appears to bind one CO per binuclear site,[3] synthetic complexes (1) are unreactive toward CO.

The three-coordinate arrangement of nitrogen and oxygen ligands in 1 appears to provide a very stable environment for copper(I) (displayed in the rather positive reduction potentials). This ligand environment also fosters an intermolecular Cu-Cu interaction. The crystal structure of 1 where R = 2-(2′-pyridyl) ethyl suggested a much stronger interaction between the nitrogen ligands and the copper(I) centers compared to the interaction between the oxygen and the coppers. Hence, the stability and unusual reactivity of these compounds may result from the nearly linear arrangement of nitrogen ligands.

The apparent preference of copper(I) for a two-coordinate environment of nitrogen ligands is evident in the crystal structure of 2. Again, a direct Cu-Cu interaction was observed. This complex contrasts the earlier system (1), and 2 reacts with carbon monoxide to yield the four-coordinate copper(I) centers in 3.

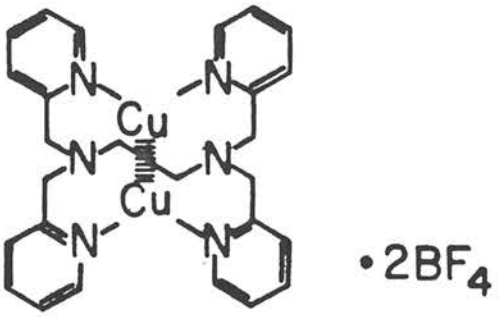

2

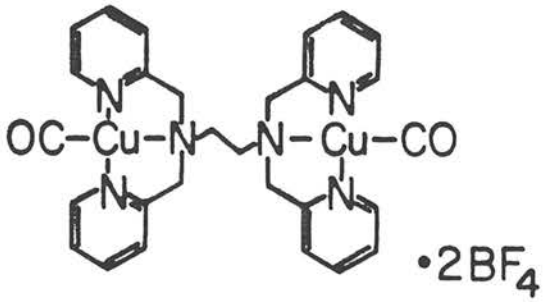

3

Based on the chemistry observed for system 1 as well as recent protein studies,[1,2] complexes 4 and 5 were designed as possible

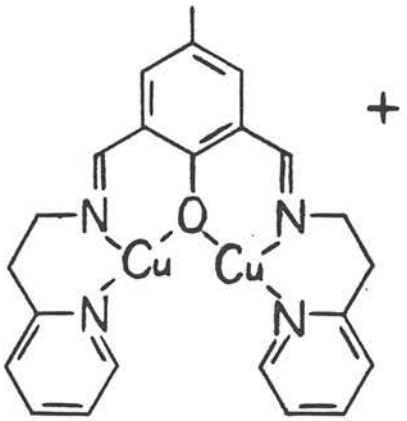

4

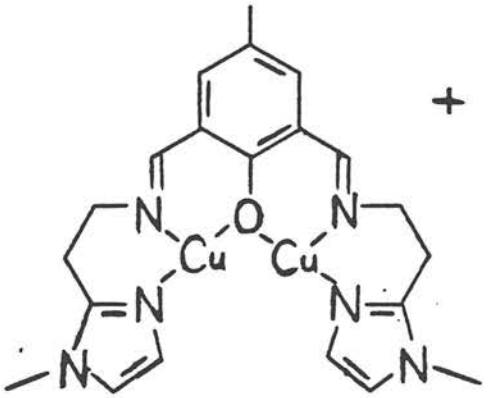

5

improved models for the binuclear copper active sites. Although the synthesis of the ligands for 4 and 5 was accomplished, the isolation of the cuprous complexes was not realized. This may reflect a thermodynamic instability of the desired products (4 and 5) or the difficulties involved in the synthesis of such copper(I) species.

Future research in this area should involve the synthesis of new

copper(I) complexes for the investigation of their dioxygen reactivity, taking into account the results presented above. Binuclear copper(I) systems such as 6 and 7 are proposed by this author. These ligands

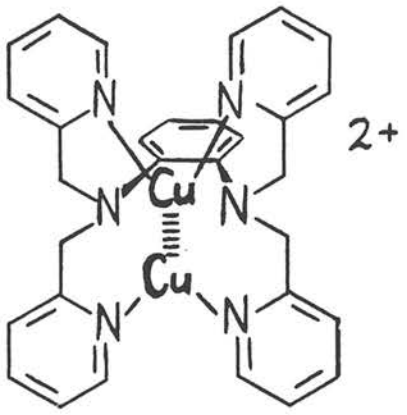

6

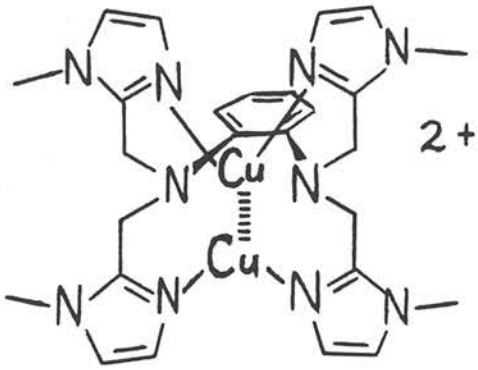

7

could provide a stable, two-coordinate environment for the Cu^I ions, and the ligand structure should be somewhat rigid due to the phenylene bridge and steric repulsions between the heterocyclic rings. This latter factor may prevent major ligand reorganization upon dissolution or reaction with O_2 or CO. Finally, the ligand can provide steric bulk around a dioxygen molecule bound in the "pocket" between the two coppers.

References

(1) Brown, J. M.; Powers, L.; Kincaid, B.; Larrabee, J. A.; Spiro, T. G. J. Amer. Chem. Soc. 1980, 102, 4210-4216.

(2) Eickman, N.; Himmelwright, R. S.; Solomon, E. I. Proc. Natl. Acad. Sci. USA 1979, 76, 2094-2098. Larrabee, J. A.; Spiro, T. G. J. Amer. Chem. Soc., 1980, 102, 4217-4223.

(3) Alben, J. O.; Yen, L.; Farrier, N. J. J. Amer. Chem. Soc. 1970, 92, 4475-4476. Fager, L. Y.; Alben, J. O. Biochemistry 1972, 11, 4786-4792.

APPENDIX I

Investigation of a Reported One-Step Two-Electron Reduction

The binuclear copper complex, 1, has been reported by Lintvedt et al.[1] to undergo a one-step, two-electron reduction at $E_{\frac{1}{2}} = -0.61$ V versus the standard calomel electrode (sce). This corresponds to

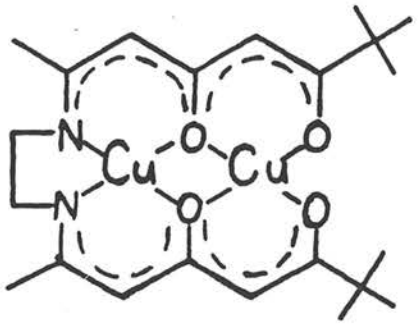

1 = $Cu_2(PAA)_2en$

approximately -0.34 V vs. nhe. This result is quite surprising since the complex is reported to be completely diamagnetic at room temperature, showing no EPR signal and sharp NMR signals. The electrochemistry observed here is in contrast to that expected for two metals which are interacting to such a large extent (indicated by the diamagnetism). Usually, the reduction of one of the metals results in a more negative environment around the remaining unreduced metal (compared to the environment about the first metal, prior to reduction), and this second metal is reduced at a more negative potential.[2] Two possible explanations for this anomalous behavior were postulated by our laboratory.[3] a) The reduction of the first Cu^{II} to Cu^{I} and its concomitant adoption of tetrahedral geometry could force a more tetrahedral geometry around the remaining Cu^{II}, making its reduction

easier. b) Due to the asymmetric nature of this complex, access to the electrode may be hindered at one of the coppers, and if the electrons are forced to enter via the Cu^{II} which is inherently more difficult to reduce, one potential may be observed for the reduction of both metals.

A one-step, two-electron reduction of a binuclear cupric complex was of great interest due to its analogy with the electrochemistry exhibited by the binuclear copper protein sites.[4] For this reason, we set out to ascertain if, indeed, the reduction of 1 was a one-step, two-electron process.

Complex 1 was synthesized by published methods (Scheme 1).[1,5] The triketone was synthesized by a modified Claisen type condensation,

Scheme 1

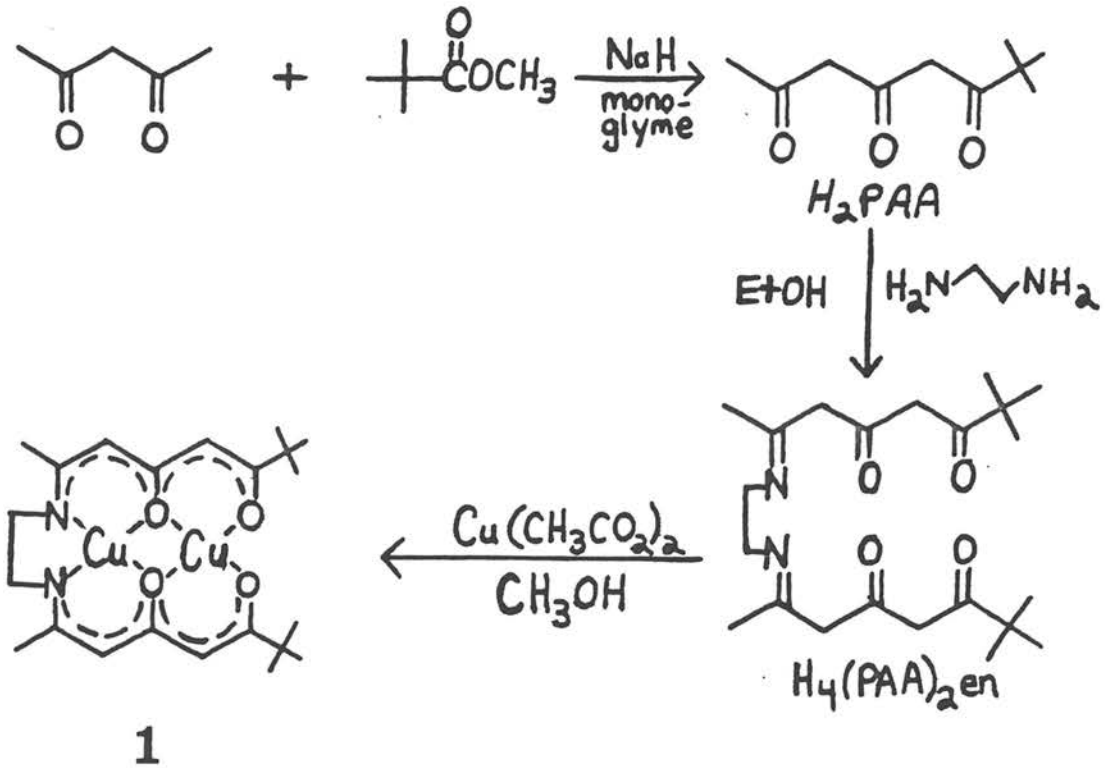

1

and this was followed directly by a Schiff base condensation with ethylenediamine. Treatment of the ligand with cupric acetate gave the desired complex, $\underset{\sim}{1}$. $Cu_2(PAA)_2en$ (H_2PAA = pivaloylacetylacetone and en = ethylenediamine).

This complex ($\underset{\sim}{1}$) appears to be only slightly paramagnetic, showing a fairly well resolved nuclear magnetic resonance (NMR) spectrum (see Figure 1). Note that the two downfield peaks due to the methine protons (A) and the methylene protons (B) are quite broad due to the possible influence of paramagnetic copper centers. It was found that this complex does give an electron paramagnetic resonance (EPR) spectrum, although the signal is quite weak (Figure 2). Note the multitude of superhyperfine splitting (vide infra).

Cyclic voltammetry of $\underset{\sim}{1}$ at a hanging mercury drop electrode is shown in Figure 3. The formal reduction potential was ca. -1.04 V vs. nhe. The measured potential was converted to vs. nhe using E^f = +0.40 V vs. nhe for ferrocene.[6,7] Cyclic voltammetry with sce as reference electrode yielded E_f = -0.93 V vs. sce. However this latter value is rather uncertain due to the unknown junction potential which exists between the aqueous calomel electrode and the dimethylformamide solution.[8] (The uncertainty which arises from the use of this electrode in a non-aqueous solvent such as DMF is evident in the 300 mV difference between the value obtained here and that from the previous study.)[1]

The peak separation (E_{p_a}-E_{p_c}) at a scan rate, ν, of 50 mV per second was 80 mV. Unfortunately this peak separation is not directly

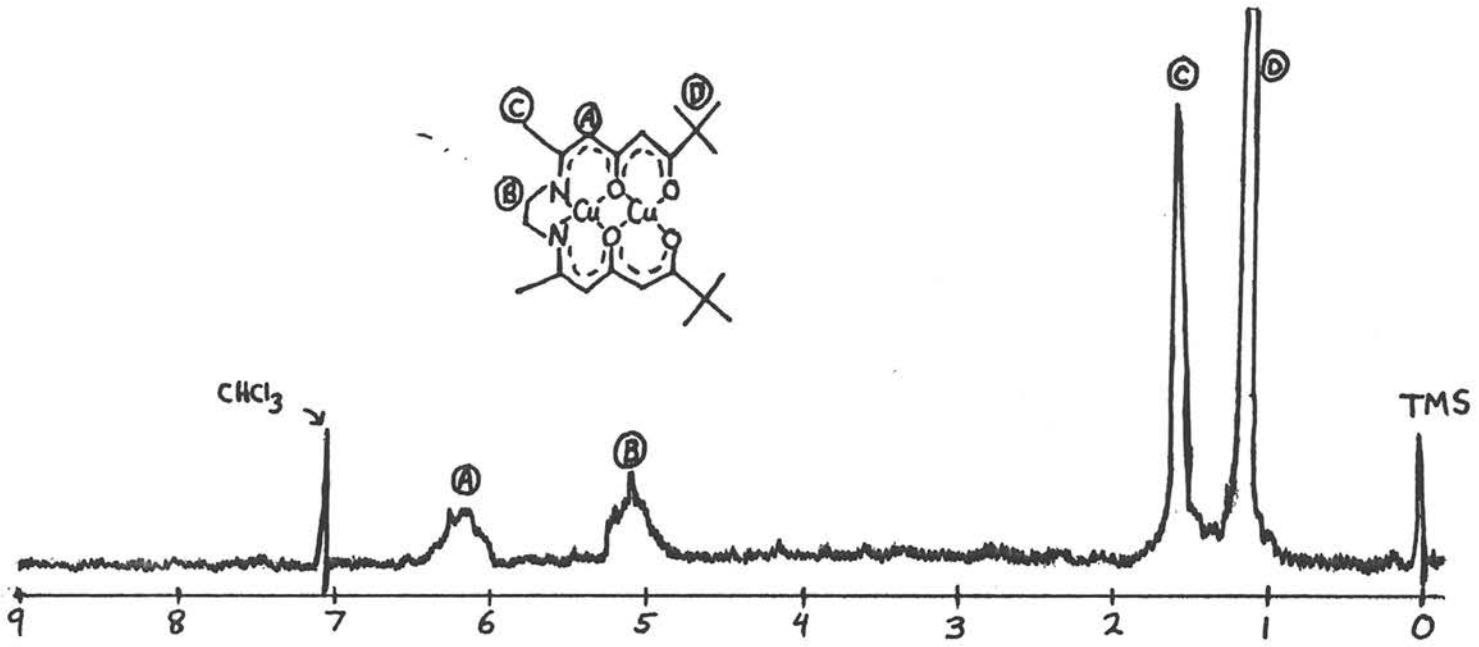

Figure 1. NMR spectrum of 1, in $CDCl_3$, (34°C).

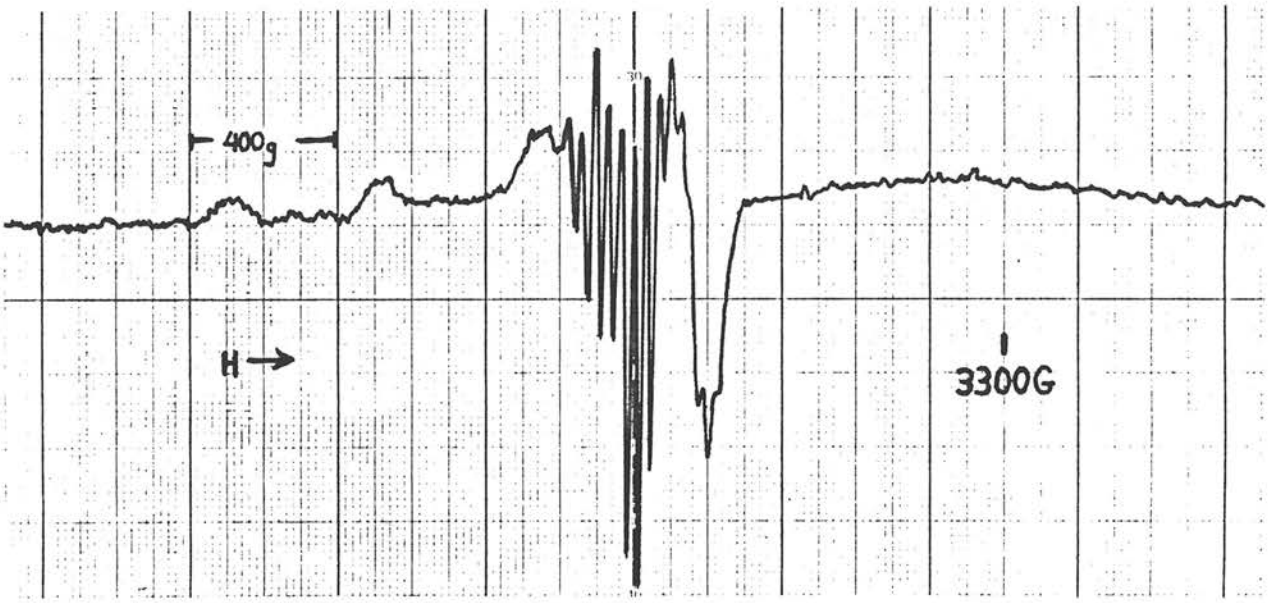

Figure 2. EPR spectrum of $Cu_2(PAA)_2en$ (1) in CH_2Cl_2 at 77°K (microwave frequency = 9.172 GHz).

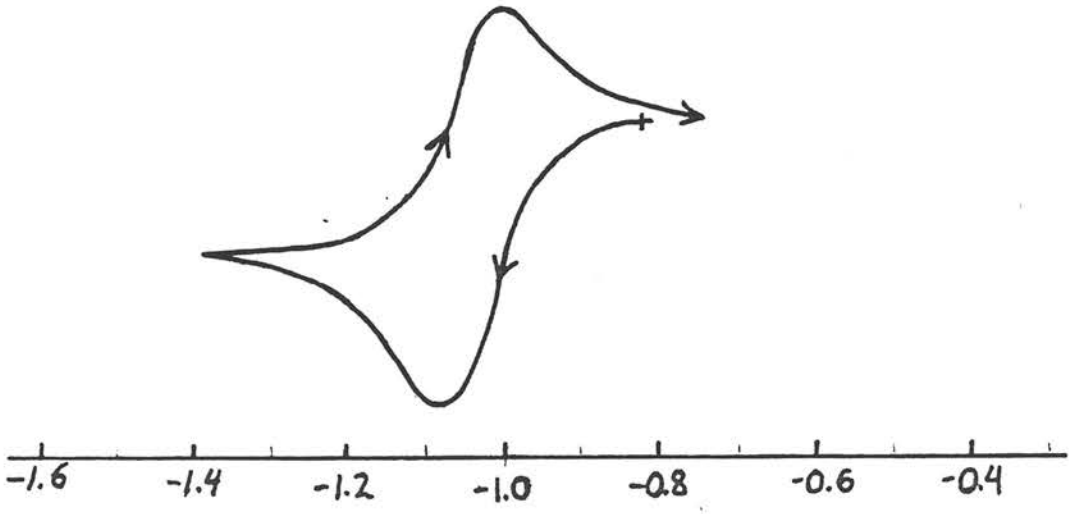

Figure 3. Cyclic voltammogram of $Cu_2(PAA)_2en$ (1) in DMF solution containing 0.1 M TBAP as the electrolyte. A hanging mercury drop electrode was used and the scan rate was 100 mV/sec.

indicative of the number of electrons involved in the process (n value). It is also related to other factors such as the scan rate, resistance between the electrodes and of course the rate of electron transfer. The value obtained here is larger than that expected for a reversible one-electron process (58 mV) or a reversible two-electron process (29 mV).[9] For this reason, constant potential electrolysis (cpe) was performed on a DMF solution of $\underset{\sim}{1}$ to determine the n value. After passing the number of coulombs corresponding to a 1-electron reduction, the current dropped to a very slow rate, and copper metal plated out on the glass walls of the electrochemical cell as further electrolysis was done. It appears that the binuclear Cu^{II} complex was being reduced by one electron to produce an unstable mixed valence species. This complex may then slowly disproportionate to give copper metal and Cu^{II} complexes which can undergo further electrolysis. For instance, consider Scheme 2.

Scheme 2

$$Cu^{II}Cu^{II}L \xrightarrow[cpe]{+1e^-} Cu^{II}Cu^{I}L^-$$

$$2Cu^{II}Cu^{I}L^- \longrightarrow Cu^0 + Cu^{II}L^{2-} + Cu^{II}Cu^{II}L$$

$$\longrightarrow \text{further reductions} \quad (L = (PAA)_2en)$$

A sample of the electrolyzed solution (after one equivalent of electrons was passed and the current had slowed to a minimum) was removed and analyzed by EPR, and an interesting result was obtained. The spectrum, including super-hyperfine peaks was identical to

Figure 2, obtained for the original binuclear Cu^{II} complex, but the signal was ca. 200 times stronger (for identical concentrations). Due to the observed super-hyperfine peaks, the reduction product appears to be the mixed valence species, 2. Very similar EPR spectra

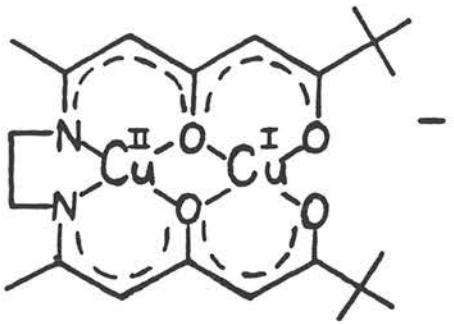

2

were observed by Lintvedt et al.[1] for both the mononuclear Cu^{II}-$[H_2(PAA)_2en]$ and the mixed metal $Cu^{II}Zn^{II}(PAA)_2en$. The Cu^{II} is believed to be nitrogen coordinated in both of these compounds. The observed EPR signal after reduction may also be due to the mononuclear Cu^{II} complex following a disproportionation reaction (see Scheme 2). Attempts to isolate 2 were unsuccessful due to further disproportionation reactions. The fact that the original binuclear Cu^{II} complex, 1, exhibited the same spectrum may be due to mononuclear impurities.

The investigation of this system was halted at this point since the complex does not appear to be reduced by a reversible two-electron process, as reported. In addition, the reduction potential (ca. -1.04 V vs. nhe) is very negative, indicating the destabilization of Cu^{I} by this ligand (which is in agreement with the observed disproportionation

upon reduction of 1). This is not surprising due to the fairly rigid, planar ligand which utilizes relatively "hard" donor atoms. The formal negative charge on the ligand (-4) should also resist the addition of electrons to the system. Neither the negative reduction potentials nor the type of ligands about the coppers are conducive to a model for copper proteins.

Experimental

All chemicals were reagent grade and were used as received unless otherwise noted. Tetrabutylammonium perchlorate (TBAP, Southwestern Analytical Chemicals) was dried exhaustively under vacuum (25° C) before use. Reagent grade N,N-dimethylformamide (DMF) was dried over $MgSO_4$ and 4A molecular sieves for 24 hrs and then vacuum distilled.

$Cu_2(PAA)_2en$, 1. The ligand, $H_4(PAA)_2en$, was synthesized by the literature methods[1,5] without isolation of the intermediate, H_2PAA. Cupric acetate monohydrate (0.40 g, 2 mmoles) was dissolved in 50 ml of hot methanol. To this solution was added $H_4(PAA)_2en$ (0.37 g, 1 mmole), resulting in a green solution. After cooling to 5° C, green crystals of 1 were collected, and the product was recrystallized from chloroform and washed with methanol. After drying under vacuum overnight, the yield was 0.45 g (87%) of yellow-green needles. These needles decompose at ca. 244° C. Anal. Calcd. for $C_{22}H_{32}N_2O_4Cu_2$: C, 51.25; H, 6.26, N, 5.43; Cu, 24.65. Found: C, 50.88; H, 6.07; N, 5.34; Cu, 24.3.

Physical Measurements. The NMR spectrum was recorded on a Varian EM 390 spectrophotometer at 90 mHz (34° C). The solvent utilized was $CDCl_3$ containing Me_4Si as the reference. The X-band EPR spectra were recorded on a Varian E-line spectrophotometer. The EPR spectrum of the reduced species, 5, was recorded under an atmosphere of helium. Elemental Analysis was performed by the Caltech Microanalytical Laboratory.

Electrochemistry. All electrochemical measurements were performed under helium in a Vacuum Atmospheres Dri-Lab inert atmosphere chamber. A Princeton Applied Research (PAR) Model 174A polarographic analyzer was used for cyclic voltammetry. For display purposes, a Hewlett-Packard 7004B X-Y recorder was utilized. The apparatus used for constant potential electrolysis (cpe) consisted of a PAR Model 173 potentiostat-galvanostat coupled with a Model 179 digital coulometer.

Cyclic voltammetry was done in a single compartment cell with a volume of ca. 5 ml of DMF. The supporting electrolyte was 0.1 M TBAP. The working electrode consisted of a platinum button electrode or a hanging mercury drop electrode. In all cases, the auxiliary electrode was a coiled platinum wire and the reference electrode consisted of a silver wire immersed in an acetonitrile solution containing $AgNO_3$ (0.01 M) and TBAP (0.1 M), all contained in a 9 mm glass tube fitted on the bottom with a fine porosity sintered glass frit. The apparatus employed for constant potential electrolysis was similar, except a two-compartment H-cell was used to isolate the auxiliary electrode from the working compartment. A mercury pool was used as the working electrode for cpe.

All potentials are reported versus the normal hydrogen electrode, nhe. This was accomplished by the use of an internal reference redox couple, namely ferrocene, for which the formal potential is reported to be +0.400 V versus nhe in water.[6] It has been proposed that the ferrocene reduction potential changes very little in different solvents, and hence it is a good solvent-independent redox couple.[7]

Experimentally, small amounts (ca. 10^{-3} M) of ferrocene were added to solutions containing the compounds of interest, and formal potentials for both couples were measured under the same conditions.

References

(1) Lintvedt, R. L.; Tomlonovic, B.; Fenton, D. E.; Glick, M. D. Adv. Chem. Series 1975, 150, 407-425.

(2) For example see: Creutz, C.; Taube, H. J. Amer. Chem. Soc. 1973, 95, 1086-1094. Gagné, R. R.; Koval, C. A.; Smith, T. J.; Cimolino, M. C. J. Amer. Chem. Soc. 1979, 101, 4571-4580.

(3) Gagné, R. R., personal communication.

(4) See the discussion in Chapter I and references cited therein.

(5) Miles, M. L.; Harris, T. M.; Hauser, C. R. J. Org. Chem. 1960, 30, 1007-1011.

(6) Koepp, H. M.; Wendt, H.; Strehlow, H. Z. Electrochem. 1960, 64, 483-491.

(7) For a discussion of the use of ferrocene as an internal standard for electrochemistry see: Gagné, R. R.; Koval, C. A.; Lisensky, G. C. Inorg. Chem. 1980, 19, in press.

(8) Badoz-Lamblingand, J.; Bardin, J. C. Compt. Rend. Acad. Sci. 1973, 276C, 583-586. Alfenaar, M.; de Ligny, C.; Remynse, A. Rec. Trav. Chim. Pays-Bas 1967, 86, 986-992.

(9) Anson, F. C. "Electroanalytical Chemistry", A.C.S. Audio Course, 1976, Section G.

APPENDIX II

An Approach to the Synthesis of Binuclear, Tetrahedral Copper(I) Complexes

The quest for reversible oxygenation in synthetic copper(I) complexes has met with little success.[1] This is disappointing, since the protein hemocyanin employs copper in its function to bind dioxygen reversibly.[2] Careful design of the ligand system may be necessary for the realization of this behavior in model compounds. Complexes such as 1 are proposed by this author as viable candidates for reversible

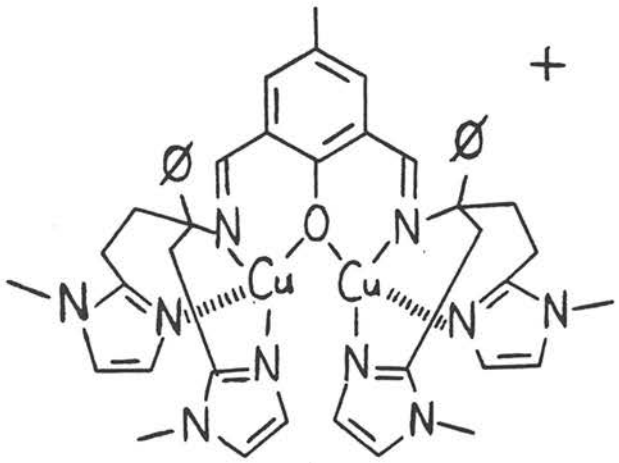

1

oxygenation. This complex includes a number of factors, based on protein and synthetic copper(I) investigations, which may be important for obtaining clean, reversible oxygenation. (a) A binuclear complex is suggested by the fact that hemocyanin appears to contain a binuclear copper active site.[2] (b) A tetrahedral ligand environment has been found to be favorable for copper(I)[3] leading to high reduction potentials,[4]

which may be desirable for reversible dioxygen binding.[5] (c) The four imidazole ligands may provide steric bulk around a dioxygen molecule bound between the two coppers. This may be necessary to prevent further reactions of bound dioxygen.[6] (d) The ligands provided by the polydentate chelate in $\underset{\sim}{1}$ are almost identical to those proposed for hemocyanin.[7] (e) The system avoids dissociable ligands and obvious activated positions (which might be subject to autoxidation).[8]

The synthesis of the binuclear copper complex, $\underset{\sim}{1}$, requires the prior synthesis of the primary amine, α,α-bis-[2-(1-methylimidazolyl)-methyl]benzylamine, $\underset{\sim}{2}$, which could then be condensed with 2-hydroxy-5-methylisophthalaldehyde to generate the polydentate ligand in $\underset{\sim}{1}$. An attempt to synthesize $\underset{\sim}{2}$ is presented in Scheme 1. Unfortunately, this approach failed at the final step. Apparently, the large amount of steric hindrance adjacent to the amide prevents its degradation to the desired amine, $\underset{\sim}{2}$. This result was surprising since the conversion of amides to amines has been affected at hindered and heterocyclic amides.[9] The reaction was also attempted using methanol as the solvent, but again starting material was recovered.

Although this attempt did not yield the desired amine, $\underset{\sim}{2}$, slight alterations in the reaction route or in the target amine may yield a bis-imidazolyl primary amine. This method may then afford interesting binuclear copper(I) complexes for investigation of their dioxygen reactivity.

Scheme 1

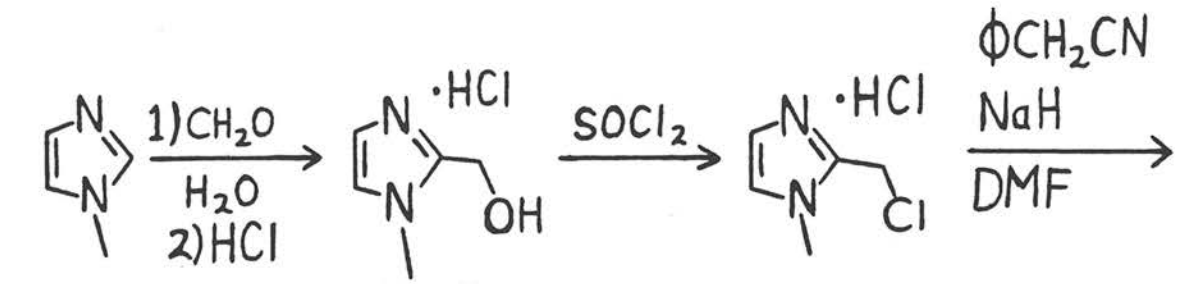
1) CH_2O
H_2O
2) HCl
·HCl
$SOCl_2$
·HCl
ϕCH_2CN
NaH
DMF
OH
Cl

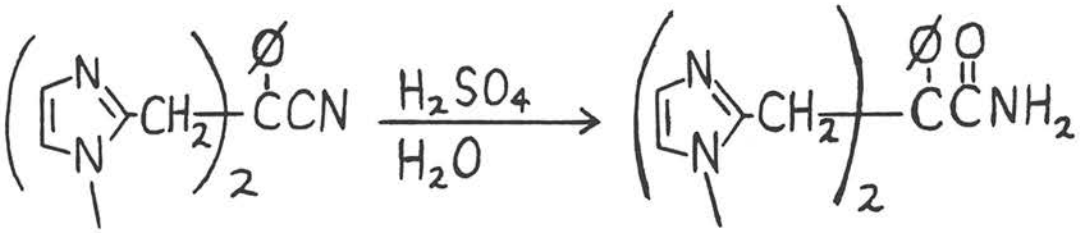
H_2SO_4
H_2O

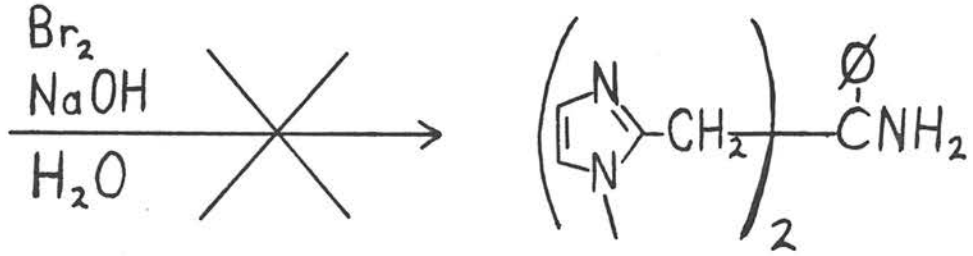
Br_2
NaOH
H_2O

2

Experimental

All chemicals were reagent grade and were used as received unless otherwise noted. N,N-dimethylformamide (DMF) was dried over $MgSO_4$ and 4A molecular sieves for 24 h and then vacuum distilled. The preparation of 2-hydroxymethyl-1-methylimidazole hydrochloride and 2-chloromethyl-1-methylimidazole hydrochloride is described in Chapter IV. Proton magnetic resonance spectra were recorded on a Varian EM390 spectrophotometer at 90 MHz (34° C, $CDCl_3$). Elemental analyses were performed by the Caltech Microanalytical Laboratory.

α,α-bis-[2-(1-methylimidazolyl)methyl]benzylcyanide.[10]

Sodium hydride (36g, 0.75 moles) was added to 500 ml of dry ($MgSO_4$) DMF under an atmosphere of nitrogen. Phenylacetonitrile (17.2 ml, 0.15 moles) was added dropwise from a dropping funnel while stirring the mixture. When the evolution of H_2 became slow, 2-chloromethyl-1-methylimidazole hydrochloride (50 g, 0.3 moles) was added in small portions over 90 min., keeping the temperature at 40-50° C by the heat from the exothermic reaction. The mixture was then heated at 80-90° C for 2 hrs and cooled to ambient temperature. Water (5 ml) was added to quench the excess NaH. The solvent was removed by rotary evaporation and 300 ml of water was added. The solution was rendered acidic with conc. HCl and extracted with 2 × 50 ml of chloroform. The chloroform extracts were discarded, and the aqueous phase was rendered alkaline by the addition of aqueous NaOH. The aqueous phase was then extracted with 4 × 50 ml of chloroform. The combined chloroform extracts were dried ($MgSO_4$), filtered,and the solvent was

removed by rotary evaporation. Addition of diethyl ether (300 ml) with stirring yielded off-white solid which was collected by filtration and washed with diethyl ether. Recrystallization from toluene gave off-white crystals of α,α-bis-[2-(1-methylimidazolyl)methyl]benzylcyanide (28 g, 61% yield). The product was washed with diethyl ether and dried overnight under vacuum. Anal. Calcd. for $C_{18}H_{19}N_5$: C, 70.82; H, 6.23; N, 22.95. Found: C, 70.71; H, 6.27, N. 22.53.

α,α-bis-[2-(1-methylimidazolyl)methyl]phenylacetamide.[11] α-α-bis-[2-(1-methylimidazolyl)methyl]benzylcyanide (12 g, 0.04 moles) was mixed with 60 ml of 80% H_2SO_4 (aq) under N_2 at ambient temperature. Most of the solid dissolved and the mixture was stirred and heated at 100° C for 90 min. The reaction mixture was then cooled in an ice bath and added to a stirred solution of 450 ml of 4N NaOH which was also cooled in an ice bath. The aqueous mixture was extracted with 4 × 50 ml of $CHCl_3$. The combined chloroform extracts were dried ($MgSO_4$), and evaporation of the solvent resulted in an oil which crystallized upon addition of a solution of 10 ml CH_2Cl_2 and 20 ml of diethylether. After cooling to 0° C, the white crystals of α,α-bis-[2-(1-methyl-imidazolyl)methyl]phenylacetamide (7.8 g, 61%) were collected by filtration, washed with diethyl ether and dried under vacuum overnight. Anal. Calcd. for $C_{18}H_{21}N_5O$: C, 66.87; H, 6.50; N, 21.67. Found: C, 66.88; H, 6.42; N, 21.99.

Attempted Synthesis of α,α-bis-[2-(1-methyl-imidazoyl)methyl]-benzylamine, 2.[9] Sodium hydroxide (0.095 g, 2.4 mmoles) was dissolved in 2 ml of water. The solution was cooled to 0° C and

bromine (0.12 g, 1.5 mmoles) was added followed by α,α-bis-[2-(1-methylimidazolyl)methyl]phenylacetamide (0.2 g, 0.6 mmoles). The mixture was stirred at 0° C for 30 min., then at 80° C for one hour. The mixture was cooled, acidified (conc. HCl) and washed with $CHCl_3$ (5 ml). The aqueous layer was then made basic (NaOH) and extracted with 2 × 5 ml of $CHCl_3$. The combined chloroform extracts were dried ($MgSO_4$) and the solvent was removed by rotary evaporation. NMR of the resulting oil indicated mainly starting material. Starting material was also recovered in an analogous procedure using methanol as the solvent.

References

(1) See: Simmons, M. G.; Wilson, L. J. J. Chem. Soc., Chem. Commun. 1978, 634-636, and references cited therein.

(2) Lontie, R. in "Inorganic Biochemistry", Eichhorn, G. I., Ed.; American Elsevier: New York, 1973, p. 344.

(3) Jardine, F. H. Adv. Inorg. Chem. Radiochem. 1975, 17, 115-163.

(4) Patterson, G. S.; Holm, R. H. Bioinorg. Chem. 1975, 4, 257-275.

(5) Reversibility of oxygenation in cobalt complexes was shown to be related to reduction potentials: Carter, M. J.; Rillema, D. P.; Basolo, F. J. Amer. Chem. Soc. 1974, 96, 392-400.

(6) This strategy was successful in preventing the irreversible decomposition of dioxygen adducts with iron porphyrins. See: Collman, J. P.; Gagné, R. R., Reed, C. A.; Halbert, T. R.; Lang, G.; Robinson, W. T., J. Amer. Chem. Soc. 1975, 97, 1427-1439.

(7) See: Brown, J. M.; Powers, L.; Kincaid, B.; Larrabee, J. A.; Spiro, T. G. J. Amer. Chem. Soc. 1980, 102, 4210-4216, and references cited therein.

(8) See Chapter IV of this thesis.

(9) Wallis, E. S.; Lane, J. F. Org. React. 1946, 3, 267-306.

(10) Zugg, H. E.; Dunnigan, D. A.; Michaels, R. J.; Swett, L. R.; Wang, T. S.; Sommers, A. H.; DeNet, R. W. J. Org. Chem. 1958, 26, 644-651.

(11) Sperber, N.; Papa, D.; Schwenk, E. J. Amer. Chem. Soc. 1948, 70, 3091-3097.

PROPOSITIONS

Abstracts

Proposition 1. The synthesis of transition metal complexes derived from "face-to-face" 1,10-phenanthroline macrocycles is proposed. The compounds will be investigated as catalysts for the reduction of oxygen to water.

Proposition 2. The synthesis of gold metallocycles and an investigation of their stability and reactivity patterns are proposed.

Proposition 3. The synthesis of models for blue copper proteins is proposed.

Proposition 4. The use of macrocyclic copper(I) complexes for the photosensitization of norbornadiene to quadricyclene is proposed.

Proposition 5. An investigation into the mechanism of the reaction between transition metal formyl complexes and carbon electrophiles is proposed.

PROPOSITION 1

Metal Complexes Derived from Face-to-Face 1,10-Phenanthroline Macrocycles

The development of fuel cell technology would represent a significant advance towards more efficient, less polluting energy.[1] A fuel cell has the potential of efficiently and cleanly converting the energy stored in fuels into useful electrical energy by the electrochemical oxidation of these fuels (e.g., H_2, hydrocarbons) with oxygen. For the fuel cell to become an efficient device for energy conversion, a catalyst must be found for the reduction of oxygen to water (equation 1). This four-electron process is

$$O_2 + 4e^- + 4H^+ \rightarrow 2H_2O \qquad (1)$$

likely to require a catalyst which can deliver four electrons to the oxygen molecule and avoid high-energy peroxide and superoxide intermediates.[2] Polynuclear transition metal complexes are good candidates for such multi-electron transfer.[3] In this light it is interesting to note that the reduction of oxygen to water is catalyzed by the natural enzyme, laccase, which contains four copper atoms per molecule, all of which appear to be necessary for enzymatic activity.[4]

This rationale has led to the synthesis of novel binucleating ligands capable of holding two metal ions in close proximity, such that these ions can react with dioxygen and possibly deliver two electrons per metal to the bound dioxygen moiety.[2,5,6] The following "face-to-face" cobalt porphyrin has been synthesized by Collman et al., and

indeed it was found to catalyze the reduction of oxygen to water at a graphite disk electrode.[6] Electrons were supplied by the electrode

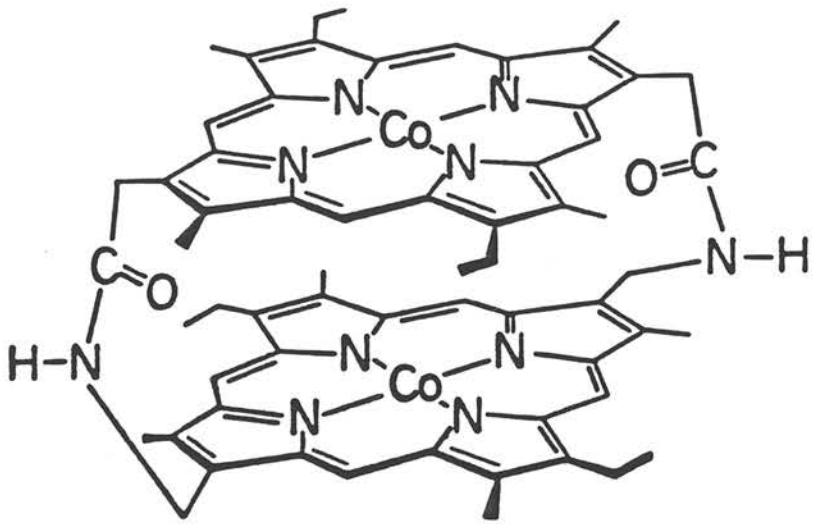

1

at a potential of ca. 0.6 volts vs. nhe, and molecular oxygen was reduced catalytically to water. This was performed at a rotating ring-disk electrode,[7] and the production of (unwanted) hydrogen peroxide was monitored at the outer ring. By this technique, it was determined that very little H_2O_2 was produced, and that oxygen was reduced to water at a turnover rate of 30/site/sec! The exact mechanism of this reaction is not known with certainty.

These results are very encouraging, but certain problems need to be overcome. The reduction of oxygen does not commence until the electrode potential is more negative than +0.7 volts vs. nhe, and this potential is well below the standard reduction potential for the four-electron reduction of oxygen to water (1.23 volts vs. nhe). For optimum voltage output from a fuel cell, the catalyst should

operate at a potential as close to 1.23 volts as possible, while still reacting rapidly with O_2. The potential at which oxygen is reduced by this system is probably limited by the Co^{3+}/Co^{2+} reduction potential of ca. 0.6 volts for these cobalt porphyrin complexes. Catalysts which exhibit more positive reduction potentials are ultimately desirable. In addition, the catalyst suffers from a gradual loss in activity, possibly due to oxidative degradation of the ligand by H_2O_2 or desorption of the catalyst from the electrode surface. Finally, the synthesis of these "face-to-face" porphyrins is a very tedious procedure involving many steps. A more simple ligand synthesis will likely be required for practical use of such catalysts.

In an effort to surmount some of these problems inherent in the "face-to-face" porphyrin system, I propose the synthesis of "face-to-face" 1,10-phenanthroline macrocycles. The synthesis of such ligands could be accomplished by condensation of 2,9-dichlorophenanthroline and a diamine such as 1,3-diaminopropane or o-phenylene diamine (equation 2).[8] Polymerization reactions will certainly be a complication

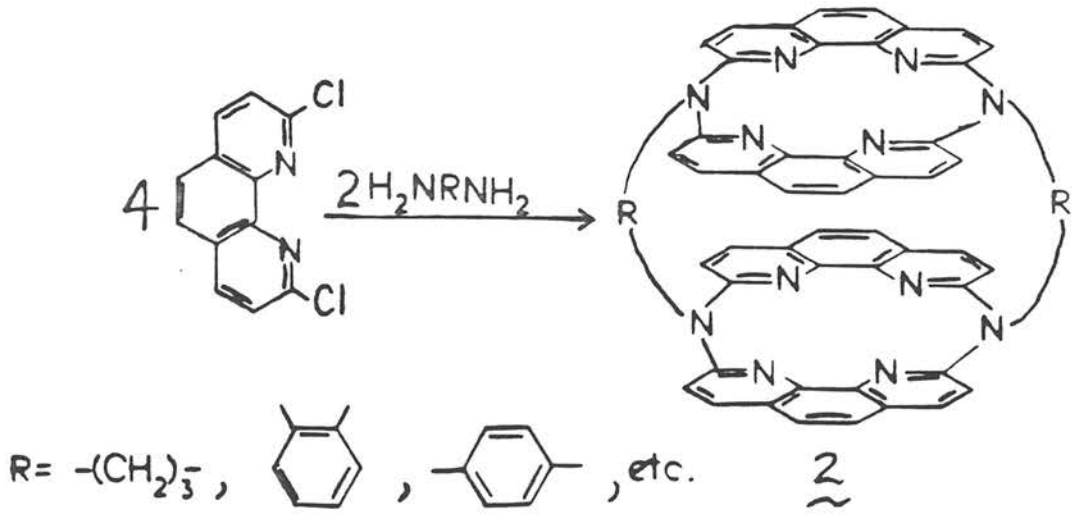

2

in such a synthesis, but high dilution may decrease the extent of polymerization. Surprisingly, polymerization was not a problem in the synthesis of the prototype macrocycle, 3, which was synthesized in 94% yield![8]

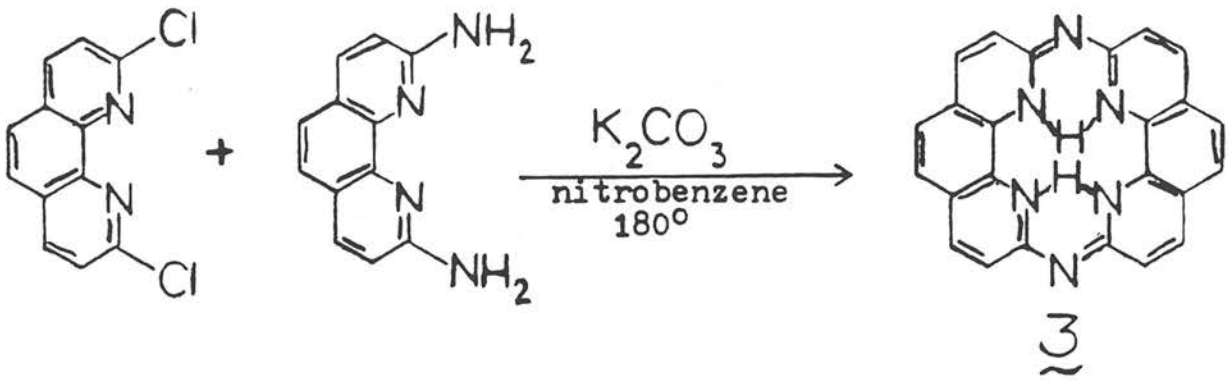

3

The variability of the R-groups which connect the two macrocycles in 2 allows for systematic changes in the metal-to-metal distance. For the species, M-O-O-M, the optimum metal-to-metal distance is ca. 4.8 Å,[2] and molecular models indicate a M-M distance of 4-5 Å for R = propylene in the proposed system.

This "face-to-face" phenanthroline ligand system, 2, possesses several advantageous features: The neutral ligand will lead to a system with a +4 overall charge including two divalent metals (such as Co^{2+}). This will certainly raise the reduction potentials for the metals relative to the overall neutral "face-to-face" metal porphyrins.[9] Since the reactivity of cobalt complexes with oxygen seems to be proportional to the amount of negative charge on the metal center,[10] a more positively charged system may show reduced oxygen affinity.

For this reason, a variety of metals such as Co^{2+}, Fe^{2+}, Ru^{2+}, and Cu^{+} will be investigated in an effort to produce the desired combination of high reduction potentials and high oxygen affinity. Metal complexes of the aromatic ligands in 2 should be resistant to oxidative degradation during oxygen reduction. Also, the overall +4 charge of the bimetallic system should increase its solubility in polar solvents and thereby aid in the characterization of these species. These highly charged compounds are likely to be water soluble, as opposed to the neutral "face-to-face" metal porphyrins. Finally, the synthesis of the proposed binucleating ligand, 2, appears straightforward and the required reactants are commercially available, or have been made in good yields by published procedures.[8] Fortunately, there are no possible isomers of proposed system 2, contrary to the syn and anti isomers which are formed in the synthesis of the "face-to-face" porphyrins. (Compound 1 is the anti isomer.)

As an alternative synthesis of 2, the macrocycle 3 could be synthesized by the published method,[8] followed by alkylation with a dihalide such as 1,3-dibromopropane to yield the desired product, 2.

An early indication of the viability of the proposed type of synthesis can be obtained from the reaction depicted in equation 4. Since 1,2-diaminobenzene is commercially available, and 2-chlorophenanthroline can be synthesized in three steps by published methods,[11] the below reaction could be consummated with relative ease. Bimetallic complexes of the ligand, 4, would be quite interesting in their own right, since molecular models indicate that these metal complexes would assume a face-to-face geometry due to the steric

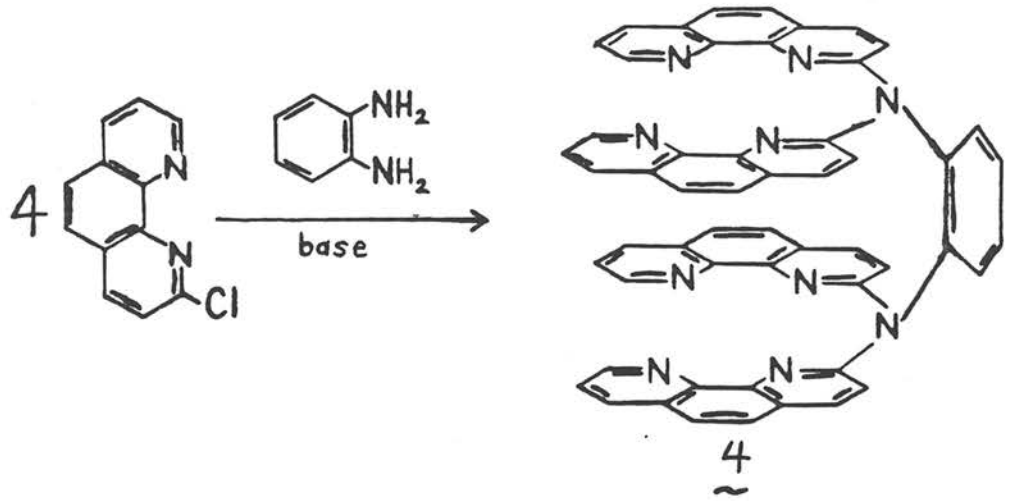

repulsion present in any other geometry. Hence, the synthesis of the ligand, $\underset{\sim}{4}$, presents a convenient starting point for this project, and it may not even be necessary to synthesize the more complicated, doubly-bridged ligand system, $\underset{\sim}{2}$.

The syntheses proposed herein should involve standard organic and inorganic laboratory techniques. No special precautions need be taken except in the handling of the low-valent metal complexes, which should be done under an inert atmosphere to prevent air oxidation. The compounds will be fully characterized by techniques such as elemental analysis, IR spectroscopy, NMR spectroscopy (for the ligands and diamagnetic metal complexes), ESR spectroscopy (for the paramagnetic metal complexes), electronic spectroscopy (for the metal complexes), and mass spectroscopy. The reduction potentials for the metal complexes will be determined by either cyclic voltammetry or differential pulse voltammetry. The catalytic activity of these com-

plexes towards dioxygen reduction will be studied at a rotating platinum ring-disk electrode consisting of a graphite disk and a concentric platinum ring. The metal complex will be adsorbed onto the graphite disk, and then the rate of oxygen reduction at the disk can be monitored electrochemically. At the same time, the amount of undesirable hydrogen peroxide can be measured at the platinum ring by reoxidation to oxygen at a potential of ca. 1.4 volts vs. nhe.

References

1. J. Bockris and S. Shrinivasan, "Fuel Cells: Their Electrochemistry", McGraw Hill, New York (1969).
2. J. Collman, C. Elliott, T. Halbert and B. Tovrog, Proc. Natl. Acad. Sci. USA, 74, 18 (1977).
3. J. P. Collman, M. Marocco, P. Denisovich, F. C. Anson, and C. Koval, J. Electroanal. Chem., 101, 117 (1979).
4. a) J. Fee, Structure and Bonding, 23, 1 (1975);
   b) Vanngård, "Biological Applications of Electron Spin Resonance Spectroscopy", H. Swartz, J. Bolton, and D. Borg, eds., J. Wiley, New York, p. 411 (1972).
5. R. R. Gagné, C. A. Koval and T. J. Smith, J. Amer. Chem. Soc., 99, 8367-8368 (1977).
6. J. Collman, private communication (1979).
7. "Ring-Disk Electrodes", W. J. Albery and M. L. Hitchman, Clarendon Press, Oxford, 1971.
8. a) S. Ogawa and T. Yamaguchi, J. Chem. Soc., Perkin, 976 (1974).
   b) S. Ogawa, J. Chem. Soc., Perkin, 214 (1977).
9. G. Patterson and R. Holm, Bioinorganic Chem., 4, 257 (1975).
10. a) F. Basolo, Chem. Comm., 810 (1973).
    b) R. D. Jones, D. A. Summerville, and F. Basolo, Chem. Rev., 79, 142 (1979).
11. B. Halcrow and W. Kermack, J. Chem. Soc., 155 (1946).

PROPOSITION 2

Gold Metallocycles

Metallocyclic compounds have been postulated as intermediates in several reactions catalyzed by transition metals. Included in these are the [2+2] cycloaddition of olefins, olefin metathesis, and isomerization of strained carbocyclic rings. For example, an iridiocyclic compound has been isolated and demonstrated as the intermediate in the iridium catalyzed dimerization of norbornadiene (equation 1).[1]

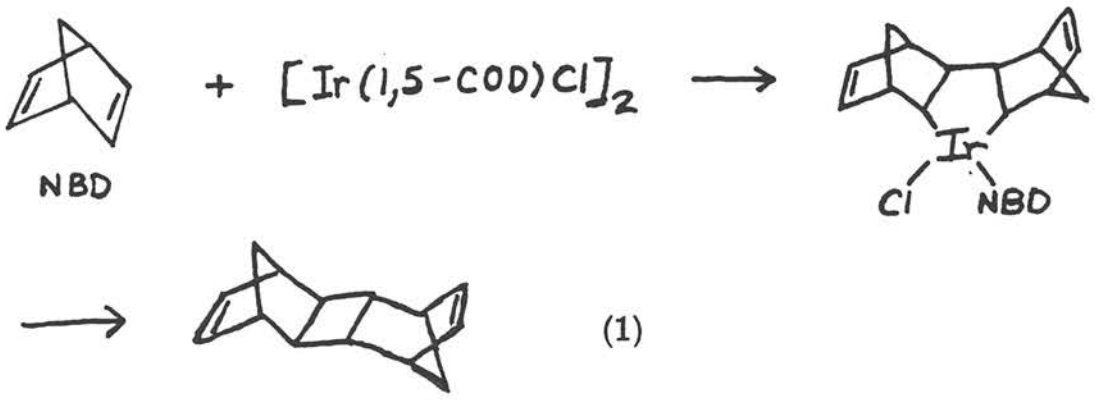

(1)

An indication that metallocyclic compounds may be involved in olefin metathesis was demonstrated by the reaction of 1,4-dilithiobutane with tungsten hexachloride (equation 2).[2] Possibly the most novel example

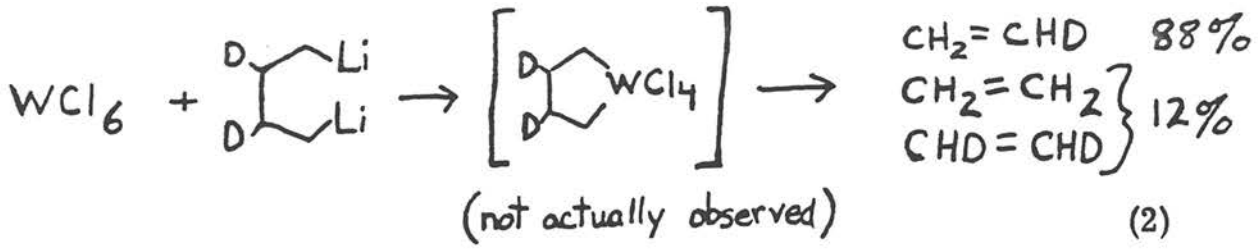

(2)

of all is the valence isomerization of cubane by rhodium shown in equation 3.[3] Here again the metallocyclic complex was not observed

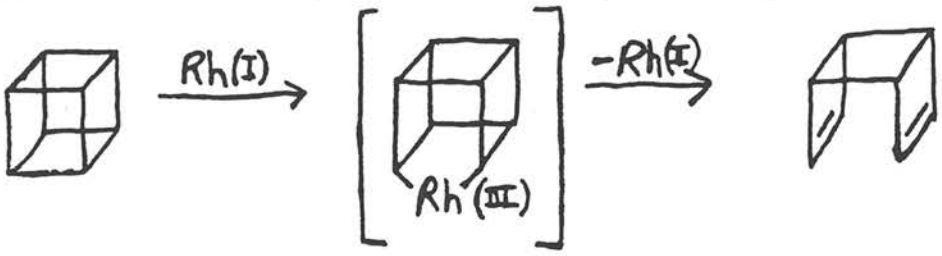

(3)

directly, but its probable existence is indicated by the isolation of the following acyl-rhodium adduct (equation 4).[3] Note that both the [2+2]

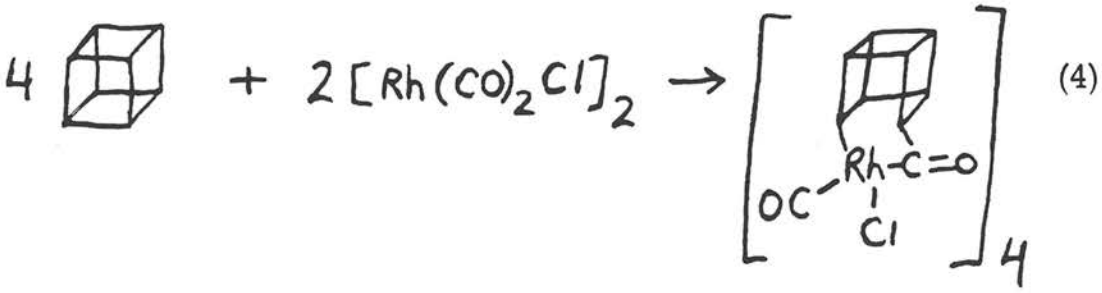

(4)

cycloaddition of olefins and the valence isomerization are thermally "forbidden" by Woodward-Hoffman orbital symmetry conservation rules.[4]

In addition to the above examples, metallocyclic complexes have been observed with titanium,[5] tantalum,[6] iron,[7] nickel,[8] and platinum.[9] The most complete studies involve nickel and platinum.

A series of platinocycles have been prepared by Whitesides et al.[9] for comparison with acyclic platinum alkyls. The platinocycle, 2, was found to be thermally much more stable compared to the acyclic analogue, 1. Complex 1 yields ethylene and ethane (1:1) upon decomposition, while complex 2 yields butene (primarily 1-butene). The

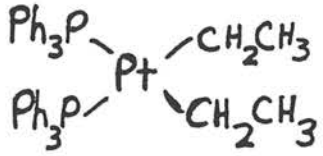

1

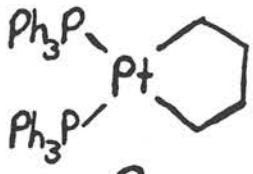

2

mechanism suggested for both decompositions is β-elimination to form a metal hydride complex, followed by reductive elimination as shown in equations 5 and 6. Presumably, β-elimination of the acyclic

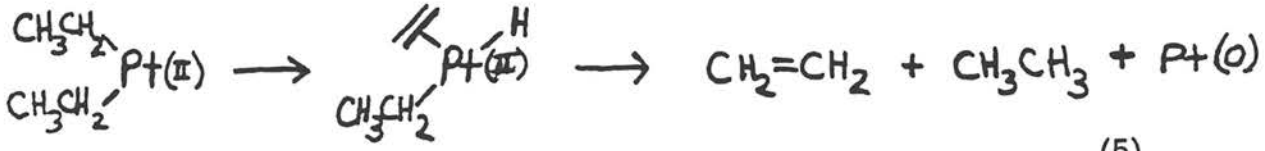

(5)

(6)

complex, 1, follows dissociation of a triphenylphosphine ligand since the rate of decomposition is greatly suppressed by excess triphenylphosphine.[10] Strangely enough, the rate of decomposition of the metallocycle, 2, is <u>accelerated</u> by excess triphenylphosphine. Hence, a different mechanism may be involved for the metallocycle. Nevertheless, the metallocyclic complex is much more stable than the acyclic analogue, indicating that the facile pathway to β-elimination observed for 1, is not as readily available for the metallocyclic

complex 2. It is postulated that these β-eliminations occur most readily when the M-C-C-H dihedral angle is 0°. For this reason, the tetramethylene metallocycle, 2, in which M-C-C-H dihedral angles would be greater than 90°, is expected to show a decreased rate of β-elimination, as observed.[9] The rate of decomposition is also lowered for the analogous pentamethylene and hexamethylene platinocyclic complexes.

Since these metallocycles exhibit increased resistance to thermal decomposition via β-elimination, other pathways of decomposition may become available for metallocyclic compounds. These include reductive elimination with concomittant carbon-carbon bond breaking and/or carbon-carbon bond formation (i.e., equation 7). The only platinocycle

(7)

which gave a significant amount of decomposition other than β-elimination was the tri-n-butylphosphine analogue of 2 (equation 8).[9]

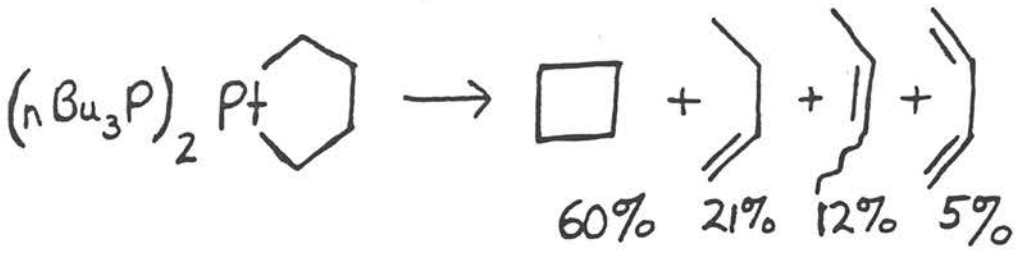

(8)

The multitude of decomposition pathways available to metallocycles is demonstrated by nickelocyclopentanes, in which different

major products are observed depending upon the concentration of tricyclohexylphosphine (L) (Scheme 1).[8] The three-coordinate complex,

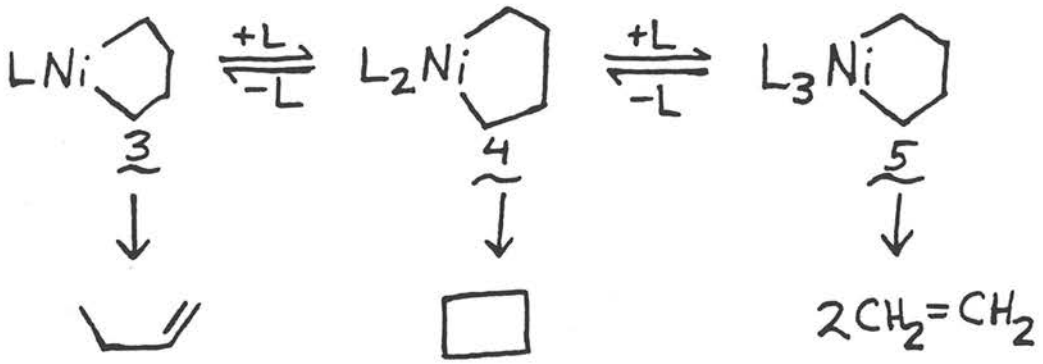

Scheme 1

3, decomposes via β-elimination. This is not surprising since a vacant coordination site is available for coordination of the β-hydrogen. The mechanism of decomposition of the four- and five-coordinate complexes is unknown. In all three cases, a mixture of products is observed, which may be a result of the equilibrium present between the three-, four-, and five-coordinate complexes. A very clean product was obtained from the bidentate ligand, diphos, which should exist almost entirely as the four-coordinate complex, 6 (equation 9). Clean products

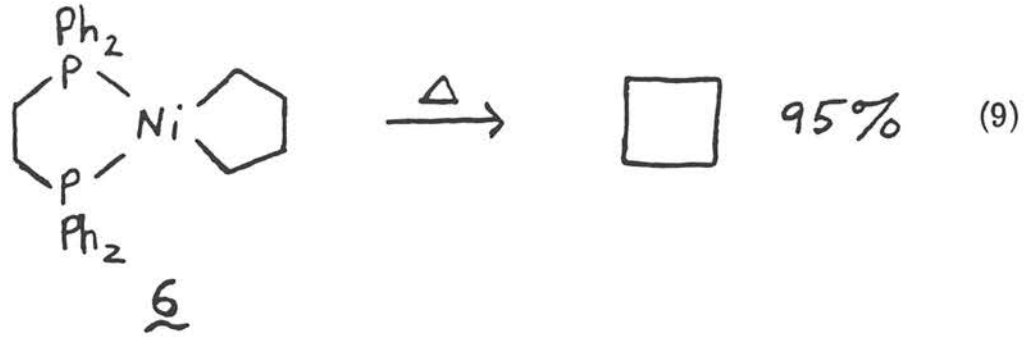

(9)

are also obtained by oxidation with dioxygen, followed by decomposition (equation 10). In each case, cyclobutane was formed as the major

(10)

product (>85%). Photochemical decomposition resulted in a higher yield of ethylene in all cases as shown in equation 11. The results

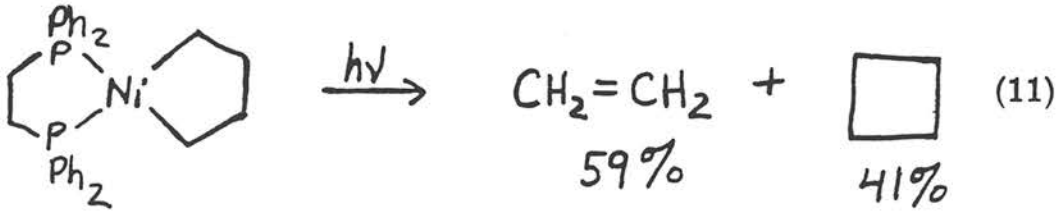

(11)

from oxidation and photolysis have not been explained,[8] and further study is certainly warranted.

To augment the information known about the formation and decomposition of metallocycles, I propose a study of gold(III) metallocycles. These metallocycles would be of special interest for comparison to the metallocycles discussed above, especially those of nickel and platinum. The modes of decomposition of such gold metallocycles may be sensitive to changes in geometry, coordination number, oxidation state, and orbital occupancy as was observed with the nickelocyclic compounds.[8] A comparison of the stability and modes of decomposition between aurocycles and their acyclic analogues may provide additional information about the nature of metallocyclic compounds (vide infra). Gold metallocycles could be synthesized in a

manner analogous to known acyclic alkyl gold compounds (Scheme 2).[12,13]

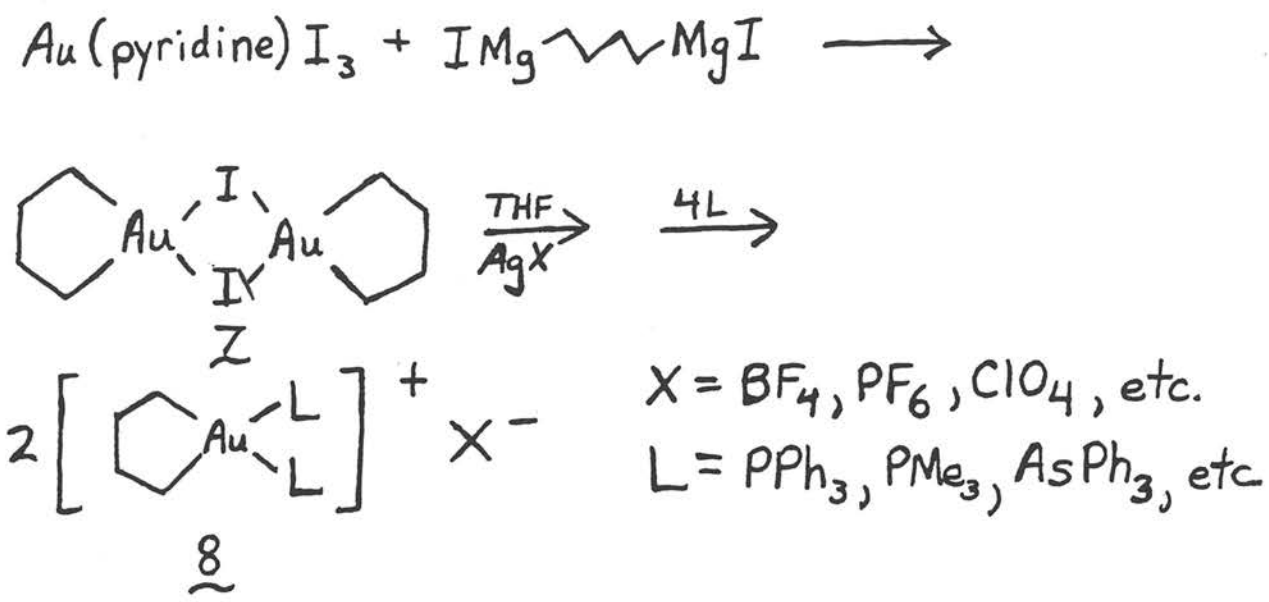

8

Scheme 2

Acyclic alkyl gold complexes such as 9, decompose exclusively by reductive elimination to give alkyl-coupled products (e.g., equation 12).[13]

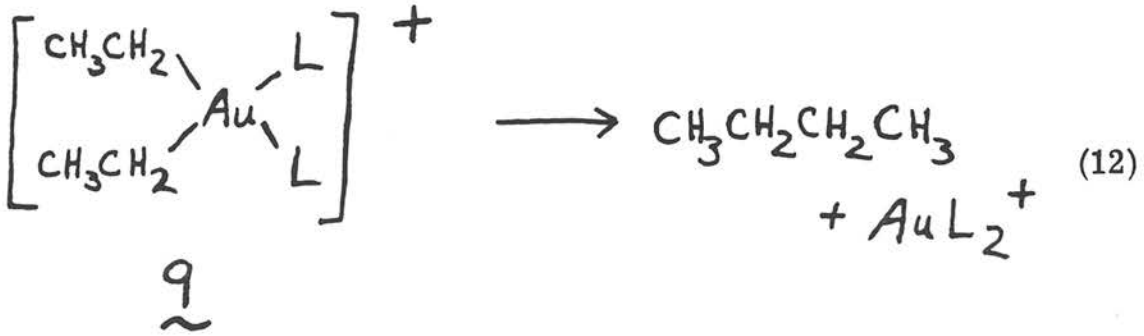

(12)

9

A number of factors influence the stability of these dialkylgold complexes. Cationic complexes such as 9 eliminate faster than neutral analogues. Bulky ligands increase the rate of reductive elimination, while excess ligand (L) and bidentate ligands decrease the rate of elimination. This and other mechanistic information indicate that the mechanism involves dissociation of a ligand, L, followed by intramolecular, concerted reductive elimination from an unstable three-coordinate intermediate.

A similar investigation of the mechanism for decomposition of metallocyclic gold compounds is proposed. A mechanism similar to that described above for the acyclic complex, 9, may be expected; however, platinocyclic compounds were shown to decompose by a different mechanism than their acyclic analogues, although the overall process appeared to be the same (vide supra).[9] For this reason, the dependence of rate on phosphine (L) concentration will be examined to determine if dissociation of ligand is involved in the rate-determining step. A free radical process can be discovered by use of a radical trap such as di-t-butyl nitroxide, radicals of which could be observed by EPR.[13] Intermolecular processes would be evidenced by the formation of larger rings as shown in Scheme 3.

Intermolecular decompositions would not be expected for cationic aurocycles such as 9, since the dialkyl acyclic analogues seem to proceed via an intramolecular mechanism. However, an intermolecular mechanism has been suggested for neutral trialkyl gold(III) compounds such as 10.[14] The mechanism, however, is solvent-

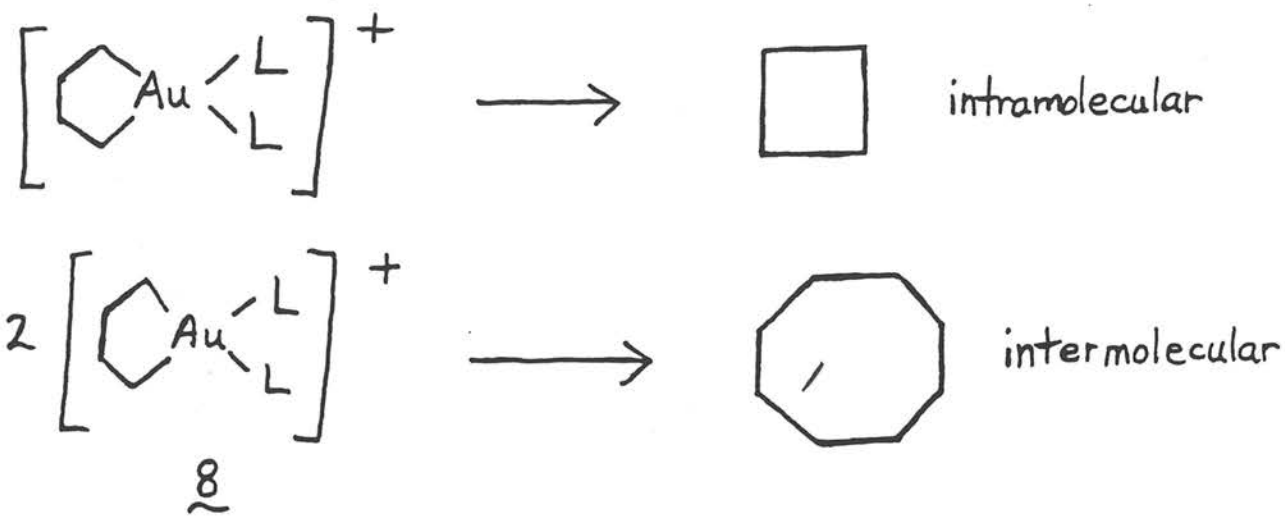

8

Scheme 3

dependent, showing only intramolecular coupling in donor solvents such as dimethyl sulfoxide (DMSO) (Scheme 4). Yet this result contra-

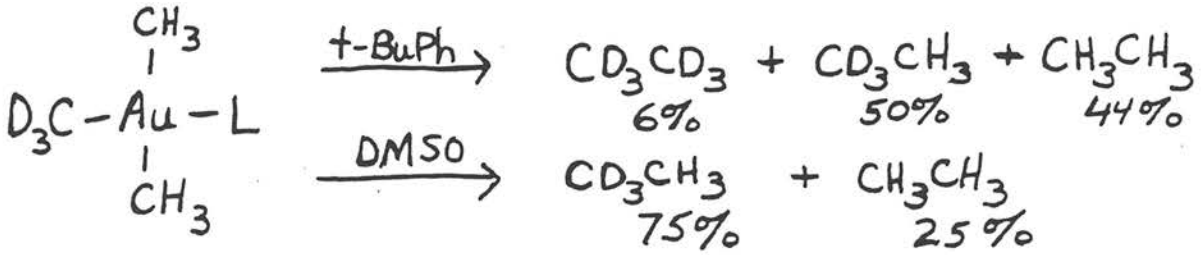

10

Scheme 4

dicts an earlier study by the same group in which the decomposition of trialkyl gold complexes in tert-butyl benzene was claimed to be intramolecular.[15] The inconsistency here may be due to difficulty in quantitatively analyzing the amount of deuterated products, which was done by mass spectroscopy. It should be easy to differentiate between the intramolecular and intermolecular routes for the aurocycles,

since the products differ greatly as shown above. Tri-alkyl substituted aurocycles should be prepared for comparative purposes. These cyclic derivatives could be prepared as shown in Scheme 5, which is similar to the synthesis of acyclic analogues such as 10.[15,16,17]

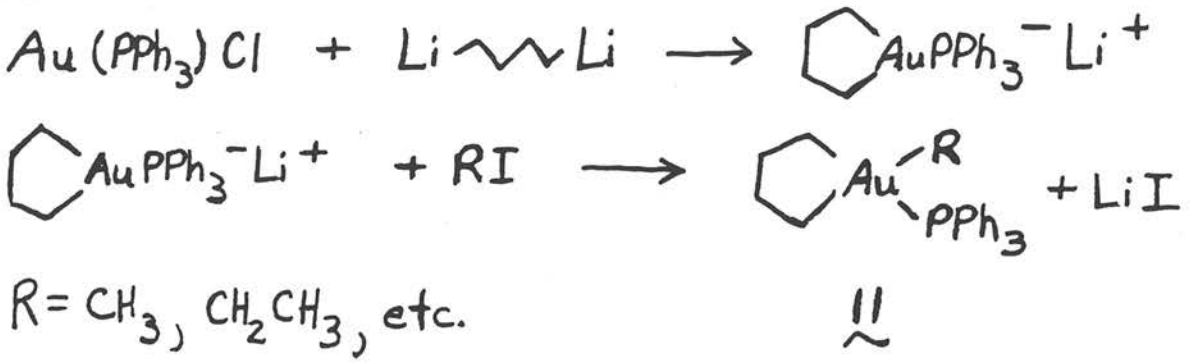

Scheme 5

Derivatives such as 11 may undergo an intermolecular mechanism more readily than cationic complexes such as 9, which will exhibit electrostatic repulsions when approaching one another.

Another interesting mechanistic application would be the synthesis of labeled derivatives of 9 and 11, proposed in Scheme 6.

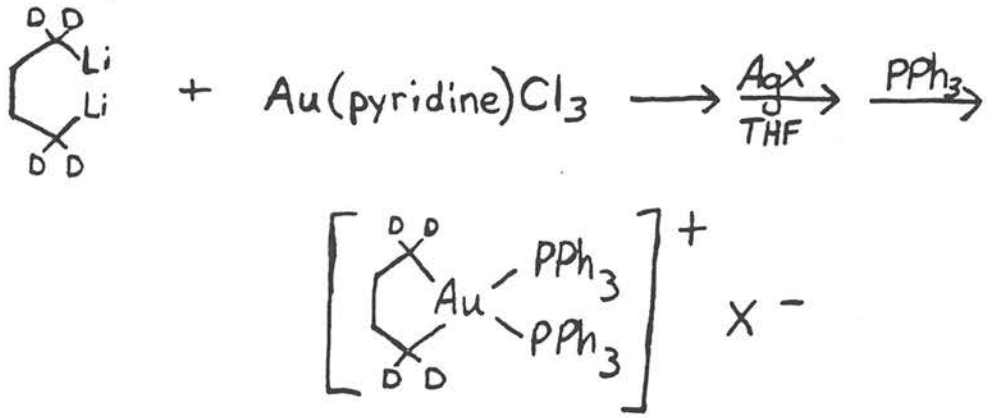

Scheme 6

Scrambling of the deuteriums in the decomposition products would indicate more complicated rearrangements rather than simple concerted reductive elimination. For instance, Scheme 7 is a possibility:

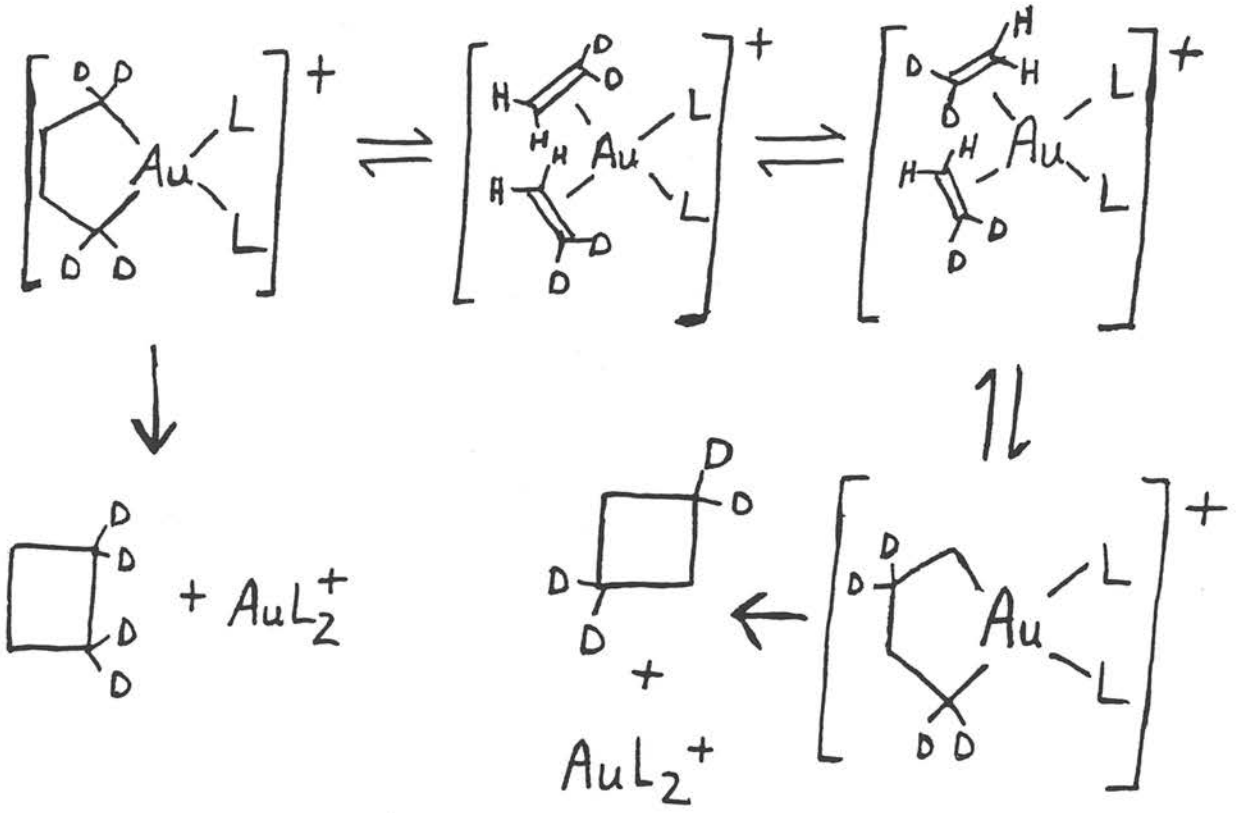

Scheme 7

In contrast to nickel[11] and platinum[10] acyclic dialkyl complexes, which tend to decompose via β-elimination as a major route, acyclic trialkyl gold(III) complexes decompose exclusively via reductive elimination and coupling of alkyl groups (equation 13).[13,15] For this

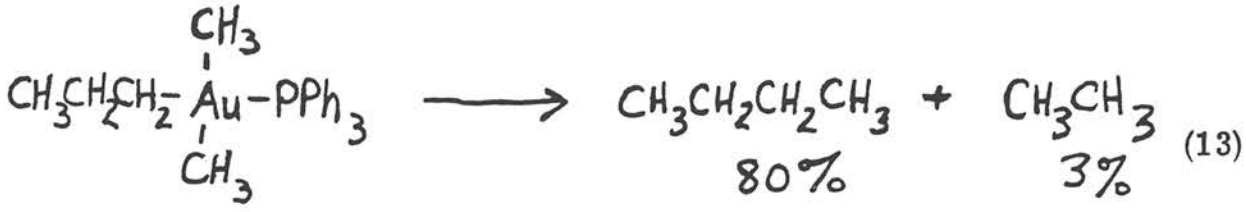

(13)

reason, the decomposition of gold metallocycles may not be complicated with the β-elimination products as in the nickel and platinum cases. Accordingly, aurocyclic complexes may give the first good comparison between the stabilities of acyclic and cyclic transition metal alkyl complexes for which the exclusive mode of decomposition is reductive elimination and concerted carbon-carbon bond formation. Complexes such as 11 are very intriguing in this respect. The products from decomposition of 11 should indicate whether elimination of two cyclic groups or one cyclic and one acyclic group is faster (Scheme 8). These

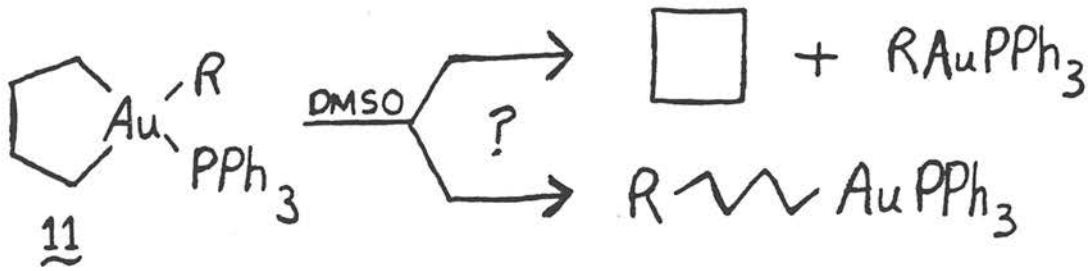

11

Scheme 8

two routes should easily be distinguished by analysis of the gaseous products and by NMR of the resulting solution. Alkyl coupling between alkyl groups in the Au(I) products shown above is a possibility, but this reaction is slower and can be completely eliminated by a slight excess of triphenylphosphine.[14]

As was true with the nickelocycles, ethylene may be a decomposition product from aurocycles such as 9 and 11. An attempt could be made to induce the formation of ethylene by photolysis. (Recall that photolysis of nickelocycles favors production of ethylene.) Excess ligand also resulted in the formation of ethylene (reason unknown).[8]

Hence, it would be useful to study the effect of excess triphenylphosphine on the product distribution. Since Au(III) complexes are rarely 5-coordinate,[18] this effect should be slight, if any; however, the potentially three-coordinate ligand, 1,1,1-tris-(dimethylphosphinomethyl) ethane[19] as well as the potentially bidentate diphos ligand may provide interesting results. For instance, consider the following possible complexes, 12 and 13.

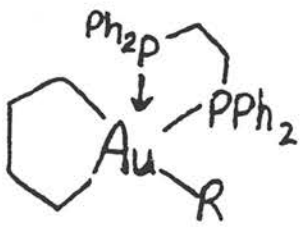

12

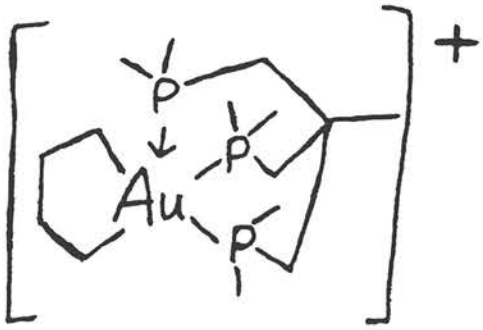

13

Finally, the effect of oxidation on these complexes should be investigated. As was the case with nickel,[8] rapid reductive elimination to form cyclobutane would be expected, but the situation is somewhat different here in that oxidation of Au(III) complexes by one electron followed by reductive elimination would yield an Au(II) complex. Gold(II) complexes are extremely unstable[20] and generally lead to disproportionation. Two reasonable possibilities for the oxidative decomposition of these aurocycles are shown on Scheme 9. The second case, which shows disproportionation of the Au(II) intermediate accompanied by alkyl transfer, was observed in the oxidative decomposition of tetramethylaurate(III) compounds (equation 14).[21] In the above reaction, triphenylphosphine was required, presumably to

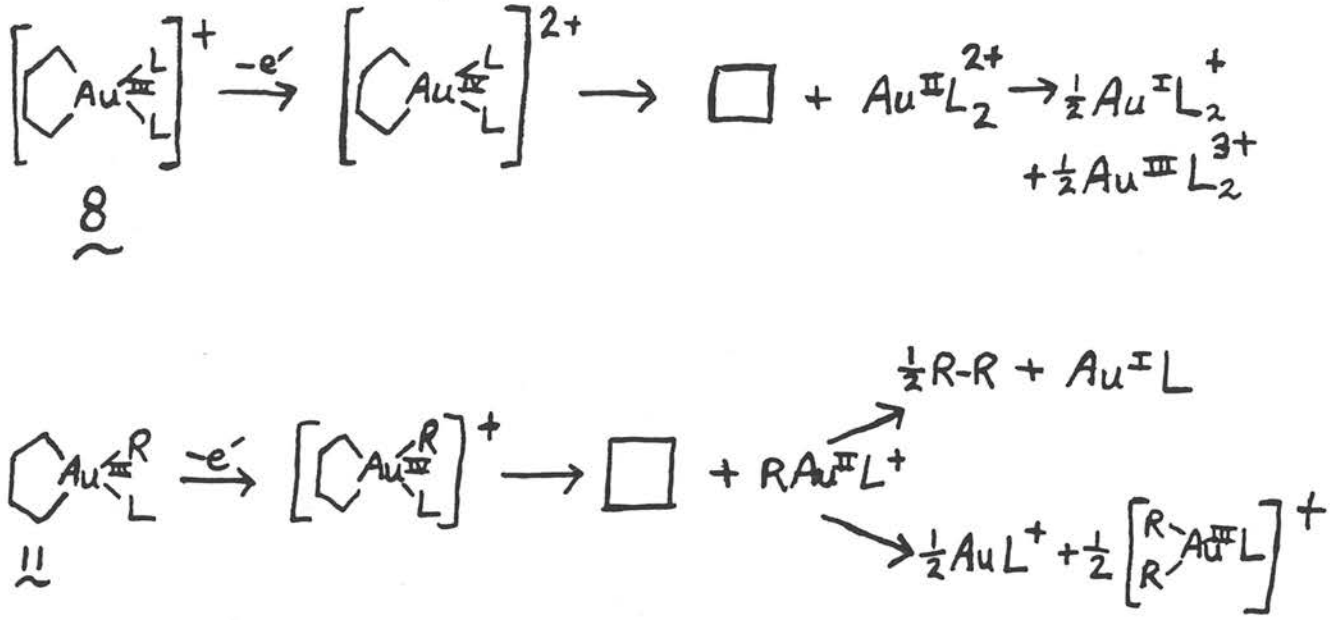

Scheme 9

$$(CH_3)_4AuLi(PPh_3) \xrightarrow{O_2} CH_3CH_3 + CH_3AuPPh_3 + (CH_3)_3AuPPh_3 \quad (14)$$

stabilize the Au(II) intermediate; otherwise reductive elimination directly to Au^0 was observed. The effect of triphenylphosphine (L) concentration on the oxidative decomposition of 11 merits investigation.

Oxidation of these complexes could be affected by adding molecular oxygen, but this presents an added variable due to the possibility of O_2 complexing to the metal. Complexation of dioxygen to nickel may be involved in the decomposition of nickelocycles by O_2.[8,22] Olefins with electron-withdrawing substituents were shown to bind to dialkyl nickel compounds and promote reductive coupling of the alkyl groups.[11] A similar process could occur with dioxygen. Therefore, in addition to decomposition by dioxygen, decomposition could be generated by

electrochemical oxidation, in which the oxidation is most likely a simple electron-transfer. Also, the effect of electrochemical reductions could be easily studied electrochemically, and cyclic voltammetry will show the relative stability of any oxidized or reduced species. Finally, the rate constants of follow-up chemical reactions (i.e., reductive elimination) can possibly be determined by double potential-step chronocoulometry and/or current reversal chronopotentiometry.[23]

References

1. A. R. Fraser, P. H. Bird, S. A. Bezman, J. R. Shapley, R. White, J. A. Osborn, J. Amer. Chem. Soc., 95, 597 (1973).
2. R. Grubbs and T. Brunck, J. Amer. Chem. Soc., 94, 2538 (1972).
3. L. Cassar, P. Eaton, and J. Halpern, J. Amer. Chem. Soc., 92, 3515 (1970).
4. R. B. Woodward and R. Hoffmann, Angew. Chem., Int. Ed. Engl., 8, 781 (1969).
5. G. Whitesides and J. McDermott and M. Wilson, J. Amer. Chem. Soc., 98, 6259 (1976).
6. S. J. McLain, C. D. Wood, and R. R. Schrock, J. Amer. Chem. Soc., 99, 3519 (1977).
7. M. L. H. Green, Adv. Organomet. Chem., 8, 29 (1970).
8. R. H. Grubbs, A. Miyashita, M. Liu, and P. Burk, J. Amer. Chem. Soc., 100, 2418 (1978).
9. G. Whitesides, J. White, and J. McDermott, J. Amer. Chem. Soc., 98, 6521 (1976).
10. G. Whitesides, J. Gaasch, and E. Stedronsky, J. Amer. Chem. Soc., 94, 5258 (1972).
11. T. Yamamoto, A. Yamamoto, and S. Ikeda, J. Amer. Chem. Soc., 93, 3350 (1971).
12. F. H. Brain and C. S. Gibson, J. Chem. Soc., 762 (1939).
13. P. Kuch and R. Tobias, J. Organomet. Chem., 122, 429 (1976).
14. S. Komiya, T. A. Albright, R. Hoffmann and J. K. Kochi, J. Amer. Chem. Soc., 98, 7255 (1976).

References (continued)

15. A. Tamaki, S. Magennis, and J. Kochi, J. Amer. Chem. Soc., 96, 6140 (1974).

16. A. Tamaki and J. Kochi, J. Organomet. Chem., 61, 441 (1973).

17. A. Tamaki and J. Kochi, J. Organomet. Chem., 51, C39 (1973).

18. F. Cotton and G. Wilkinson, "Advanced Inorganic Chemistry", Interscience, New York, 1972, p. 1054.

19. G. Whitesides, C. Casey, and J. Krieger, J. Amer. Chem. Soc., 93, 1379 (1971).

20. J. Huheey, "Inorganic Chemistry", Harper & Row, New York, 1972, p. 334.

21. S. Komiya, T. A. Albright, R. Hoffman, J. K. Kochi, J. Amer. Chem. Soc., 99, 8440 (1977).

22. M. Almemark and B. Akerkmark, J.C.S. Chem. Comm., 67 (1978).

23. R. W. Murray in "Physical Methods of Chemistry, Part IIA: Electrochemical Methods", A. Weissberger and B. Rossiter, Eds., Wiley Interscience, New York, 1971, Ch. VIII.

PROPOSITION 3

Models for Blue Copper Proteins

The Type 1, or "blue" copper, protein site is present in a large number of proteins including azurin, stellacyanin, plastocyanin and laccase.[1] This site is characterized by an intense absorption envelope centered around 600 nm and an EPR spectrum having an unusually small hyperfine coupling constant ($A_{||}$). These properties suggest a novel coordination environment for copper(II) in these protein sites, and a considerable amount of research has been directed toward the full characterization of the Type 1 site. The blue copper site in poplar plastocyanin has been characterized by X-ray diffraction, and the copper was found in a distorted tetrahedral geometry, the ligands being a cysteine thiolate, a methionine thioether, and two histidine imidazole nitrogens.[2] An X-ray structural analysis for P. aeruginosa azurin was also performed and although the resolution was poor, the probable ligands are the same as in the plastocyanin site.[3] This would seem to indicate a common copper(II) coordination environment in all the Type 1 sites, but at least stellacyanin must be different since it does not contain methionine.[4] In addition, the large range of reduction potentials (200-800 mV vs. nhe) exhibited by the Type 1 binding sites suggests a variation in structure and/or ligands.[1] There could be a common feature (e.g., mercaptide coordination) which is responsible for the characteristic Type 1 properties, while other features may vary among the different protein sites.

Numerous spectroscopic studies are in agreement with a near tetrahedral arrangement of sulfur and nitrogen ligands around copper in the Type 1 sites.[5] The intense absorption at ca. 600 nm in these blue copper proteins has been assigned to a S(cysteine) → Cu(II) σ-LMCT.[6] The small hyperfine splitting ($A_{||}$) observed in the EPR spectra of these sites has been accounted for by assuming a tetragonally flattened tetrahedral copper(II) geometry.[5]

While the novel properties and structures of the blue copper protein sites are beginning to be understood, these sites have yet to be effectively modeled by synthetic complexes. The difficulty in obtaining such model complexes is largely due to the tendency of copper(II) compounds to instantaneously oxidize mercaptides to disulfides. Mercaptide coordination to copper(II) has been observed in some complexes at low temperature, and indeed, strong absorption bands attributable to S(thiolate) → Cu(II) LMCT are observed for these compounds.[6,7] However, the other ligands in these complexes bear little resemblance to the proposed protein sites. The electronic spectra of a number of copper(II) complexes employing thioether coordination have been examined, and S(thioether) → Cu(II) LMCT absorptions have been identified.[7,8] The other ligands as well as the geometries in these complexes fail to mimic the blue copper protein sites. The few cases of mercaptide to copper(II) coordination which are stable at room temperature have rather complex structures, and again bear little overall resemblance to the proposed Type 1 site.[9,10] In no case has this blue copper site been mimicked completely in terms of coordination geometry and ligands, electronic absorption spectrum,

reduction potential and stability at room temperature.

As an effective model for the blue copper protein site, I propose the synthesis of the copper complex, 1. In addition to providing a tetra-

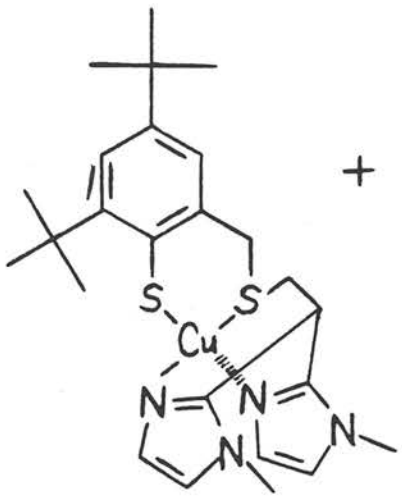

1

hedral arrangement of appropriate ligands to mimic the Type 1 site, this complex contains considerable steric bulk around the thiolate sulfur in an effort to prevent the oxidative coupling of the mercaptides. A possible synthesis of the ligand is given in Scheme 1. All of the proposed reactions have ample precedent.[11-16] If the dimethylthiocarbamate group fails as a protecting group, the p-toluenesulfonyl group may be used on 3,5-di-t-butyl-2-hydroxybenzyl alcohol and removed after formation of the thioether, prior to the reaction with dimethylthiocarbamyl chloride.[14]

Once the ligand is in hand, the desired compound, 1, could be synthesized directly from copper(II) starting materials, or, if necessary, the copper(I) complex could be synthesized, followed by

Scheme 1

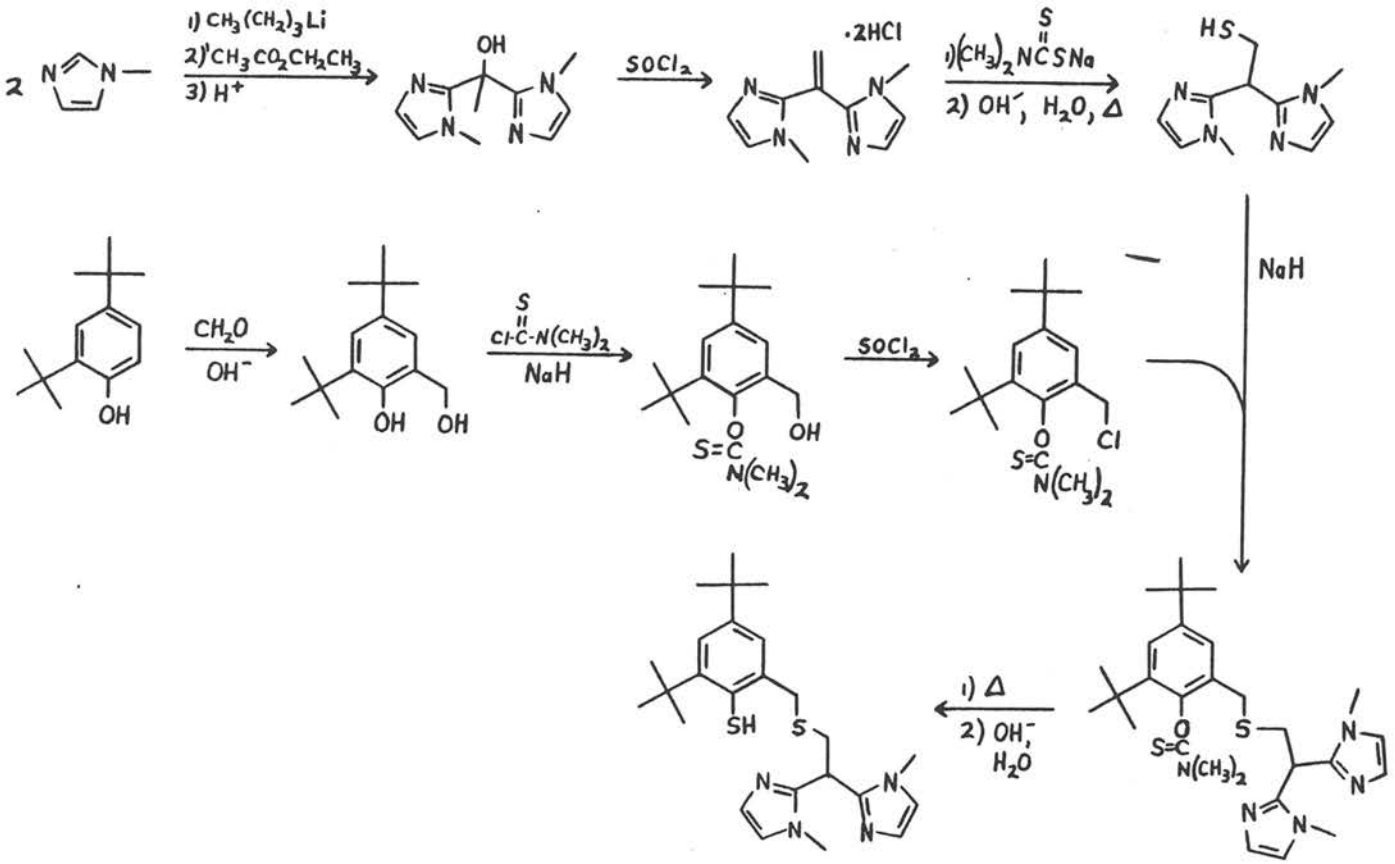

2

electrochemical oxidation to yield the desired compound. Initial studies on this complex should include electronic absorption, EPR, and electrochemistry for comparison to the blue copper protein sites. It would be of interest to investigate the effect of slight modifications in the geometry and type of ligands around copper(II). The ligand, $\underset{\sim}{2}$, appears to be amenable to systematic variations of the donor atoms. For instance, consider complexes $\underset{\sim}{3}$ and $\underset{\sim}{4}$ which could be synthesized along with $\underset{\sim}{1}$. The effects of these modifications on the electronic absorption spectrum, EPR spectrum and redox potentials could yield information about the possible factors responsible for the unique features of the Type 1 site.

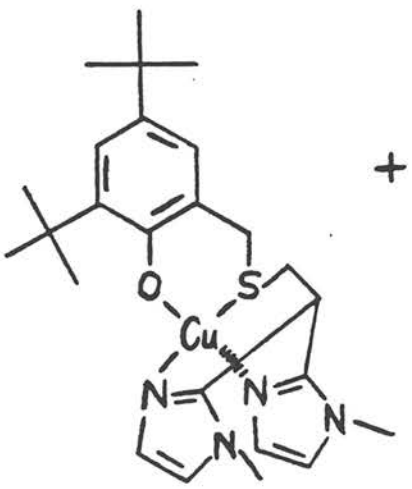

3

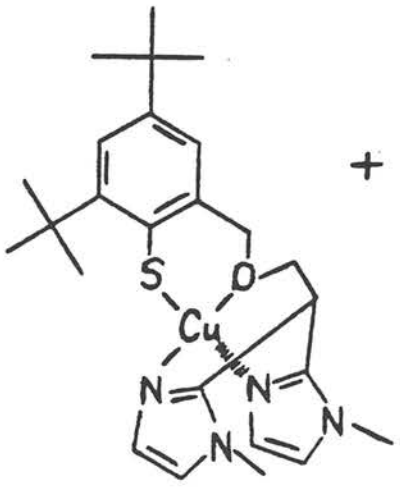

4

It is possible that complex $\underset{\sim}{1}$ may exist as Cu(I) and a sulfur radical at room temperature, rather than the desired Cu(II) and thiolate anion. This formulation, in which the mercaptide has been

oxidized instead of the Cu(II) ion, has been suggested for the "visible" copper site (Cu_a) of cytochrome c oxidase.[17] Modification of the ligand to include "harder" nitrogen or oxygen donors (e.g., complex 4) should stabilize copper(II) relative to copper(I) and favor the Cu(II)-S^- formulation. These studies may in fact yield informative comparisons to the Cu_a site in cytochrome c oxidase.

If additional steric bulk is necessary to prevent the oxidative coupling of the mercaptides, the binuclear complex, 5, could be synthesized from p-cresol in a manner analogous to the synthesis of 1. In this binuclear system, the best model for the blue copper sites would probably be the mixed valence species $Cu(II)Cu(I)L^{2+}$ (L = the binucleating ligand in 5). The two copper(II) ions in the fully oxidized species are likely to be antiferromagnetically coupled, possibly leading to a diamagnetic system.[18] The extent of such coupling is relevant to both cytochrome c oxidase and hemocyanin, since both proteins contain pairs of metals which are strongly coupled, presumably through a bridging ligand.[19,20] In neither case is the identity of the bridging ligand known, and a mercaptide bridge from cysteine is a possibility. The binuclear complex, 5, or slight variations of it, may indeed be reasonable models for the binuclear copper site in hemocyanin.[20]

In conclusion, the study of a series of copper complexes such as 1, 3, 4 and 5 could yield informative comparisons with a number of copper containing proteins. The necessary ligands could be synthesized by standard organic techniques. Subsequent studies of the copper complexes should include characterization by elemental analysis, I.R. spectroscopy, NMR spectroscopy (for the ligands and

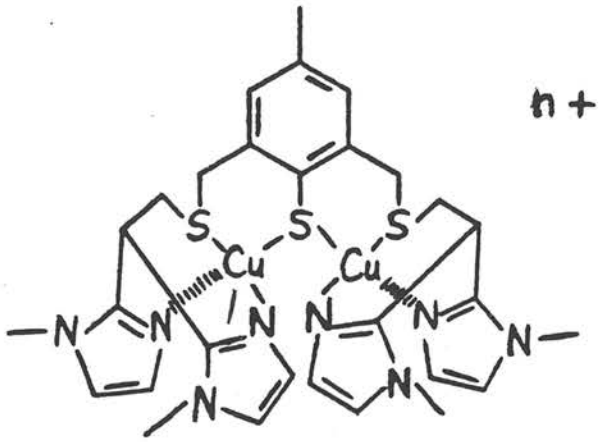

5

diamagnetic metal complexes), EPR spectroscopy, electronic absorption spectroscopy, and perhaps mass spectroscopy. The reduction potentials for the metal complexes could be determined by cyclic voltammetry, differential pulse voltammetry or by classical polarography. More sophisticated techniques such as circular dichroism and magnetic circular dichroism spectroscopy,[5] photoelectron spectroscopy,[21] variable temperature magnetic susceptibility,[22] and measurement of electron transfer kinetics[5] could be employed for further characterization and comparison to the copper protein sites.

References

1. Fee, J. A. Struct. Bonding (Berlin) 1975, 23, 1.
2. Colman, P. M.; Freeman, H. C.; Guss, J. M.; Murata, M.; Norris, V. A.; Ramshaw, J. A. M.; Venkatappa, M. P. Nature (London) 1978, 272, 319.
3. Adman, E. T.; Stenkamp, R. E.; Sieker, L. C.; Jensen, L. H. J. Mol. Biol. 1978, 123, 35.
4. Bergman, C.; Gandvik, E. K.; Nyman, P. O.; Strid, L.; Biochem. Biophys. Res. Commun. 1977, 77, 1052.
5. Solomon, E. I.; Hare, J. W.; Dooley, D. M.; Dawson, J. H.; Stephens, P. J.; Gray, H. B. J. Amer. Chem. Soc. 1980, 102, 168.
6. Thompson, J. S.; Marks, T. J.; Ibers, J. A. Proc. Natl. Acad. Sci. U.S.A. 1977, 74, 3114.
7. Amundsen, A. R.; Whelan, J.; Bosnich, B. J. Amer. Chem. Soc. 1977, 99, 6730.
8. Miskowski, V. M.; Thich, J. A.; Solomon, R.; Schugar, H. J.; J. Amer. Chem. Soc. 1976, 98, 8344.
9. Schugar, H. J.; Ou, C.; Thich, J. A.; Potenza, J. A.; Lalancette, R. A.; Furey, W. J. Amer. Chem. Soc. 1976, 98, 3047.
10. Hughey, J. L.; Fawcett, T. G.; Rudich, S. M.; Lalancette, R. A.; Furey, W. J. Amer. Chem. Soc. 1979, 101, 2617.
11. Tang, C. C.; Davalian, D.; Huang, P.; Breslow, R. J. Amer. Chem. Soc. 1978, 100, 3918.

References

12. Gagné, R. R.; Kreh, R. P.; unpublished results.

13. Bruson, H. Org. Reactions 1949, 5, 79.

14. Ullmann, F.; Brittner, K. Chem. Ber. 1909, 42, 2539.

15. Newman, M. S.; Karnes, H. A. J. Org. Chem. 1966, 31, 3980.

16. Gillis, R. G.; Lacey, A. B.; Org. Synthesis 1963, Coll. Vol. IV, 396.

17. Chan, S. I.; Bocian, D. F.; Brudvig, G. W.; Morse, R. H.; Stevens, T. H. in "Cytochrome Oxidase", King, T. E. et al. eds.; Elsevier/North-Holland Biomedical Press: Amsterdam, 1979, p. 177.

18. Copper(II) ions bridged by oxygen ligands are often strongly coupled. For example, see: Lintvedt, R. L.; Tomlonovic, B.; Fenton, D. E.; Glick, M. D. Adv. Chem. Series 1975, 150, 407.

19. Blumberg, W. E.; Peisach, J. in "Cytochrome Oxidase", King, T. E. et al. eds.; Elsevier/North Holland Biomedical Press: Amsterdam, 1979; p. 153.

20. Lontie, R.; Witters, R. in "Inorganic Biochemistry", Eichorn, G. I. ed.; American Elsevier: New York, 1973; p. 344.

21. Wurzbach, J. A.; Grunthaner, P. J.; Dooley, D. M.; Gray, H. B.; Grunthaner, F. J.; Gay, R. R.; Solomon, E. I. J. Amer. Chem. Soc. 1977, 99, 1257.

22. Solomon, E. I.; Dooley, D. M.; Wang, R.; Gray, H. B.; Cerdonio, M.; Mogno, F.; Romani, G. L. J. Amer. Chem. Soc. 1976, 98, 1029.

PROPOSITION 4

Macrocyclic Cuprous Complexes as Photosensitizers

The valence isomerization of norbornadiene (NBD) to quadricyclene (Q) has been investigated as a method for photochemical energy

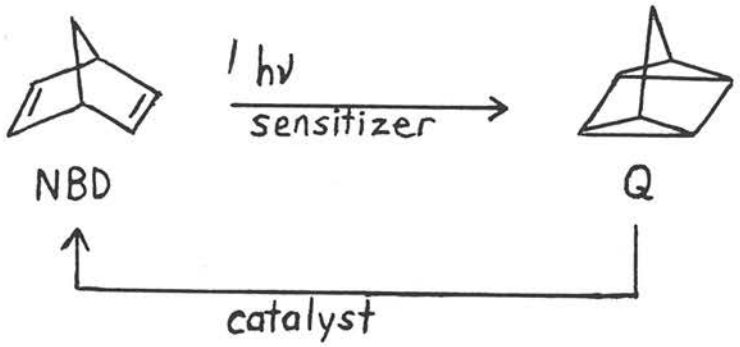

storage.[1,2] The reaction is endothermic by 21-26 kcal · mole^{-1} which corresponds to a storage capacity of 240 calories per gram of quadricyclene produced.[3] While quadricyclene is indefinitely stable at ambient temperatures, this energy can be released by exposure to appropriate catalysts.[4] Since norbornadiene does not absorb in the wavelength region (>300 nm) of available solar energy, a "sensitizer" is necessary for absorption of light at longer wavelengths. A variety of copper(I) complexes have been investigated as sensitizers.

Cuprous chloride has been found to sensitize the conversion of NBD to Q when irradiated with light at a wavelength of 313 nm.[5] A quantum yield[6] of ca. 0.39 with catalytic factors[7] up to 394 have been obtained for CuCl in neat NBD. The proposed mechanism is outlined in Scheme 1. The initially formed ClCu-NBD complex exhibits an intense charge transfer band (λ_{max} 248 nm, $\epsilon = 6.3 \times 10^3$ M^{-1} cm^{-1} in

Scheme 1

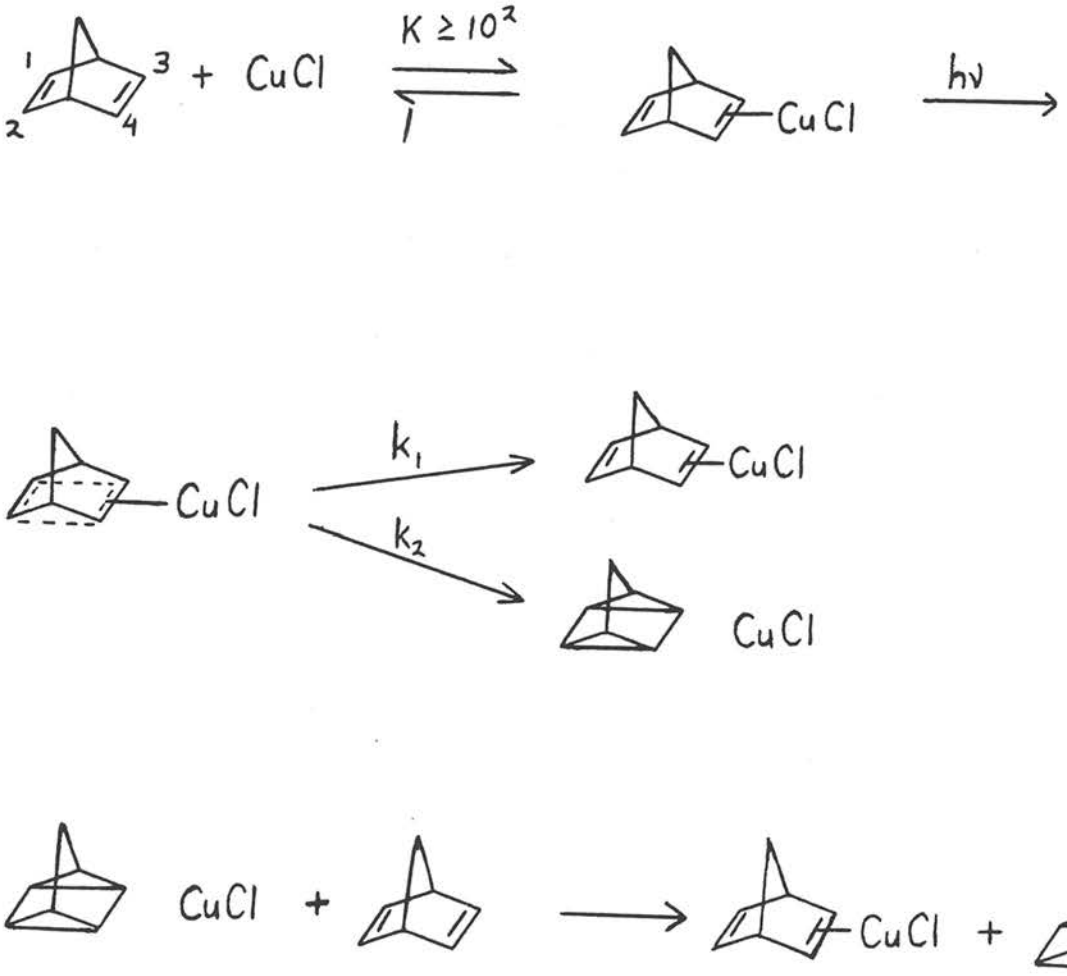

ethanol) which increases the absorption of the system out to 350 nm. The direction of this charge transfer was not assigned (MLCT or LMCT), but in either case a weakening of the bonding between C_1-C_2 and C_3-C_4 with a strengthening of the bonding between C_1-C_3 and C_2-C_4 is expected.[8] Relaxation of this excited state can then lead to either Q or NBD. Upon formation of Q, it is lost from the cuprous coordination sphere and replaced by NBD to begin the catalytic cycle again.

The conversion of NBD to Q is also sensitized by copper phosphine compounds, but the mechanism appears to be different (Scheme 2).[9] The copper complex, $\underset{\sim}{1}$, appears to be four-coordinate

Scheme 2

$$Cu(PPh)_2BH_4 \xrightarrow{h\nu} Cu(PPh_3)_2BH_4^*$$

$$\underset{\sim}{1}$$

$$\xrightarrow{NBD} [Cu(PPh_3)_2BH_4^*, NBD] \rightarrow\rightarrow Cu(PPh_3)_2BH_4 + Q$$

(with a bidentate BH_4 ligand), and there is no evidence for ground state coordination of NBD to copper. Compound $\underset{\sim}{1}$ exhibits an intense absorption centered at 257 nm, and it arises from the transfer of a lone pair electron on phosphorus to an empty antibonding π orbital centered on a phenyl ring.[9] Excitation of this transition by incident light at 313 nm produces an excited Cu(I) complex which apparently interacts with NBD to generate Q. Quantum yields up to 0.56 were observed with excess NBD in benzene solutions. Low catalytic factors ($\sim$ 10) were observed due to photodegradation of $Cu(PPh)_2BH_4$.

This sensitization can also be accomplished by a four-coordinate Cu(I) complex containing a single substitutionally labile ligand, e.g., 2.[10] The carbon monoxide ligand is replaced by NBD, and the reaction

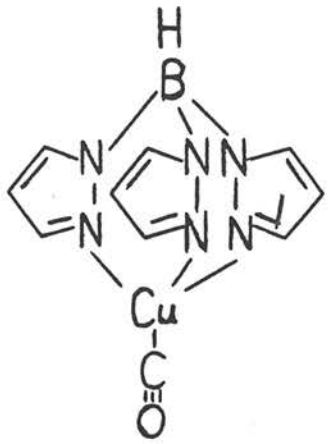

$Cu[HB(pz)_3]CO$, **2**

is proposed to proceed by the mechanism outlined in Scheme 1 (for CuCl). The complex $Cu[HB(pz)_3]$ (NBD) exhibits a charge transfer absorption which extends out to 370 nm. Irradiation (313 nm) of a solution of 2 and excess NBD produces Q with a quantum yield of 0.6 and catalytic factors ≥ 65.

The present proposition suggests the investigation of four-coordinate macrocyclic copper(I) complexes as sensitizers for the photochemical conversion of NBD to Q. The cuprous complexes shown in Figure 1 have recently been prepared electrochemically from the copper(II) analogues.[11] The majority of these compounds bind carbon monoxide as a fifth ligand (Table 1).[11-13] While the binding of these compounds to olefins has not been investigated, it is likely that they will also bind NBD as a fifth ligand. Thus, these macrocyclic copper(I) complexes are candidates for the sensitization of the conversion of NBD to Q by a mechanism similar to Scheme 1.

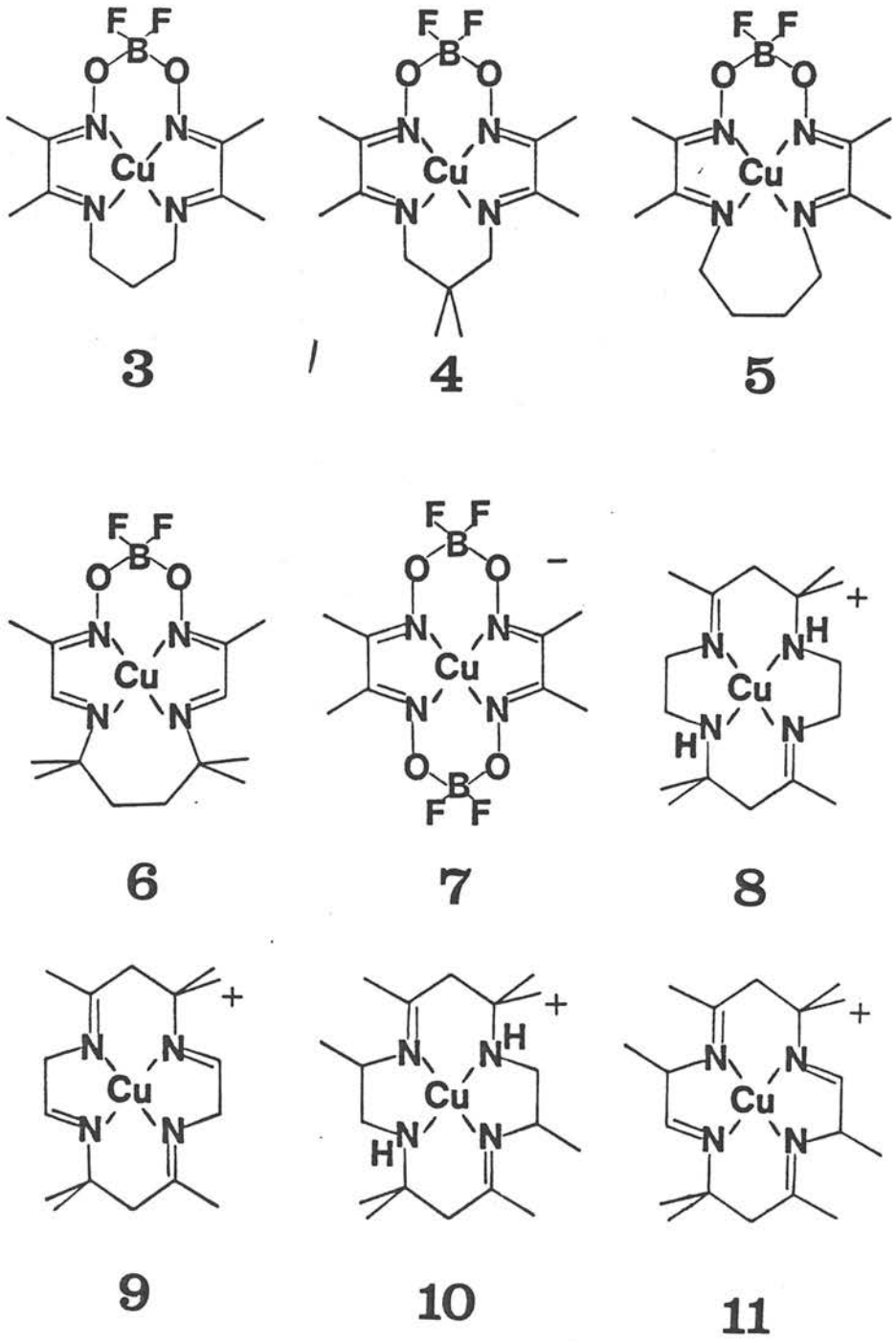

Figure 1. Macrocyclic copper(I) complexes which are proposed as sensitizers for the conversion of norbornadiene to quadricyclene.

Table 1

Complex	E_f^*	K_{CO}**	Reference
11	-0.762	6.1×10^4	11
9	-0.683	2.5×10^4	11
8	-0.656	4.7×10	15
10	-0.594	< 10	11
3	-0.456	1.2×10^5	15
4	-0.451	1.5×10^3	13
7	-0.438	8.8×10^5	15
5	-0.270	1.2×10^3	15
6	-0.169	5.3×10^3	13

*On Pt or Hg electrode (no significant differences noted) in dimethylformamide. Potentials converted to values versus nhe using ferrocene as an internal standard.[16]

**By the method in reference 15.

The complexes shown in Figure 1 present several possible advantages as sensitizers over the previously studied systems. A major problem with the systems presented thus far is the lack of light absorption in the visible region (400-800 nm) where the intensity of sunlight is greatest. The complexes shown in Figure 1 are all colored due to visible or near U.V. absorptions. Most notably, complex $\underset{\sim}{3}$ is blue, due to an absorption at 677 nm.[12] Also the charge transfer absorptions, Cu $\rightarrow$ NBD MLCT, are likely to be at longer wavelengths than those observed for ClCu-NBD and Cu[$HB(pz)_3$] (NBD). This is predicted for the (presumed) more electron-rich copper(I) centers which result from the high σ-donating character of the "hard" imine nitrogens. The high σ-donating character of these ligands also results in a relative destabilization of Cu(I) vs. Cu(II) when bound to these ligands. This is manifested by rather negative reduction potentials (Table 1).

In the event that these macrocyclic cuprous compounds do not bind NBD, they may still sensitize the conversion of NBD to Q by an excited state interaction with NBD (see Scheme 2). In this case, the visible absorptions (e.g., at 677 nm for $\underset{\sim}{3}$) may be useful. The binding constants for NBD to these Cu(I) compounds can be determined spectrophotometrically or electrochemically.[12]

These macrocyclic cuprous compounds present two additional attractive features as sensitizers. First, the presence of a single coordination site favors the desired intramolecular rearrangement rather than oligimerization or fragmentation processes which appear to be favored by multiple coordination sites on the metal.[14] Finally,

the organic framework of these macrocyclic ligands provides positions which can be functionalized for attachment to a solid support. This is desirable for the isolation of the sensitizer from the catalyst (to prevent cross-contamination) and to facilitate the replacement of the sensitizer in a working solar energy storage device.[3,4]

References

1. Kutal, C. Adv. Chem. Ser. 1978, 168, 158.
2. Kutal, C.; Grutsch, P. A. Adv. Chem. Ser. 1979, 173, 325.
3. Kutal, C.; Schwendiman, D. P.; Grutsch, P. Sol. Energy 1977, 19, 651.
4. Sweet, E. M.; King, R. B.; Hanes, R. M.; Ikai, S. Adv. Chem. Ser. 1979, 173, 344.
5. Schwendiman, D. P.; Kutal, C. J. Amer. Chem. Soc. 1977, 99, 5677.
6. Quantum yield (ϕ) is defined by

$$\phi = \frac{\text{number of molecules undergoing a particular change}}{\text{number of quanta absorbed}} .$$

7. Catalytic factor ≡ moles of Q produced per mole of sensitizer present.
8. Schwendiman, D. P.; Kutal, C. Inorg. Chem. 1977, 16, 719.
9. Grutsch, P. A.; Kutal, C. J. Amer. Chem. Soc. 1979, 101, 4228.
10. Sterling, R. S.; Kutal, C. Inorg. Chem. 1980, 19, 1502.
11. Lisensky, G. C., Ph.D. Disseration, California Institute of Technology, 1981.
12. Allison, J. L., Ph.D. Dissertation, California Institute of Technology, 1979.
13. Ingle, D. M., Ph.D. Dissertation, California Institute of Technology, 1980.
14. Salomon, R. G.; Kochi, J. K. J. Amer. Chem. Soc. 1974, 96, 1137. Salomon, R. G.; Sinha, A.; Salomon, M. F. J. Amer. Chem. Soc. 1978, 100, 520; Evers, J. T. M; Mackor, A.

References (continued)

Tetrahedron Lett. 1978, 2317.

15. Gagné, R. R., Allison, J. L., Ingle, D. M., Inorg. Chem. 1979, 18, 2767.

16. Gagné, R. R., Koval, C. A., Lisensky, G. C., Inorg. Chem. 1980, 19, in press.

PROPOSITION 5

Transition Metal Formyl Chemistry

The current energy shortage has prompted much interest in the Fischer Tropsch synthesis reaction.[1] This process involves the metal catalyzed reduction of CO by H_2 to yield mixtures of paraffins, olefins, alcohols, etc. Metal formyl complexes, 1, have been proposed as

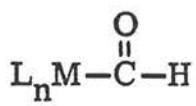

1

intermediates in this process, and as a result they are the subject of numerous current investigations. These studies have involved the synthesis and reactivity of transition metal formyl complexes.

The most general preparative route is given in equation 1.[2-4]

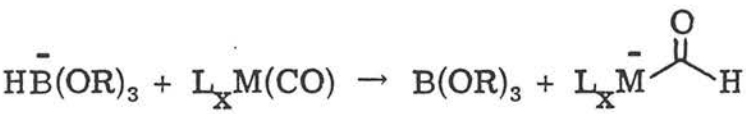

(1)

L = PPh_3, $P(OPh)_3$, CO

R = $-CH_3$, $-CH(CH_3)_2$

M = Cr, W, Re, Fe

The most stable formyl complexes have been formed with rhenium and iron. The normal method of decomposition involves loss of CO, followed by hydride migration to yield a metal hydride complex (e.g., equation 2).[5] Alternatively, these formyl compounds can act as

$$(CO)_4\bar{F}e\text{-}\overset{\overset{O}{\|}}{C}H \underset{+CO}{\overset{-CO}{\rightleftharpoons}} (CO)_3\bar{F}e\text{-}\overset{\overset{O}{\|}}{C}\text{-}H \rightarrow (CO)_4\bar{F}eH \qquad (2)$$

hydride donors to a number of electrophiles (e.g., Scheme 1).[4]

Scheme 1

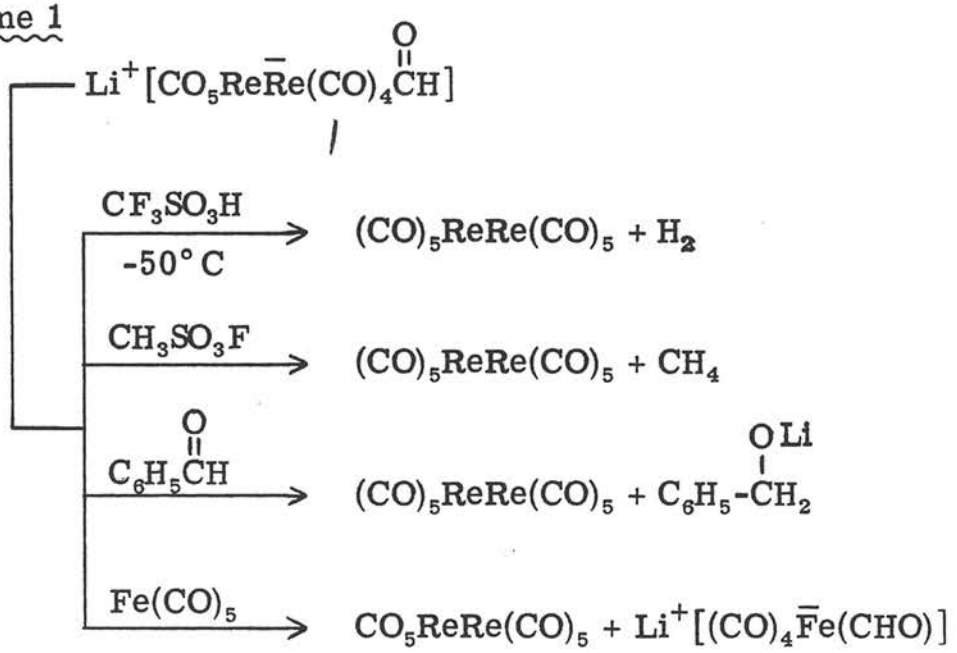

In contrast to these reactions, the iron formyl compounds, 2 and 2a, react differently toward acid.[3-5] The reason for this different

$$N(P\phi_3)_2^+[(CO)_4\bar{F}e(CHO)] \xrightarrow{H^+} \underset{H}{\overset{O}{\diagup\!\!\diagdown}}\!\!\underset{H}{} \qquad (3)$$

2

$$Et_4N^+[(\phi O)_3P(CO)_3\bar{F}e\text{-}\overset{\overset{O}{\|}}{C}H \xrightarrow{H^+} CH_3OH \qquad (4)$$

2a

reactivity is not obvious, but it may be related to the presence of an available coordination site on iron (for H^+). The reactivity of these compounds apparently does not directly reflect the relative stability of

the metal formyl complexes which was determined to be: $[(C_6H_5)_3P]_2N^+(CO)_4FeCHO^- > Et_4N^+$ cis-$(CO)_9Re_2CHO^- > Et_4N^+$ trans-$[C_6H_5O]_3P(CO)_3FeCHO^-$.[3] The mechanisms for these processes are unknown, but two proposed routes for the production of methanol are outlined in Scheme 2.

Scheme 2

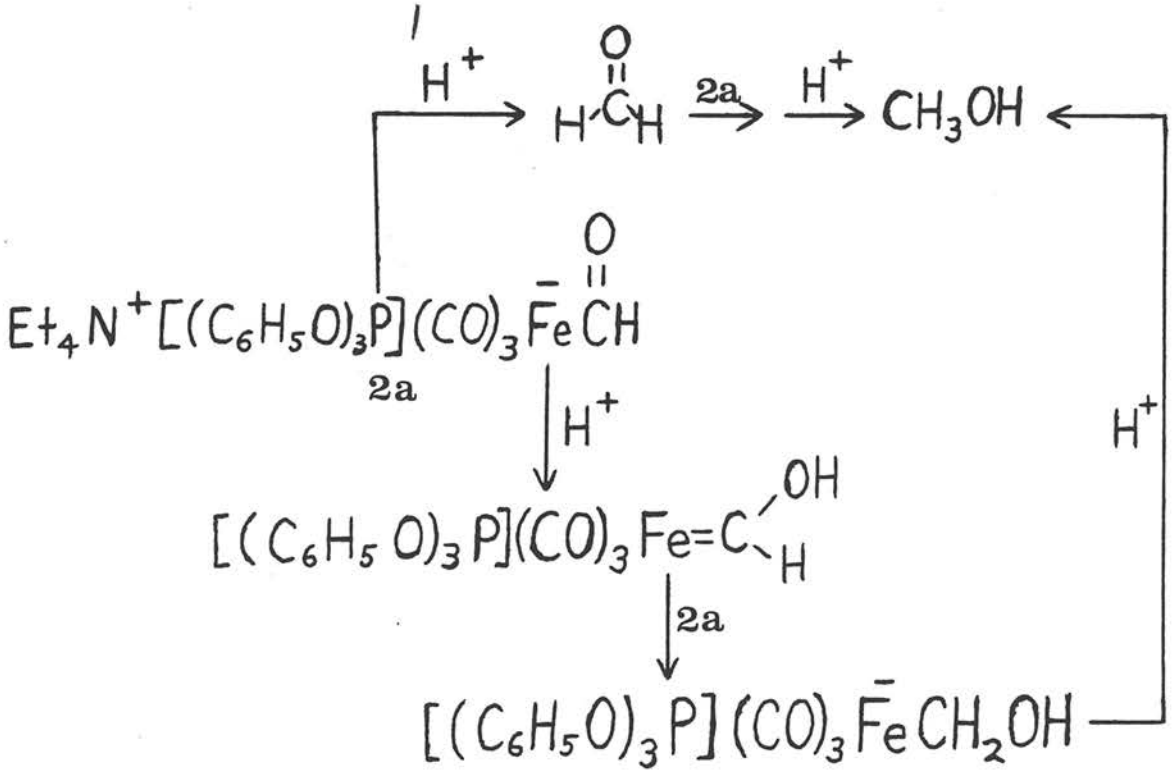

The analogous reactions of $\hat{2}$ and $\hat{2}$a with carbon electrophiles do not yield aldehydes as would be predicted from the above acid reactions. For instance, complex $\hat{2}$ reacts with 1-iodooctane to give octane and only a trace of nonanal. This result is consistent with direct nucleophilic displacement of iodide by the formyl hydrogen atom[3] or with the more complicated mechanism shown in Scheme 3.[5]

Scheme 3

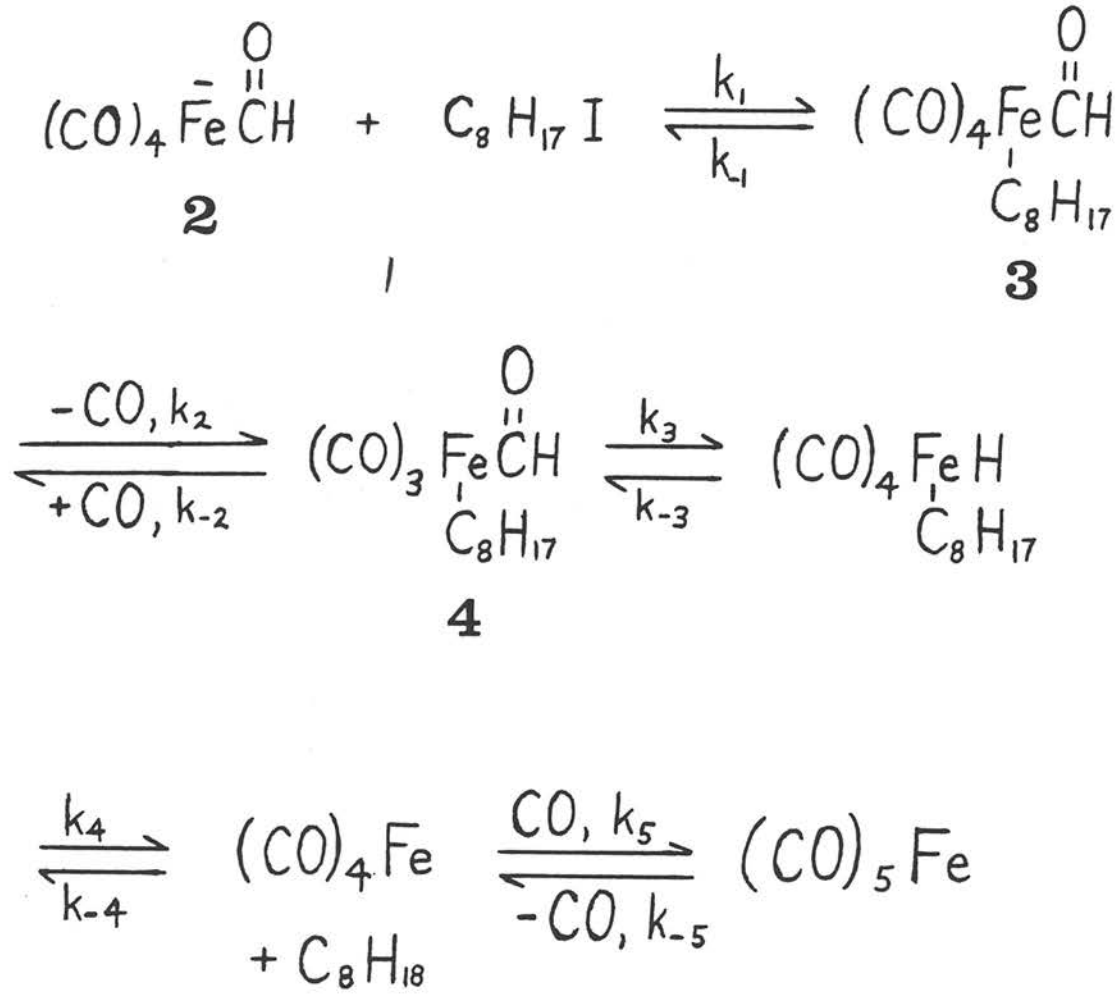

An investigation into this mechanism is proposed. In particular, the dependence of the reaction rate on carbon monoxide pressure will be investigated. While the direct hydride transfer mechanism should show no dependence on the CO pressure, the mechanism in Scheme 3 indicates that the reaction should be inhibited by CO. Assuming that $k_3 \gg k_{-3}$ and that processes k_4 and k_5 are fast and irreversible leads to the following rate expression (equation 5) when steady-state kinetics

$$\frac{-d[\underset{\sim}{2}]}{dt} = \frac{k_3 k_1 k_2 [\underset{\sim}{2}][C_8H_{17}I]}{k_{-1}k_3 + k_2 k_3 + k_{-1}k_{-2}[CO]} \quad (5)$$

$$\frac{-d[\underset{\sim}{2}]}{dt} = k_{obs}[\underset{\sim}{2}][C_8H_{17}I] \quad (5a)$$

are applied to $\underset{\sim}{3}$ and $\underset{\sim}{4}$.[6-8] A plot of k_{obs}^{-1} versus $[CO]^{-1}$ should yield a straight line. Even if the assumptions used here are invalid, the rate should be affected by [CO], contrary to the direct hydride attack mechanism.

The reaction can be conveniently monitored by the disappearance of the metal formyl proton magnetic resonance (pmr) signal at 14.95, δ versus TMS in THF.[5] Low temperature and/or high CO pressure may slow down the reaction such that intermediate $\underset{\sim}{4}$ can be observed by pmr.

Evidence supporting the mechanism in Scheme 3 would be significant for several reasons. It suggests the direct attack of electrophile on the metal center, with possible ramifications for the reactions of iron formyl complexes with acids (equations 3 and 4). Also the mechanism would seem to suggest either a greater tendency for reductive elimination with hydride and formyl substituents compared to alkyl and formyl substituents or a favoring of CO extrusion (reverse migratory insertion) from the formyl ligand when an alkyl ligand is bound to the iron.

To supplement this study, an analogous investigation into the products and mechanism of the reaction between $\underset{\sim}{2}$ and a smaller

carbon electrophile (e.g., CH_3I) may be of interest. Also, the effect of [CO] on the reaction rates for the processes in Scheme 1 (for $[(CO)_5ReRe(CO)_4C(O)H]^-$) could be examined for comparative purposes.

References

1. Olivé, G. H.; Olivé, S. Angew. Chem., Int. Ed. Engl. 1976, 15, 136.
2. Casey, C. P.; Neumann, S. M. J. Amer. Chem. Soc. 1976, 98, 5395.
3. Casey, C. P.; Neumann, S. M. J. Amer. Chem. Soc. 1978, 100, 2544.
4. Gladyz, J. A.; Tam, W. J. Amer. Chem. Soc. 1978, 100, 2545.
5. Collman, J. P.; Winter, S. R. J. Amer. Chem. Soc., 1973, 95, 4089.
6. It is reasonable to assume $k_3 \ll k_{-3}$ since migratory insertion of CO into a M-H bond is unknown. (See reference 5.)
7. Reductive elimination of an alkyl and a hydride from a transition metal (k_4) is usually fast and almost never reversible. See: Abis, L.; Sen, A.; Halpern, J. J. Amer. Chem. Soc., 1978, 100, 2915.
8. The unsaturated 16-electron species, $Fe(CO)_4$, should quickly bind another CO ligand (k_5), and the equilibrium should lie far to the right. See: Basolo, F.; Pearson, R. G.; "Mechanisms of Inorganic Reactions"; John Wiley and Sons, Inc., New York, 1967, pp. 533-578.